

Spring 2012

Using Landsat 5 TM Data to Identify and Map Areas of Mangrove in Tulum, Quintana Roo, Mexico

Samuel Standish Meachum
University of New Hampshire, Durham

Follow this and additional works at: <https://scholars.unh.edu/thesis>

Recommended Citation

Meachum, Samuel Standish, "Using Landsat 5 TM Data to Identify and Map Areas of Mangrove in Tulum, Quintana Roo, Mexico" (2012). *Master's Theses and Capstones*. 707.
<https://scholars.unh.edu/thesis/707>

This Thesis is brought to you for free and open access by the Student Scholarship at University of New Hampshire Scholars' Repository. It has been accepted for inclusion in Master's Theses and Capstones by an authorized administrator of University of New Hampshire Scholars' Repository. For more information, please contact nicole.hentz@unh.edu.

**Using Landsat 5 TM Data to Identify and Map Areas of
Mangrove in Tulum, Quintana Roo, Mexico**

BY

SAMUEL STANDISH MEACHAM
B.A., The University of Vermont, 1990

THESIS

Submitted to the University of New Hampshire
in Partial Fulfillment of
the Requirements for the Degree of

Master of Science
in
Natural Resources

May, 2012

UMI Number: 1518012

All rights reserved

INFORMATION TO ALL USERS

The quality of this reproduction is dependent upon the quality of the copy submitted.

In the unlikely event that the author did not send a complete manuscript and there are missing pages, these will be noted. Also, if material had to be removed, a note will indicate the deletion.

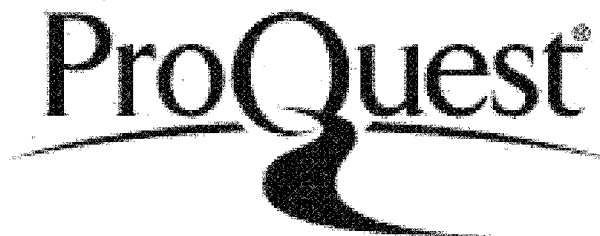


UMI 1518012

Published by ProQuest LLC 2012. Copyright in the Dissertation held by the Author.

Microform Edition © ProQuest LLC.

All rights reserved. This work is protected against unauthorized copying under Title 17, United States Code.

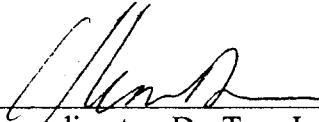


ProQuest LLC
789 East Eisenhower Parkway
P.O. Box 1346
Ann Arbor, MI 48106-1346

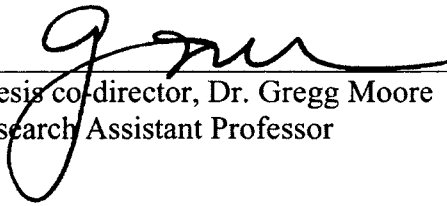
This thesis has been examined and approved.



Thesis co-director, Dr. Barrett N. Rock
Professor Forestry/Botany/Remote Sensing



Thesis co-director, Dr. Tom Lee
Associate Professor Forest Ecology



Thesis co-director, Dr. Gregg Moore
Research Assistant Professor

DECEMBER 22, 2011

Date

Acknowledgements

I am extremely grateful to many people and organizations who have made this project possible. First and foremost I owe so much to Dr. Barry Rock, NASA and the New Hampshire Space Grant Consortium for getting me to UNH and helping me realize my potential. Dr. Gregg Moore endured a trial by fire in the mangrove swamps of Mexico and has been an invaluable source of knowledge and drive throughout. I also appreciate the guidance of Dr. Tom Lee. I have learned so much from Dr. Russ Congalton and have benefited greatly from his input and interest in this project. Meghan MacLean and Mickey Campbell were invaluable in helping me find solutions to problems I encountered along the way. Michael Routhier and Stanley Glidden in the Morse Hall GIS lab were steadfast companions and helped a great deal as I waded through the actual process of image analysis. Fellow students Mike Gagnon and Natasha Leuchanka braved the harsh elements of Mexico and helped in collecting much of the data that is presented here. My dear friends Dr. Dominique Rissolo and Dr. James Rotenberg have been supportive from day one. In Mexico, a great deal of thanks to Paul Sanchez Navarro and the folks at El Centro Ecologico Akumal for all of their logistical support. Gonzalo Merediz and Miriam Reza at Amigos de Sian Ka'an also helped in making available data to the project. Access to the Sian Ka'an Biosphere Reserve would not have happened without the support of its Director Francisco Ursua and Sub Director Angel Omar Ortiz. I am also grateful to the Ejido Tulum which granted access to the inland mangrove areas of Laguna Union and Laguna Chumkopo. Fundacion Selva Maya and Manuel Orvañanos granted access to Laguna Selva Maya. Field work was made much more

tolerable in May of 2011 thanks to Gary and Kay Walten who made their beautiful home available to us. In the field, I could not have made it without Olmo Torres-Talamante who is an excellent 'compadre'. We share many good memories from our walks and talks.

Finally, my dear wife Orane and my boys Benjamin and Matteo deserve my greatest thanks for letting me transplant us from beautiful (warm) Mexico to beautiful (not as warm) New England. It has been quite an adventure.

Table of Contents

Acknowledgements	iii
List of Tables	vii
List of Figures.....	viii
Abstract.....	ix
1.0 Introduction.....	1
1.1 Study Area	1
1.2 Worldwide Status of Mangrove	2
1.3 Status of Mangrove in Mexico.....	3
1.4 Mangrove Distribution and Classification	6
1.5 Mangrove Leaf Anatomy	8
1.6 The Mangrove species of Mexico	8
1.6.1 Red Mangrove (Rhizophora mangle).....	8
1.6.2 Black Mangrove (Avicennia germinans)	9
1.6.3 White mangrove (Laguncularia racemosa)	10
1.6.4 Buttonwood (Conacarpus erectus)	10
1.7 Remote Sensing Overview	11
1.7.1 The Landsat 5 Thematic Mapper	14
1.7.2 Data Exploration	15
1.7.3 Image Classification.....	16
1.7.4 The Visible Infrared Intelligent Spectrometer (VIRIS)	17
1.7.5 Leaf Anatomical/Spectral Characteristics	18
1.7.6 Remote Sensing and Mangroves	19
1.8 Accuracy Assessment	20
1.9 Hypotheses	23
1.10 Goals	23
1.11 Objectives.....	23
2.0 Methods and Materials.....	25
2.1 Overview	25
2.2 Selection of Landsat Data	25
2.2.1 Image Stacking.....	26
2.3 Image Exploration.....	27
2.3.1 Unsupervised Classification.....	28
2.3.2 Derivative Bands.....	30
2.4 Image Preprocessing	30
2.4.1 Image Subsetting.....	30
2.4.2 Image Masking.....	31
2.5 Classification Scheme.....	33
2.6 Reference Data Collection and Areas of Interest	33
2.7 Supervised Classification	34
2.8 Accuracy Assessment	35
2.8.1 Reference Data Collection and Classification Scheme	35
2.9 Spectral Characterization and Anatomical Study of Mangrove Leaf Samples.....	37
2.9.1 Study Area for Foliar Collection.....	38
2.9.2 Collection Methods for Leaf Samples	40
2.9.3 Measuring Spectral Reflectance Properties of Leaf Samples	42

2.9.4 Mangrove Leaf Anatomy Analysis	43
3.0 Results	44
3.1 Mangrove Leaf Anatomical Analysis.....	44
3.1.1 Avicennia germinans (Black mangrove).....	44
3.1.2 Rhizophora mangle (Red mangrove)	45
3.1.3 Laguncularia racemosa (White mangrove).....	47
3.2 Spectral Characterization of Mangrove.....	48
3.2 Thematic Map Results	55
3.2.1 Thematic Map Accuracy Assessment	55
3.2.2 Thematic Map Classifications.....	56
4.0 Discussion.....	60
4.1 Leaf Anatomy and Reflectance Properties of Mangrove.....	60
4.2 Map Accuracy.....	62
4.3 The Thematic Map	63
4.3.1 Forest Classification.....	63
4.3.2 Sawgrass Classification.....	66
4.3.3 Mangrove Classification	67
4.4 Inland Mangrove Habitats	71
4.5 Comparison of CONABIO and UNH studies	76
4.6 Implications for Mangrove Conservation	79
5.0 Conclusions	81
Hypothesis 1	83
Hypothesis 2	83
Hypothesis 3	83
Hypothesis 4.....	83
References	84
Appendices.....	88
Appendix A:	89

List of Tables

<i>Table 1 Landsat 5 TM Bands and Uses, adapted from Jensen (2007)</i>	15
<i>Table 2 Classification scheme for Reference Data Collection</i>	33
<i>Table 3 Areas of Interest for Training the Computer</i>	34
<i>Table 4 Accuracy Assessment Field Form</i>	36
<i>Table 5 Data field form for Solimon Bay Study Site</i>	41
<i>Table 6 Average Spectral Indices (REIP, 5/4) for Solimon Bay Mangrove Samples and Two Non-Mangrove Samples</i>	51
<i>Table 7 Mangrove Accuracy Assessment Error Matrix</i>	55
<i>Table 8 Comparison of Classified Mangrove and Not-Mangrove Areas</i>	56
<i>Table 9 Supervised Mangrove Polygons by Size (ha)</i>	68
<i>Table 10 Mangrove Areas (ha) and Number of Polygons by Type</i>	69
<i>Table 11 Characteristics of Inland Mangrove Areas</i>	74
<i>Table 12 Comparisons of Results Between CONABIO and UNH Studies</i>	76

List of Figures

<i>Figure 1 The Municipality of Tulum and the Solimon Bay Study Site.....</i>	<i>1</i>
<i>Figure 2 Evidence of the Growth of the Town of Tulum 1984-2000.....</i>	<i>5</i>
<i>Figure 3 Evidence of Construction on top of Mangrove Habitat, Chemuyil, Mexico</i>	<i>6</i>
<i>Figure 4 The Electromagnetic Spectrum, adapted from Jensen (2007)</i>	<i>11</i>
<i>Figure 5 Landsat 5 TM Bandwidths and Resolutions, adapted from Jensen (2007).....</i>	<i>13</i>
<i>Figure 6 Spectral Curve of White Pine and Landsat Band Regions (Forestwatch, 2011)</i>	<i>18</i>
<i>Figure 7 Example of Error Matrix, derived from Jensen (2007).....</i>	<i>22</i>
<i>Figure 8 Detail of 10 Class Unsupervised Classification demonstrating Confusion with Urban, Overwash Mangrove and Beach Areas</i>	<i>29</i>
<i>Figure 9 Processes of Subsetting and Masking the Image</i>	<i>32</i>
<i>Figure 10 Municipality of Tulum including the Town of Tulum and the Solimon Bay Study Site</i>	<i>38</i>
<i>Figure 11 Foliar Sample Ready for Scan.....</i>	<i>40</i>
<i>Figure 12 The VIRIS in use with leaf samples in the foreground.....</i>	<i>42</i>
<i>Figure 13 Thin Section of A. germinans Leaf (100x).....</i>	<i>44</i>
<i>Figure 14 Thin Section of R. mangle leaf (100x).....</i>	<i>45</i>
<i>Figure 15 R.mangle water storage cells (400x).....</i>	<i>46</i>
<i>Figure 16 Thin section of L. racemosa leaf (100x).....</i>	<i>48</i>
<i>Figure 17 Plot of the mean 5/4 ratio for Black Mangrove (AG), Ficus cotinifolia (FC), Ficus maxima (FM), Red Mangrove Medial (RM-M), and White Mangrove (LC). Overall analysis by ANOVA followed by multiple comparisons using Student's t (<0.05). Error bars constructed using 1 standard error from the mean.....</i>	<i>52</i>
<i>Figure 18 Plot of the mean REIP value for Black Mangrove (AG), Ficus cotinifolia (FC), Ficus maxima (FM), Red Mangrove Medial (RM-M), and White Mangrove (LR). Overall analysis by ANOVA followed by multiple comparisons using Student's t (<0.05). Error bars constructed using 1 standard error from the mean.....</i>	<i>52</i>
<i>Figure 19 Reflectance Curves for 3 Mangrove Species, Solimon Bay, Mexico</i>	<i>53</i>
<i>Figure 20 Comparison of Average Reflectance of Three Mangrove Species with Two Non-Mangrove Species</i>	<i>54</i>
<i>Figure 21 Final Supervised Classification Showing Polygons Meeting the MMU</i>	<i>57</i>
<i>Figure 22 Areas of Mangrove Identified by this Study by Class.....</i>	<i>59</i>
<i>Figure 23 Comparison of potential moisture conditions in the.....</i>	<i>62</i>
<i>Figure 24 Final Supervised Classification of the Study Area (Showing all polygons)</i>	<i>64</i>
<i>Figure 25 Unprotected Inland Areas of Mangrove.....</i>	<i>72</i>
<i>Figure 26 Overlays of CONABIO and UNH Studies.....</i>	<i>78</i>
<i>Figure 27 Areas of Mangrove, Protected vs. Unprotected.....</i>	<i>79</i>
<i>Figure 28 Unprotected Areas of Mangrove Identified by the UNH Study</i>	<i>80</i>
<i>Figure A 1 Flowchart for Image Stacking in ERDAS Imagine V.10.....</i>	<i>89</i>
<i>Figure A 2 Full Extent of Landsat 5 TM Image (FCC bands 4,3,2) Path 19 Row 46, Acquired February 9th, 2000 with Tulum Municipal Boundary.....</i>	<i>90</i>
<i>Figure A 3 Full Extent of Landsat 5 Image (FCC Bands 4,3,2) Path 19 Row 46, Acquired April 17th, 1984 with Tulum Municipal Boundary</i>	<i>91</i>
<i>Figure A 4 10 Class Unsupervised Classification of the Study Area</i>	<i>92</i>
<i>Figure A 5 Derivative Band Creation (5/4 ratio, Principal Components Analysis) in ERDAS imagine V.10</i>	<i>93</i>
<i>Figure A 6 Derivative Band Creation (NDVI, Tasseled-Cap) in ERDAS Imagine.....</i>	<i>94</i>
<i>Figure A 7 Flowchart for Landsat Image Subset and Masking in ERDAS Imagine.....</i>	<i>95</i>
<i>Figure A 8 Accuracy Assessment Reference Points.....</i>	<i>96</i>

Abstract

Using Landsat 5 TM Data to Identify and Map Areas of Mangrove in Tulum, Quintana Roo, Mexico

By

Samuel S. Meacham

University of New Hampshire, May, 2012

Mangroves are recognized worldwide as a major ecosystem that provides significant ecosystem services. They are threatened due to rising pressures from human overpopulation and economic development. The Caribbean Coast of Mexico's Yucatan Peninsula contains mangrove habitat that have been negatively impacted by the development of the region's tourist industry. However, little research has been done to map and quantify the extent of mangrove in the region. This study used remote sensing techniques to identify mangrove in the Municipality of Tulum located in Quintana Roo, and to produce an accurate vector based thematic map that inventories these areas. Anatomical differences were analyzed and related to high-resolution field spectral data for each mangrove species. A vector map of mangrove habitat, including areas of inland mangrove, was produced with an overall accuracy of 88%. The 19,262 ha. of mangrove identified by this study represents a 140% increase in area over previous studies.

1.0 Introduction

1.1 Study Area

This research project was conducted in the Mexican state of Quintana Roo within and around the Municipality of Tulum (Figure 1), which was incorporated as a municipality in 2008 (Congreso del Estado de Quintana Roo, 2008). Located along the Caribbean coastline and stretching west to the town of Coba, it incorporates 2,040 km², contains 170 populated localities and according to the 2010 census has a population of 28,263 (Instituto Nacional de Estadística y Geografía, 2010). This does not, however, take into account a floating population of workers involved in construction, the tourism industry and the tourists that visit the area.

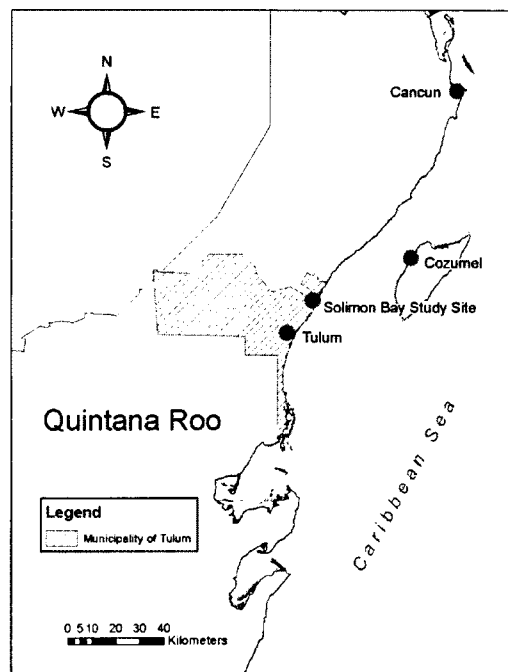


Figure 1 The Municipality of Tulum and the Solimon Bay Study Site

The area's climate is tropical and receives an annual mean precipitation of 1230 mm (Lee, 1996). Mean monthly temperatures range from 34°C in August to 20°C in

February (Lee, 1996). There is a marked rainy season from May through November and a dry season from December through April (Beddows, 2004). Tropical storm and hurricane activity frequently affect the area. The geology of the region is karst with large, submerged solution cave systems serving as conduits that discharge freshwater along the Caribbean coastline while allowing seawater to infiltrate to inland areas (Beddows, 2004). Saltwater circulation could play a significant role in mangroves existing in inland areas.

1.2 Worldwide Status of Mangrove

The term 'mangrove' is used to describe both the plant families and ecosystems that have adaptations allowing them to live in the highly saline conditions between terrestrial and marine ecosystems (Tomlinson, 1986). Mangroves dominate the coastlines of the world's tropical and subtropical regions, i.e. they are pantropical in their distribution. Estimates in the coverage of mangroves worldwide vary widely from 12 to 20 million hectares (FAO, 2007). This large discrepancy only highlights the need for more accurate remote sensing methods of identifying and mapping mangrove forests. Because of their unique positioning, worldwide distribution, and high productivity, mangroves provide many important functions to the millions of people inhabiting subtropical and tropical coastlines (Polidoro et al., 2010). Their position in the transitional area between terrestrial ecosystems and the marine environment allows them to act as buffers and, as such, help to mitigate coastal erosion especially in the case of extreme events such as tsunamis and hurricanes (Alongi, 2008).

Mangroves also support and protect biological diversity as they provide habitat to a wide variety of mammals, birds, reptiles, amphibians, fish and plants (Kathiresan and

Bingham, 2001). Humans depend on mangroves both directly and indirectly for their economic well being (Cornejo et al., 2005; Ewel et al., 1998; Kaplowitz, 2000; Kaplowitz, 2001). Wood and tannins are harvested commercially from mangrove forests worldwide (Terchunian et al., 1986). Shellfish and mollusks are collected from them, and many commercial and sporting fish species use mangroves as nurseries and breeding grounds (Ellison and Farnsworth, 1996; Kathiresan and Bingham, 2001). The rise of ecotourism worldwide has also seen a new-found interest in mangrove ecosystems as a sustainable source of economic development (FAO, 2007).

At the same time, increases in the world's human population, and its associated development, are putting mangrove ecosystems at risk (Polidoro et al., 2010). Current estimates are that since 1980, 3.6 million hectares of mangrove have been destroyed (FAO, 2007). Long perceived of as unhealthy mosquito-ridden swamps (Lugo and Snedaker, 1974), developers have removed mangrove in order to further expand recreational and urbanized areas. They have also been used historically as dumping grounds for sewage and industrial waste (Kathiresan and Bingham, 2001). In addition, many developing nations are promoting the use of mangroves for aquaculture such as shrimp ponds (Terchunian et al., 1986; Valiela et al., 2001). While these types of exploitation may have short-term economic benefits, they also may have long-term negative impacts on the environment and local economies if they are not managed in a sustainable manner.

1.3 Status of Mangrove in Mexico

Due to its geographic location within subtropical and tropical regions, and its extensive coastlines on both the Pacific and Atlantic coasts, Mexico is ideally situated for

mangrove to proliferate. A total of 770,057 hectares of mangrove habitat were identified in a 2008 study of Mexico that employed remote sensing techniques by the Comisión Nacional para el Conocimiento y Uso de la Biodiversidad (CONABIO, 2009). The CONABIO study was conducted using remote sensing (SPOT 5, Système Probatoire d'Observation de la Terre) and photogrammetric techniques (digital aerial imagery) and covered the coastal sections of the entire nation. While Mexico only contains four species of mangrove (*Rhizophora mangle*, *Avicennia germinans*, *Laguncularia racemosa*, *Conocarpus erectus*), it does contain 5% of all the mangrove in the world (FAO, 2007). Mangrove is protected under the Mexican *Ley General de la Vida Silvestre NOM 60 Ter* (Poder Ejecutivo Federal, 2011), yet it is threatened from a number of different forces. The same intensive study in 2008 by CONABIO to quantify areas of mangrove within Mexico, identified agriculture, cattle ranching, aquaculture and tourism as the principal threats to mangrove habitats (CONABIO, 2009). Of these threats, the development of tourism along Mexico's Caribbean coast is of greatest concern to this study. Hoteliers, developers and state governors in areas of Mexico where tourism infrastructure is present have challenged the law arguing that the protection of mangrove is hampering job growth by limiting development. A total of 16 non partisan governors in coastal states have opposed the laws protecting mangroves urging amendments that would loosen the laws and allow more development (AllBusiness.com, 2007). Thus, the conservation of mangrove in the region is of critical importance.

Of particular interest to this study is the recently established Municipality of Tulum. Tulum is rich in its cultural and natural history. It is the home to two major Maya archeological sites, Tulum and Coba, an abundance of submerged cave systems

(Beddows, 2004; Meacham, 2007) that serve as the regions aquifer, portions of the Mesoamerican Barrier Reef and the UNESCO World heritage Site of the Sian Ka'an Biosphere Reserve. For these reasons and in addition to its white sand beaches, Tulum and the surrounding destinations of Cozumel, Cancun and the Riviera Maya are magnets for international tourism (Mazzotti et al., 2005) and tourist development. The growth of the town of Tulum and the impact that growth is having within its municipal boundaries are already visible in comparative satellite images (Figure 2, Figure 3). Evidence of these impacts helps to rationalize a study of this nature.

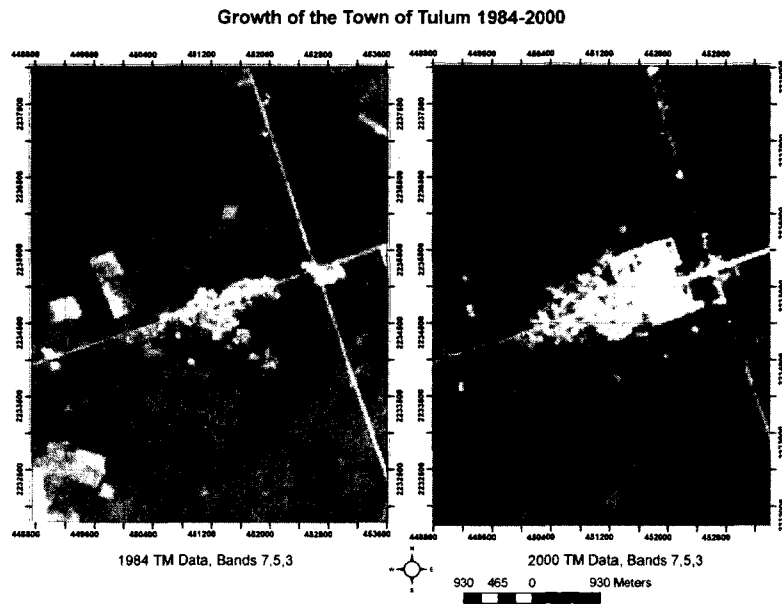


Figure 2 Evidence of the Growth of the Town of Tulum 1984-2000

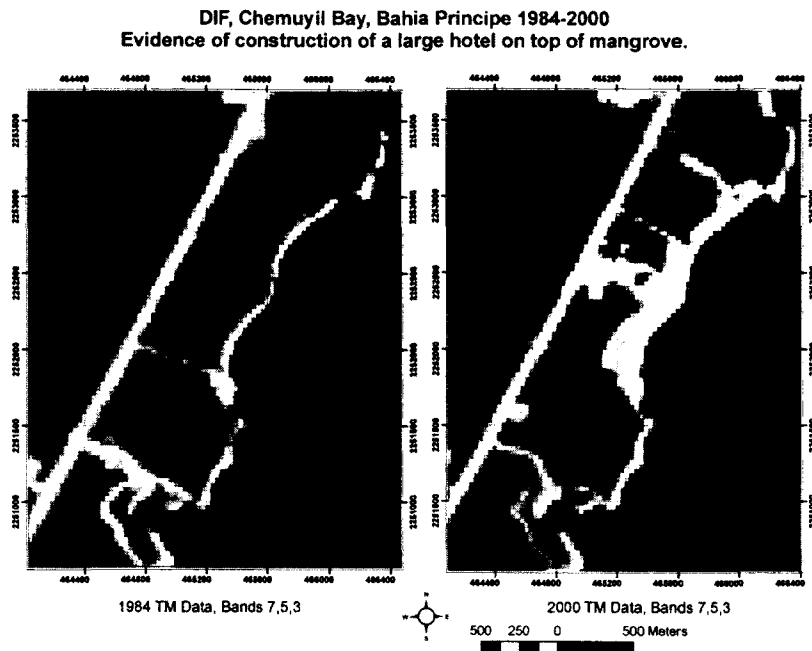


Figure 3 Evidence of Construction on top of Mangrove Habitat, Chemuyil, Mexico

Established in 2008, Tulum has adopted a conservation action plan presented to them by local NGOs's working in concert with The Nature Conservancy that identifies the conservation of mangroves as one of its priorities.

1.4 Mangrove Distribution and Classification

The main limiting factor attributed to the global distribution to mangrove is temperature (Hogarth, 1999; Tomlinson, 1986). Hogarth (1999) states that the distribution of mangroves is more closely correlated to sea temperatures as they are confined mainly by the winter position of the 20°C isotherm. Thus, the great majority of mangrove species are confined to the subtropical and tropical regions of the world. The relationship to sea temperature is demonstrated by the fact that in the Americas, the distribution of mangroves along the Atlantic coast of South America extends to 33° South due to warmer sea temperatures, while the furthest southern extent on the Pacific coast

goes only as far as 3° South due to the colder currents associated with the Humboldt Current (Hogarth, 1999).

Lugo and Snedaker (1974) established a classification of mangroves using an ecosystem approach that incorporated, ‘...the essential structural and functional attributes of mangrove as well as the principal external energy sources and stresses that affect that system.’. They describe a system of flux where the zonation of mangroves may be most influenced by ‘external forces’ acting on them. They consider that the substrate and water regime are two of the main factors influencing mangrove zonation. The categories include the *fringe forests* that occur along protected shorelines and that are above the high tide mark; *riverine forests* that occur along rivers or creeks and that are influenced by the presence of freshwater; *overwash forests* are small mangrove fingers and islands that occur in shallow bays and estuaries. They are most influenced by tidal fluctuation and are dominated by *Rhizophora mangle*, the red mangrove; *basin forests* that occur inland and along areas of drainage to the sea. Where they are still influenced by tides *R. mangle* dominates. Moving further inland mixing of *Laguncularia racemosa* (white mangrove) and *Avicennia germinans* (black mangrove) will occur; and *dwarf forests* are typified by the stunted growth of mangrove that is usually >1.5m in height. Snedaker postulates that the stunting could be attributed to a lack of nutrient sources. (Lugo and Snedaker, 1974)

In their study of Belizean mangroves Murray et al. (2003) further narrowed the limiting factors of mangrove to a local scale that is more meaningful to my proposed study. They state that among other things, the factors controlling mangrove distribution are influenced by the presence of the Mesoamerican Barrier Reef, the coastlines shallow

gradient, narrow tidal range, geomorphology, drainage and past hurricane tracks. These conditions mirror those found along the coast of Quintana Roo.

1.5 Mangrove Leaf Anatomy

Mangroves species share a common set of anatomical features including, ‘water storage’ tissue, short tracheids terminating in vein endings, and the absence of sclerotic vein sheaths (Tomlinson, 1986). Jensen (2007) states that the three dominant factors controlling leaf reflectance are the leaf pigments contained in the palisade mesophyll, the scattering of Near-IR energy in the spongy mesophyll, and the amount of water in the foliage.

Of greatest interest to this study is the common feature of ‘water storage’ tissue, known as a hypodermis, and resulting leaf succulence. Tomlinson (1986) states that mangrove leaf succulence varies according to the degree of salinity and leaf age. This suggests that the reflective properties of mangrove would be influenced by the salinity in which the mangrove grows. This idea is supported by the findings of Camilleri and Ribi (1983) who found leaf thickness to increase with higher salinity levels. One of the goals of this project is to characterize the reflectance response pattern of the dominant species of mangrove and relate it to leaf anatomy. It is expected that the ‘water storage’ tissue common to all 3 species of mangrove present will be an important factor in being able to spectrally characterize them.

1.6 The Mangrove species of Mexico

1.6.1 Red Mangrove (Rhizophora mangle)

Rhizophora mangle belongs to the family *Rhizophoraceae* that includes 16 genera and 20 species. It can attain a maximum height of 20m and while it does occur on the

west coast of Africa, it is mainly confined to the Old World on both the Pacific and Atlantic coasts. It is most easily identified by its large prop roots and is the dominant species to be found along the Caribbean Coast of Mexico (Mazzotti et al., 2005). It is viviparous and can also be easily identified by its distinctly shaped propagules. *R. mangle* uses the mechanisms of exclusion (at the roots) and accumulation in order to cope with high levels of salinity. Of the four species found in Mexico it is the one that is most tolerant to high salinity and therefore is found closest to the interface of marine and terrestrial ecosystems. The leaf arrangement of *R. mangle* is arranged in such a way that self-shading is minimized and reflectance is maximized (Tomlinson, 1986).

1.6.2 Black Mangrove (*Avicennia germinans*)

Avicennia germinans belongs to the family *Avicenniaceae*. The genus has about 8 species that are difficult to distinguish. It is a New World species and is distributed along both the Pacific and Atlantic coasts of the Americas. *A. germinans* can grow up to 30m tall and occupies diverse mangrove habitats. It is very tolerant to hypersaline conditions and uses the mechanism of exclusion, secretion and accumulation to cope with high levels of salinity. *A. germinans* is most easily distinguished by its pneumatophore root systems that can stick up to 30 cm. It has a rough black bark that is the source of its name. The leaves of *A. germinans* are also diagnostic, the lower leaf surface is white and hairy, and the upper surface is dark green. Salt crystals can be seen on the surface of the leaves. It has a large white flower, the fruit is viviparous and deposits a germinated seedlings to the ground or water below.

1.6.3 White mangrove (*Laguncularia racemosa*)

Laguncularia racemosa belongs to the family Combretaceae that contains 20 genera and 500 species. Similar to *R. mangle*, *L. racemosa* is found only in America and the West Coast of Africa. It can grow to 12-18 m and is viviparous. It is generally found on the landward fringe of mangrove communities and may or may not have pneumatophores. It can be identified by its solitary trunk and rough textured bark. It is also characterized by an abundance of dead or dying branches (Tomlinson, 1986) due to rapid branch growth and subsequent branch abortion. *L. racemosa* uses the mechanism of secretion in order to cope with high levels of salinity. Three kinds of secretory structures have been found on the leathery textured leaves of *L. racemosa*, the most obvious of which are the two glands located on the petiole of each leaf (Tomlinson, 1986).

1.6.4 Buttonwood (*Conocarpus erectus*)

Conocarpus erectus, like *L. racemosa*, belongs to the family Combretaceae, a large family of 20 genera and 500 species. It is within a genus of 2 species, one distributed in East Africa, while *C. erectus* is confined to the Americas and West Africa. Of the four species of mangrove found in Mexico, *C. erectus* is the only one that is not considered a 'true mangrove' (Tomlinson, 1986). Since it lacks vivipary and pneumatophores it is considered a 'mangrove associate'. It is tolerant to a range of conditions from freshwater to hypersaline. Its button shaped seed that is the source of its name easily distinguishes it. A variety of the species *C. sericeus*, known commonly as 'silverleaved buttonwood', can be easily identified by the hairy, silver colored leaf surface.

1.7 Remote Sensing Overview

Remote sensing is defined as, *the measurement of some property of an object by a device not in contact with the object* (Jensen, 2007). Remote sensing data can be collected by satellite, airborne or ground based sensors. The data detected by the sensors and recorded by the instrument are measurements of electromagnetic (EM) radiation (Figure 4). Sensors are designed to record and detect EM radiation along different portions of the electromagnetic spectrum and at differing resolutions or bandwidths. Each area along the EM spectrum is able to impart information about conditions on Earth's surface. For example, the visible and infrared portions of the EM spectrum allow scientists to study and understand the health of vegetation (Rock et al., 1986). The key to remote sensing is to understand the spectral response pattern of an object, or surface, seen in an image, and relating it to what is happening on the ground.

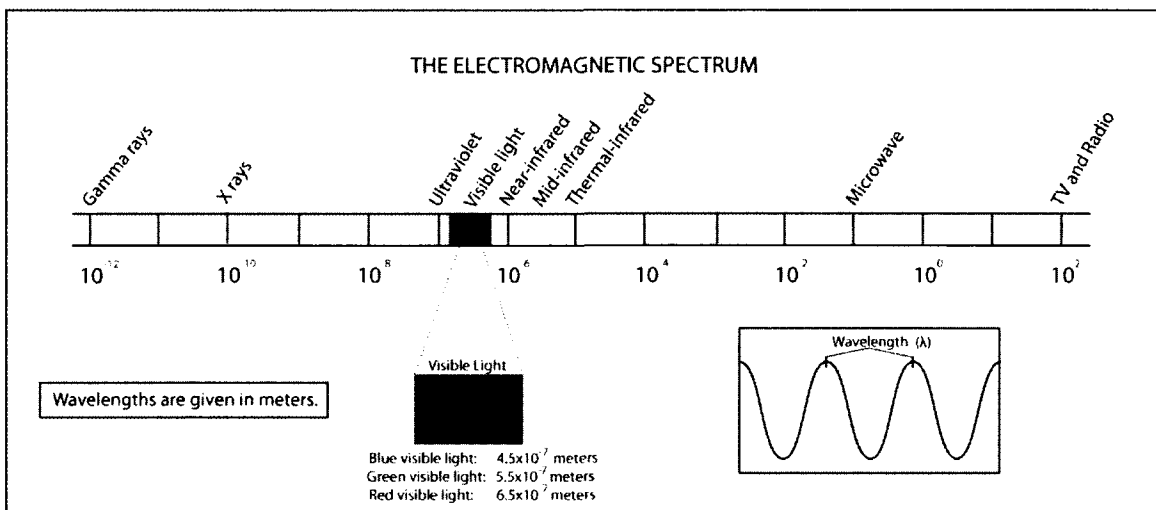


Figure 4 The Electromagnetic Spectrum, adapted from Jensen (2007)

By using a variety of sensors and platforms, remote sensing analysts can provide solutions to real world problems. Large-scale human issues such as overpopulation, the

earth's finite landscape and diminishing natural resources are the main drivers behind remote sensing analysis (Congalton, 2011). The sensors and platforms used in remote sensing provide timely and accurate information that help us to study and understand these issues so that informed decisions can be made.

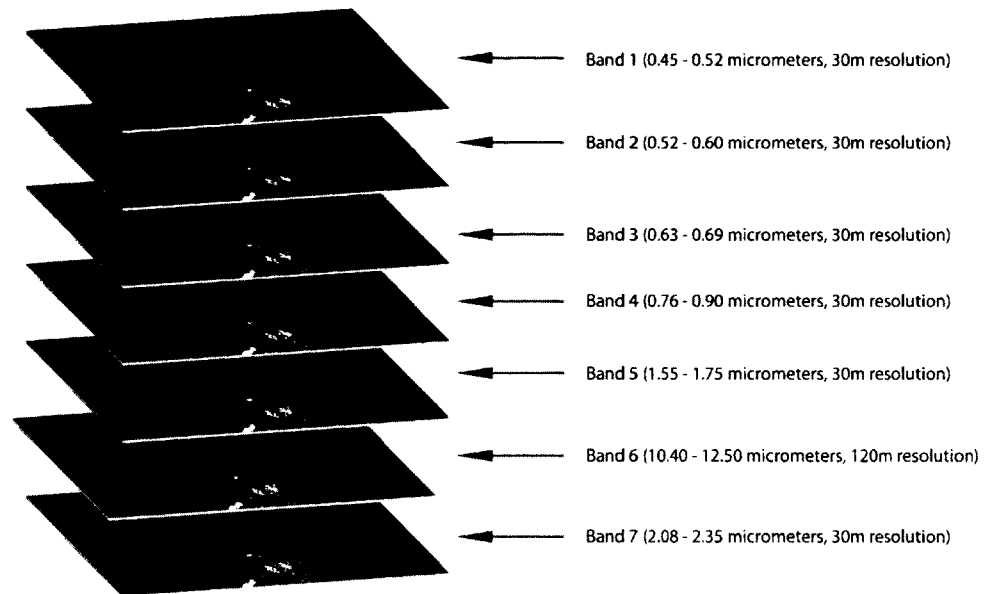
There are many clear advantages to using remote sensing. It is generally less expensive than traditional land based studies, allowing scientists to cover much larger areas more effectively and efficiently. It provides us with a synoptic view, a perspective that allows us to see the 'big picture' of issues across time and space. Furthermore, remote sensing allows us to see things that the human eye cannot. This capability allows us to, among many things, study the health of forest vegetation (e.g. using the visible and the NIR and SWIR spectrum). Additionally, remote sensing allows for various spatial and temporal scales that permit detailed studies of specific areas and change detection.

The common factors that are essential to choosing the right system for a project should be based on the following factors; *spatial resolution*, *spectral resolution*, *radiometric resolution*, *extent* and *temporal resolution*.

Spatial resolution is the size of the smallest pixel (picture element) captured by a sensor. High-resolution images have fine levels of detail (smaller pixels) while low-resolution images have coarse levels of detail (larger pixels).

Spectral resolution is the number of wavelengths of electromagnetic energy that a sensor is able to detect. The more wavelengths a sensor is able to detect, the higher its resolution will be. For example, a multispectral sensor (e.g. Landsat 5 TM, 7 spectral bands) (Figure 5) detects wide wavelengths with breaks, while a hyperspectral sensor

(e.g. Hiperion, 220 spectral bands) detects narrow wavelengths and is continuous in its measurements.



Landsat 5 TM Bandwidths and Resolutions

Figure 5 Landsat 5 TM Bandwidths and Resolutions, adapted from Jensen (2007)

Radiometric resolution is the amount of light that is being reflected and sensed. Radiometric resolution determines the dynamic color range for each individual pixel. The higher the radiometric resolution, the more range is available to each pixel. Most remotely sensed satellite data are 8-bit (2^8) which gives a potential dynamic range of 0-256. With higher levels of radiometric resolution, more subtlety and variation can be sensed.

Extent is the size of an area that a single scene covers. Typically sensors that have high spatial resolution have small extents (more detail over a smaller area).

Finally, *temporal resolution* is how often the sensor passes over the same point on planet earth. It is the temporal resolution of a sensor that allows the powerful application of change detection to be used allowing impacts on the earth's surface to be quantified.

1.7.1 The Landsat 5 Thematic Mapper

For this study, data will be used from the Landsat 5 Thematic Mapper (TM). Launched in 1984, Landsat 5 TM data has a spectral resolution of 30m. When compared to more recent advances in high spatial resolution image data (e.g. Ikonos, Quickbird) the Landsat 5 TM imagery has a lower quality that may lead some to question its effectiveness as a tool. However, the 30m resolution has an advantage, especially when looking at large stands of homogeneous vegetation, as in the case of this study. Systems that have higher spatial resolution can suffer from too much detail and the effects of shadows, thus making the process of classification more difficult (Congalton, 2011). An additional benefit of the Landsat 5 TM data is the spectral coverage that they possess. Landsat 5 TM is a multispectral platform that acquires seven bands of electromagnetic energy from the visible, near infrared, mid infrared and the thermal infrared spectrum (Figure 5 and Table 1). It is the spectral coverage that gives the Landsat data the power to discriminate a wide variety of surface and atmospheric features and vegetation types that other systems are not capable of. Each of the seven spectral bands that Landsat 5 TM measures were specifically chosen for their ability to help scientists study a variety of conditions on Earth (Table 1).

<u>Band #</u>	<u>Bandwidth</u>	<u>Use</u>
Band 1 (blue)	0.45-0.52 μm	Penetrates water bodies, supports analysis of land-use, soil, and vegetation characteristics.
Band 2 (green)	0.52-0.60 μm	Reacts to the green reflectance of healthy vegetation.
Band 3 (red)	0.63-0.69 μm	Very useful for discrimination of vegetation. Also useful for determining soil and geologic boundaries.
Band 4 (near-infrared)	0.76-0.90 μm	Very responsive to amount of vegetation biomass. Placed above 0.75 μm to increase accuracy of vegetation studies. Useful for crop identification.
Band 5 (mid-infrared)	1.55-1.75 μm	Sensitive to turgidity/amount of water in plants. Can discriminate among clouds, snow and ice.
Band 6 (thermal infrared)	10.4-12.5 μm	Measures infrared radiant energy emitted from surfaces.
Band 7 (mid-infrared)	2.08-2.35 μm	Able to discriminate geologic rock formations.

Table 1 Landsat 5 TM Bands and Uses, adapted from Jensen (2007)

Because the temporal resolution of the Landsat 5 TM is every 16 days since its launch in 1984 it is an excellent platform for detecting changes on the Earth's surface. Perhaps the greatest benefit to the Landsat data is that they are now provided free of charge through the USGS. This makes it available to a worldwide market and will only promote further use and development of remote sensing as a tool to power informed decision making.

1.7.2 Data Exploration

Data exploration is an essential step in the process for digital image analysis. Data exploration employs numerous techniques that can be done during the pre or post processing of image data. These techniques allow the remote sensing analyst to better understand the quality of the data being used, and select individual bands and derivative bands that best separate designated classes for image classification (Jensen, 2007).

Visual interpretation, masking, spectral pattern analysis, unsupervised classification, and

spectral transformations (e.g. derivative bands; principal components analysis, vegetation indices) (Jensen, 2007) are all examples of data exploration techniques. Derivative bands combine ratios to further enhance the differences between the raw data bands. The creation of derivative bands gives more power to discriminate land cover and vegetation types in a supervised classification.

1.7.3 Image Classification

Image classification can be defined as assigning pixels from remotely sensed data to classes. As Jensen (2007) notes, this is a process where, ‘data are transformed into information.’ There are two widely accepted methods for doing this; unsupervised and supervised classification. Unsupervised classification is a technique whereby the computer statistically clusters image pixels with similar spectral properties together. It is a useful tool that allows the remote sensing analyst to begin to see and understand spectral patterns within an area of interest before visiting the site. In the case of an unsupervised classification, the number of clusters is determined by the analyst and the computer groups the spectrally similar pixels in to the spectral ‘bucket’ it determines is the best fit. It is then up to the analyst to identify and label the clusters based on their own interpretation of ground conditions.

Supervised classification of image data is designed to mimic the concepts of photo interpretation (Congalton, 2011). Supervised image classification uses one’s own knowledge of a given area and/or ancillary reference data to ‘train’ the computer to differentiate between different classes (e.g. Urban, water, forest, wetland) using a signature field. Thematic maps can be derived from either technique. For this study, the final thematic map is a product of a supervised classification.

1.7.4 The Visible Infrared Intelligent Spectrometer (VIRIS)

The VIRIS is a passive hyperspectral remote sensing instrument that utilizes either a natural or an artificial illumination source, measuring percent reflectance in the wavelength range of 350-2500 nm in 600 discrete spectral bands. The VIRIS provides spectral coverage from 400-2500 nm with 2-nanometer spectral resolution from 400-1100 nm and 4-nanometer resolution from 1100-2500 nm. The high spectral resolution of the VIRIS makes it useful for detecting variations in the anatomy and physiology of vegetation. A total of 81 different reflectance, derivative and wavelength parameters can be extracted from VIRIS data. Three of the most often utilized parameters that are used are the Red Edge Inflection Point (REIP) the Normalized Difference Vegetation Index and the 5/4 ratio. The two indices of interest to this project are the Red Edge Inflection Point (REIP) which is an indicator of foliar chlorophyll concentration, a measure of plant health, and the TM 5/4 ratio which is an indicator of foliar moisture content. The REIP's position is determined by calculating the first derivative of the spectral curve data in the wavelength range of 680-750 (Rock et al., 1986; Vogelmann et al., 1993). Generally, values below 710nm are considered unhealthy. The TM 5/4 ratio is calculated by taking the average reflectance in the Thematic Mapper band 5 and dividing it by the average reflectance in TM band 4. (Hunt et al., 1987). TM 5/4 values below 0.55 are an indication of adequate water within a vegetation sample, values between 0.55 and 0.60 indicate the beginnings of water stress and values above 0.60 are indication of higher degrees of water stress ((Forestwatch, 2011)).

Reflectance curves derived from VIRIS scans are diagnostic tools that allow

scientists to determine a wide range of conditions with regards to the health and cellular structure of vegetation (Figure 6). It is thought that by selecting Landsat data from dates within the dry season of the study area that the more moist and healthy reflective qualities of mangrove will be accentuated when compared to surrounding and potentially drier non-mangrove vegetation such as forest.

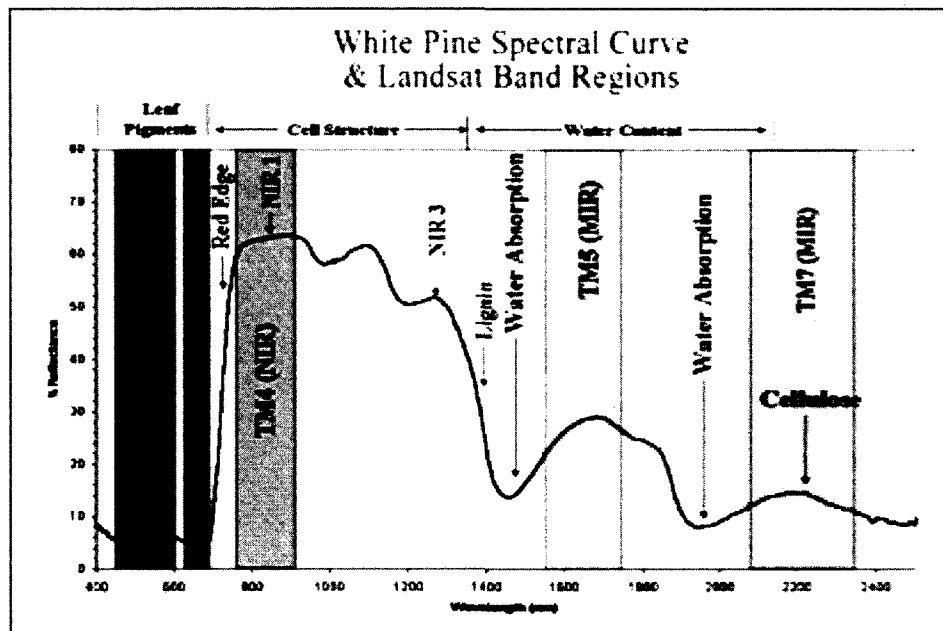


Figure 6 Spectral Curve of White Pine and Landsat Band Regions (Forestwatch, 2011)

1.7.5 Leaf Anatomical/Spectral Characteristics

Plant anatomy and leaf cell structure varies between species and the environmental conditions in which it grows. Studies have shown that these differences can be detected by looking into the reflectance curves produced by field and laboratory spectrometers (e.g. the VIRIS) allowing each species to be spectrally characterized (Gates et al., 1965; Rock et al., 1988; Rock et al., 1986; Rock et al., 1994).

The advantage of combining ground based hyperspectral sensors to characterize the dominant mangroves of the Mexican Caribbean is that it will provide important

information for identifying which bands will of the Landsat 5 TM will best discriminate mangrove. Understanding what is being seen in satellite data and linking it to what is happening on the ground is the key to remote sensing. Studies of leaf anatomy and the spectral characteristics of mangroves will be essential to making these linkages.

Past studies have been able to link cellular structure to not only reflectance values (Gates et al., 1965) but also to the overall health of forests (Rock et al., 1986). Since leaf cell structure varies depending on the species and the environmental conditions where the plant is found, it is quite probable that the reflectance of mangrove species will vary from that of surrounding forest vegetation.

1.7.6 Remote Sensing and Mangroves

There are clear advantages to using remote sensing techniques to study mangroves. Remote sensing provides the potential for a fast and efficient means to monitor mangrove forests both on a spatial and temporal scale. Tropical conditions of high heat and humidity combined with the difficulty of moving through mangrove habitat makes remote sensing an ideal alternative to traditional field based mapping methods. In addition, the low species diversity of mangrove in areas like the Yucatan Peninsula and the fact that they occupy an ecological zone distinct from other forest vegetation make them desirable a habitat to test using such technology. However, there are also disadvantages with working in the tropical environment with satellite imagery, particularly the fact that there is an increased chance of cloud cover that can obscure the area one is trying to study. This factor can significantly reduce the quality and availability of data for a given area.

Many studies over the years have used remote sensing to monitor mangrove forests (Blasco et al., 1998; Heumann, 2011). The most common methods have used satellite imagery to classify the area of interest and then field studies and aerial imagery to verify (Heumann, 2011; Rasolofoharinoro et al., 1998). Recently, more studies have begun to incorporate higher airborne hyperspectral and radar sensors to increase the definition and accuracy of the study (Held et al., 2003; Heumann, 2011; Pasqualini et al., 1999). The use of airborne sensor systems can guarantee cloud free imagery. The higher spectral resolution from air borne hyperspectral sensors allows for the potential differentiation of mangrove species that Landsat data cannot obtain (Held et al., 2003). Few, if any, studies have incorporated both a ground based spectrometer and an airborne/satellite sensor to characterize or monitor the mangrove habitat.

1.8 Accuracy Assessment

Accuracy assessment is a vital, and often ignored, procedure in map making. Many people assume, incorrectly, that all maps are right (Congalton, 2011). Error can enter the process of mapmaking at many points along the way. Accuracy assessment can help identify and eliminate sources of error so that what is represented on a map is indeed what it claims to be (Congalton, 2011). In general, anyone using accuracy assessment is using it for the following reasons; to assess how good a job they have done in producing a map; to make comparisons between different methods (e.g. supervised classification vs. unsupervised classification) to see if one gives better results than another; to understand the errors present in their work, where they come from and how they might be eliminated; to determine the accuracy of layers as the information produced as they will

potentially drive important decisions to be made; because they are required to by contract (Congalton, 2011; Congalton et al., 1998; Gopal and Woodcock, 1994)

As one goes through the process of making a map error accumulates and compounds on itself. Image acquisition, processing, analysis, conversion and sampling can all contribute to degrees of error. While all factors cannot realistically be controlled, accuracy assessment allows GIS technicians and remote sensing specialists to identify where error has occurred so that it can be corrected and taken out of the daisy chain.

Sample design is a critical part of the process for accuracy assessment. It is essential to determine how many samples will be taken, how sample sites will be selected, what the minimum mapping unit will be and how samples will be collected.

Once ground reference data has been collected, it is then compared with the classified data on the thematic map. The most commonly used technique to do this is an error matrix (Congalton, 1991) (Figure 7). An error matrix provides three important measures of thematic map accuracy; overall accuracy, producer's accuracy and user's accuracy. The overall accuracy is computed by dividing the total number of correctly classified pixels (the main diagonal) by the total number of pixels. The resulting percentage represents the overall accuracy of the map. The producer's accuracy, which is a measure of omission error, is calculated by dividing the number of correctly classified pixels of reference data (column data), by the total number of pixels for that category. The results allow one to know how well a particular area has been classified. The user's accuracy is a measure of commission error and is calculated by dividing the number of correct pixels in a category by the total number of pixels that were classified for that category (row

data). User's accuracy is a measure of whether or not a classified pixel is actually what it says it is on the ground.

Classified Data	Reference Data				
		Urban	Wetland	Forest	Water
Urban	65	0	10	0	75
Wetland	0	90	0	0	90
Forest	0	9	40	0	49
Water	0	0	0	121	121
Column Total	65	99	50	121	335

Overall Accuracy $316/335 = 94\%$

Producer's Accuracy

Urban $65/65 = 100\%$

Wetland $90/99 = 91\%$

Forest $40/50 = 80\%$

Water $121/121 = 100\%$

User's Accuracy

Urban $65/75 = 87\%$

Wetland $90/90 = 100\%$

Forest $40/49 = 82\%$

Water $121/121 = 100\%$

Figure 7 Example of Error Matrix, derived from Jensen (2007)

1.9 Hypotheses

H1: Detailed hyperspectral analysis (i.e. VIRIS data) of foliage of mangrove leaves will allow species of mangroves to be spectrally characterized, based on diagnostic reflectance properties.

H2: The diagnostic reflectance properties will be related to differences in leaf anatomical properties.

H3: Analysis of Landsat Thematic Mapper multispectral imagery, combined with the VIRIS data, will allow dominant mangrove types to be detected and mapped.

H4: Use of this model will allow the detection of mangrove in areas where it was previously not known to exist.

1.10 Goals

The goals for this project are as follows:

- Map the distribution of mangroves in the area surrounding the municipality of Tulum, Mexico;
- Extend the areas of known mangrove beyond previously mapped extent;
- Positively influence the conservation of mangroves in the Tulum Municipal area through the dissemination of this map.

1.11 Objectives

The objectives of this research effort are as follows:

- Conduct field research;
- Conduct leaf analysis using GER 2600 (VIRIS);
- Prepare and analyze leaf thin sections of collected mangrove;

- Select and analyze Landsat 5 imagery;
- Create a predictive model using Digital Image Processing and GIS techniques;
- Conduct in field accuracy assessment of predictive model;
- Create GIS geodatabase, Google Earth compatible .kmz files and educational material for Centro Ecologico Akumal, Municipal Government and other interested parties.

2.0 Methods and Materials

2.1 Overview

This project called for the creation of a spatially and thematically accurate vector map of mangrove communities in the area surrounding the Municipality of Tulum, Quintana Roo, Mexico. In order to achieve this, a process was undertaken to select, analyze and classify Landsat 5 TM data using field reference data and leaf spectral characteristics collected in the field. Image preprocessing, analysis and classification was done using ERDAS Imagine v.10 (ERDAS, 2010)* and ArcMap v.10 (ESRI, 2010)*. Accuracy assessment was conducted by field visits using the same classification scheme as the supervised classification. Additional field data were observed and collected at each site to assess model results and provide anecdotal data to facilitate further analysis.

2.2 Selection of Landsat Data

Landsat 5 TM data were provided by the United States Geological Survey (USGS) Global Visualization Viewer (GloVis) website (www.glovis.usgs.gov). The Municipality of Tulum falls entirely within images associated with Landsat 5 TM Path 19 Row 46. The Landsat 5 TM data measures reflectance in 6 bands (bands 1,2,3,4,5,7) at a pixel resolution of 30m, and thermal (band 6) at a pixel resolution of 120m (Jensen, 2007).

Landsat TM data were selected based on the following three criteria to maximize model accuracy; that they contained minimal cloud cover; they were acquired during the annual dry season from December through April (Beddows, 2004) to highlight differences between drier forest vegetation types and more moisture rich mangrove

* Specific brand name is cited for clarity and does not imply endorsement.

habitats; that they be as close temporally as possible to dates of the field studies being conducted in March, 2010 and June, 2011.

Data received from the USGS GloVis site for Path 19 Row 46 were projected using WGS84 UTM Zone 16Q and were provided with Level 1T corrections (GloVis, 2011) with an accuracy of ± 0.5 pixels (15 meters) (Congalton et al., 1998). Based on this accuracy, the minimum mapping unit (MMU) was set to 3x3 pixels (1 pixel = 30m², total MMU area $\geq 8,100\text{m}^2$) in order to reduce positional error for classification and accuracy assessment. Neither geometric nor radiometric corrections were needed for the data because only one image would be used to generate the classification.

Landsat TM5 data acquired on February 9th, 2000 came closest to meeting all three criteria. Additionally, Landsat data from April 17th, 1984 were downloaded to provide a basis for comparison and to provide evidence of change detection for the 16-year period between the data sets.

2.2.1 Image Stacking

The seven raw bands of Landsat 5 TM data were stacked in ERDAS Imagine V.10 following the manufacturers specifications (ERDAS, 2010). Particular attention was paid to each bands individual histogram (Salvador and San-Miguel-Ayanz, 2003). The mean, standard deviation, shape, and maximum and minimum DN values were recorded for each band.

2.3 Image Exploration

The 1984 image and the 2000 image were analyzed and compared visually. Using simple combinations of the seven spectral bands, basic image exploration was performed. In particular, the 4,3,2 False Color Composite (FCC) and the 7,5,3 and 7,5,2 combinations were observed with interesting results. The 4,3,2 FCC gives a good indication of the health of vegetation. Band 4, which is near infrared, is the key to seeing where healthy vegetation is or is not. This was telling in the comparison of the 1984 image to the 2000 image. Areas that indicate healthy vegetation in the 2000 image did not appear to be healthy in the 1984 image. When examining the 7,5,3 band combination, areas that are known to be mangrove appeared to stand out from areas of non-mangrove vegetation. These combinations, particularly the 7,5,3 make sense as band seven accentuates moisture content in vegetation and soils, which points towards mangrove leaf succulence and the areas of inundation that mangrove prefer. Band 5 indicates moisture content in vegetation that, during the dry season, should be accentuated between the drier forest vegetation and the more moist and succulent vegetation associated with mangroves. Similarly the distinction of chlorophyll present within vegetation that band 3 demonstrates should also be accentuated due to the distinct wet and dry conditions that mangrove and non-mangrove vegetation occupy.

Further observation revealed that areas of known sawgrass (*Cladium jamaicense*) appeared to have very different spectral reflectance properties in the image when compared to areas of known mangrove or forest. The ability to discriminate *C. jamaicense* from mangrove and forest would be an unexpected outcome of this project. If supported by accuracy assessment, this would begin to help managers, especially in the

SKBR better understand the distribution of vegetation types within the reserve. What is interesting is that although mangrove and sawgrass share similar habitats and conditions, their spectral reflectance characteristics are distinct. Based on the visual observations made in this phase, *C. jamaicense* was added as a non-mangrove class for the supervised classification.

A last area that was of interest in the initial stages of image exploration were cenotes known to have mangrove and also the features (lakes and depressions) associated with the Holbox fracture (Beddows, 2004). Once again the 7,5,3 band combination was able to clearly show larger cenotes that contain mangrove as distinct from the surrounding forest vegetation. The Holbox fracture features appear to contain areas of mangrove. These observations helped to determine the overall scope of the project area.

2.3.1 Unsupervised Classification

Unsupervised classification was used in order to establish how well certain classes would separate and in turn see if there was any confusion between classes. This was possible through the use of ancillary data and sound knowledge of the Tulum Municipal area through my previous work there (Meacham, 2007). Unsupervised classification was performed using ERDAS Imagine V.10 according to the manufacturers specifications (ERDAS, 2010). Differing cluster sizes were assigned to the TM data to ascertain similarities and differences in the spectral reflectance of different landcover types within the data (e.g. urban, water, beach, mangrove, forest, sawgrass, agriculture). The more clusters that are assigned, the more subtle variations can be teased out of the image. The advantage to unsupervised classification is the fact that it incorporates all the spectral variability within an image (Congalton, 2011). The resulting 10 class

unsupervised classification (Figure 8) helped demonstrate that the main classes of mangrove, sawgrass and forest were spectrally different. It also showed that urban, beach and overwash mangrove areas had the same spectral characteristics. Due to the similarities of these areas, and the difficulty in separating areas of overwash mangrove by masking, it was decided to eliminate areas of overwash from the study. This information was an important step in confirming the feasibility of a supervised classification and in helping determine what areas could be further masked out from the subset image.

10 Class Unsupervised Classification demonstrating Confusion between Urban, Overwash Mangrove and Beach areas

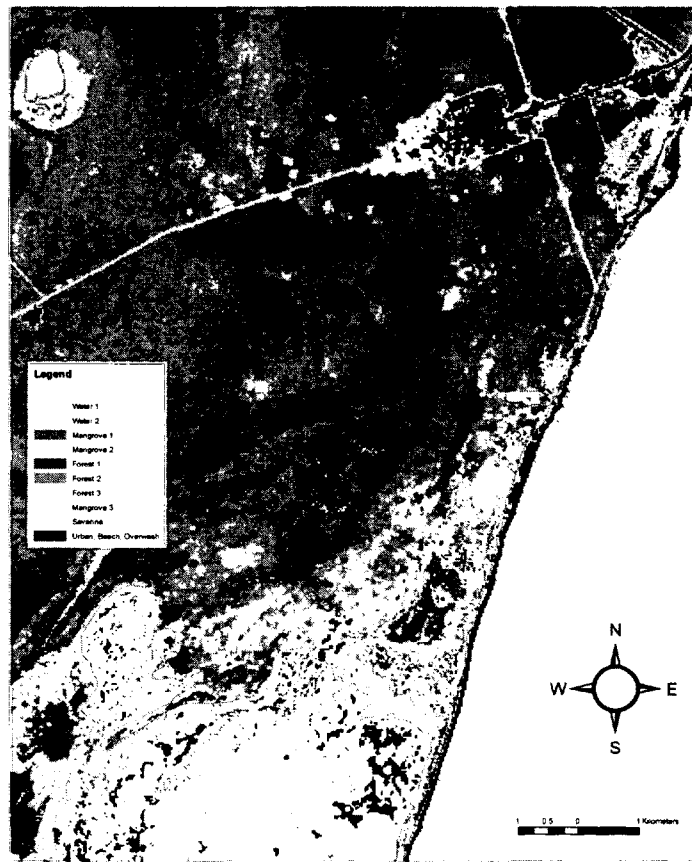


Figure 8 Detail of 10 Class Unsupervised Classification demonstrating Confusion with Urban, Overwash Mangrove and Beach Areas

2.3.2 Derivative Bands

Derivative bands were created after analysis of leaf spectral characterizations, leaf anatomical analysis and a literature review. As a result, the 5/4 ratio, NDVI, Principal Components Analysis and Tasseled Cap Transformation were created (Crist and Cicone, 1984; Green et al., 1998; Heumann, 2011; Jensen, 2007; Vogelmann et al., 1993). Six new bands (5/4, PCA 1, NDVI, Tasseled Cap 1,2,3) were created following the manufacturers specifications (ERDAS, 2010) and added to the original seven bands of the Landsat 5 TM data using image stack in ERDAS Imagine V. 10. Derivative bands were restretched to match the dynamic range of the original TM data.

2.4 Image Preprocessing

2.4.1 Image Subsetting

Because the study was focused only on the area surrounding the Municipality of Tulum, and because mangrove communities were not expected to be found across the entire extent of the image, the image was subset. The subset area was defined by my own knowledge of the location of mangrove habitats (e.g. inland cenotes and lakes), existing information on the extent of mangroves (CONABIO, 2009), and the boundaries of the Municipality of Tulum and of the Sian Ka'an Biosphere Reserve where large homogeneous areas of mangrove exist (Mazzotti et al., 2005). Large inland depression features that form part of the Holbox Fracture (Lineament) Zone (Beddows, 2004) were also included within the subset and represent the northwestern limit of the subset image.

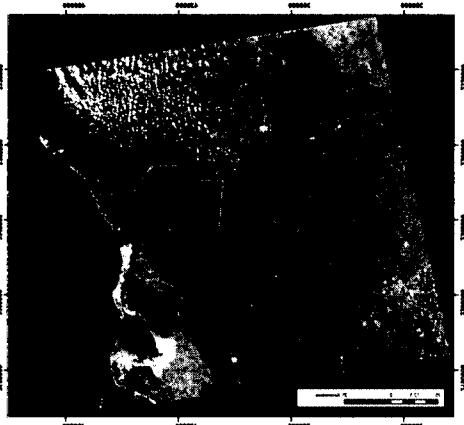
Based on this knowledge and using ArcMap v.10 a shapefile was created to define the subset area (Figure 9). A *Shapefile* is a digital storage format for storing geometric location and associated attribute information. A process was developed so that a

shapefile could be imported to ERDAS Imagine and converted to an AOI file so that the image could be subset. Thus, a preliminary subset image was created to allow the supervised classification to focus on the true areas of interest.

2.4.2 Image Masking

Image masking took place after analysis of the unsupervised classification and spectral pattern analysis results (Figure 9). Masking was performed in order to decrease the spectral variation of the image so that 'mangrove' and 'not mangrove' classes could be the focus of the classification. Masking eliminated areas on the image that could have caused confusion in the final supervised classification (e.g. water, urban, agriculture, clouds, cloud shadow). Masking was done in the same way as subsetting by creating polygons in ArcMap V.10 and converting them to AOI's in ERDAS Imagine v.10.

Figure 9 Processes of Subsetting and Masking the Image



Full Image Tile (FCC 4,3,2)

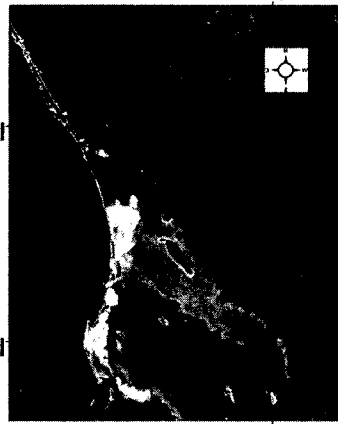


Image centered on study area (FCC 4,3,2)

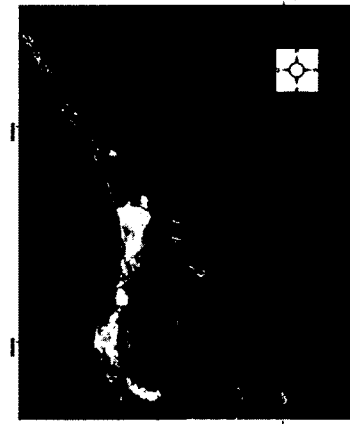
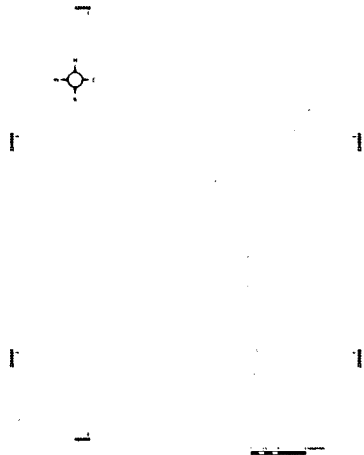


Image after subset (FCC 4,3,2)



Clipping Path Created in ArcMap

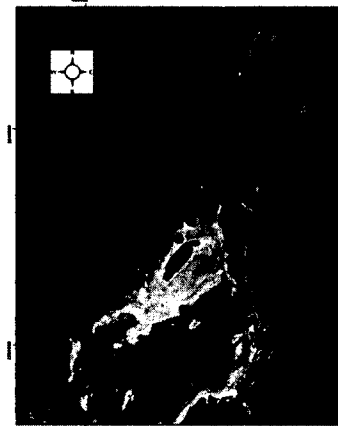


Image after application of clipping path (FCC 4,3,2)

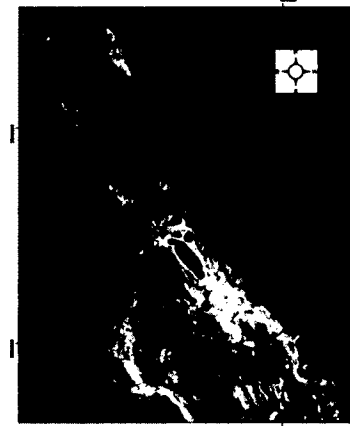


Image after application of clipping path (FCC 7,5,3)

2.5 Classification Scheme

As the purpose of this study was to discriminate areas of mangrove from non-mangrove vegetation, a simple classification scheme was developed (Congalton, 1991; Congalton et al., 1998) (Table 2). This classification scheme is an important step required for a supervised classification and later for the determination of accuracy assessment. In this step a set of labels and rules for two, mutually exclusive classes were created (e.g., mangrove and not-mangrove) with the 'not-mangrove' class having a hierarchical system that included both 'forest' and 'sawgrass' habitat types.

Mangrove	Not-mangrove
>65% mangrove present	>65% forest present
	>65% sawgrass present

Table 2 Classification scheme for Reference Data Collection

All other habitat types that occurred within the study area but that were not captured by these classification categories (e.g. beach, water, urban, agriculture) were masked out of the final subset image in order to reduce error in the computer-generated classification. This process is explained in more detail below.

2.6 Reference Data Collection and Areas of Interest

Field collected reference data are required to train the computer for the supervised classification. In this step, data are collected in the field from various sites documenting vegetation classes (i.e., mangrove, non-mangrove, forest, and sawgrass) to provide the basis for subsequent model preparation. Data were collected from Solimon Bay in March, 2010 and from previous field excursions and aerial flights related to the work I have conducted in the area around Tulum (Meacham, 2007). In the majority of cases, a

GPS unit was used to record the position or track of areas that were visited. However, dead reckoning was used for a few sites based where GPS tracking was not possible (i.e., some flight paths). All GPS data collected were exported from Trimble SoloField® software in the RECON unit as shapefiles and integrated into the geodatabase file for the project. All reference data were recorded in WGS84 UTM Zone 16Q. Shapefiles then could be superimposed with the Landsat 5 TM data to help aid in establishing the areas of interest (AOI's) for training the supervised classification (Table 3).

	Class Name	Mangrove type	Area
1	Forest 1		West of Akumal
2	Forest 2		West of Xel Ha
3	Forest 3		West of Solimon Bay
4	Forest 4		Tulum on Coba Highway
5	Forest 5		Ejido Jose Maria Pino Suarez
6	Forest 6		South of Lake Chumkopo
7	Forest 7		Sian Ka'an Biosphere
8	Forest 8		Sian Ka'an Biosphere
9	Forest 9		Sian Ka'an Biosphere
10	Forest 10		Sian Ka'an Biosphere
11	Mangrove 1	Dwarf	Solimon Bay
12	Mangrove 2	Fringe	Tankah
13	Mangrove 3	Dwarf	Ejido Jose Maria Pino Suarez
14	Mangrove 4	Fringe	Ejido Jose Maria Pino Suarez
15	Mangrove 5	Dwarf	Ejido Jose Maria Pino Suarez
16	Mangrove 6	Dwarf	Sian Ka'an Biosphere
17	Mangrove 7	Dwarf	Sian Ka'an Biosphere
18	Mangrove 8	Fringe	Ejido Jose Maria Pino Suarez
19	Mangrove 9	Fringe	Ejido Jose Maria Pino Suarez
20	Mangrove 10	Fringe	Ejido Jose Maria Pino Suarez
21	Sawgrass 1		Sian Ka'an Biosphere
22	Sawgrass 2		Sian Ka'an Biosphere
23	Sawgrass 3		Sian Ka'an Biosphere
24	Sawgrass 4		Sian Ka'an Biosphere

Table 3 Areas of Interest for Training the Computer

2.7 Supervised Classification

The supervised classification of the data for this project was done using ERDAS Imagine V.10 software and reference data collected in March, 2010 and through previous experience in the field (Meacham, 2007). Reference data were used to create areas of

interest (AOI's) using the 'seed' tool within ERDAS Imagine V.10. A signature file was created to include all vegetation classes (e.g. mangrove, forest, sawgrass). In most cases, a minimum of 10 training areas were established for each vegetation class with the exception of 'sawgrass' where only four training areas were created. This was due to a lack of sufficient areas where sawgrass could be certain to exist. Therefore, sawgrass and forest were collapsed into one class of 'not-mangrove'. The supervised classification for this project used the minimum distance algorithm. This classification method works by calculating the distance of one pixel to other pixels and deciding on the class based on the smallest distance.

2.8 Accuracy Assessment

2.8.1 Reference Data Collection and Classification Scheme

Accuracy assessment for this study was conducted from June 5th-13th, 2011 by means of field visits that compared thematic map data with reference data collected with a Trimble GPS unit. All reference data were recorded in WGS84 UTM Zone 16Q. Sampling for thematic accuracy was performed using a Trimble NOMAD® GPS unit¹. The NOMAD® incorporates an integrated high-sensitivity 12-channel SiRF Star III GPS/SBAS2 receiver^{**} and antenna with accuracy of 2-5 meters (Trimble, 2011). Additionally, the NOMAD® has the capability of recording offset points that allowed the team to extend a point into an area where the terrain prohibited entry. Any time this was done, line of site into the area of extension was maintained, a compass bearing was taken and a distance was estimated.

^{1,**} Specific brand name is cited for clarity and does not imply endorsement.

A field form was created using Tripod Data Systems SoloField® software running on the NOMAD® GPS unit (Table 4). The exact same set of labels and rules for classification that were used for the supervised classification were used again for accuracy assessment. Percent coverage was estimated visually for each point and not measured. When possible as much of the field form was completed at each sample site.

<ul style="list-style-type: none"> • Accuracy <ul style="list-style-type: none"> ○ > 65% Mangrove ○ >65% Not Mangrove <ul style="list-style-type: none"> ▪ >65% Forest ▪ >65% Sawgrass 	<ul style="list-style-type: none"> • Mangrove characterization <ul style="list-style-type: none"> ○ Dwarf ○ Fringing
<ul style="list-style-type: none"> • Salinity at surface 	<ul style="list-style-type: none"> • Salinity at 30cm
<ul style="list-style-type: none"> • Canopy closure 	<ul style="list-style-type: none"> • Road
<ul style="list-style-type: none"> • Trail 	<ul style="list-style-type: none"> • Generic Point
<ul style="list-style-type: none"> • Generic Polygon 	<ul style="list-style-type: none"> • Generic Line
<ul style="list-style-type: none"> • Soil type 	<ul style="list-style-type: none"> • Comment

Table 4 Accuracy Assessment Field Form

For each vegetation class, at least 30 sample points were recorded. Sample sites were chosen from the thematic map that met the minimum mapping unit. Due to pressures of time, terrain, weather and access to sites, sampling sites were not chosen randomly; rather they were chosen on a daily basis according to the four aforementioned variables. Sampling sites were distributed throughout the study area in order to minimize error associated with spatial autocorrelation and to allow sampling of as many diverse sites as was possible. In order to increase accuracy and reduce error associated with spatial autocorrelation (Congalton, 1988; Congalton, 1991), rules for sampling stipulated that each sample site needed to be a minimum distance of 300 meters from other samples

of the same class type and from training areas of the same class type. To ensure positional accuracy, each point collected was required to have at least 200 averaged points.

A Nikon D80 digital SLR camera (18-128mm lens) and a GoPro Hi-Definition digital video camera were used to record the field teams observations. Salinity of surface water was measured directly in the field using an Orion 5-Star Plus multimeter with DuraProbe conductivity cell calibrated daily. Soil pore water was sampled using the sipper method (Portnoy and Valiela, 1997) which extracts water trapped in pore spaces using a 1mm diameter stainless steel tube fitted with a 60cc plastic syringe. Pore water was sampled at two depths within the rhizosphere (20cm and 40cm) at each site to document salinity, redox potential, sulfide concentration and pH. Pore water salinity was determined in the field as stated above, as was redox potential using the Orion 5-Star fitted with a platinum electrode. All data collected were exported as shapefiles from the NOMAD® using SoloField®.

A standard error matrix was created to perform quantitative accuracy assessment using the classification map and the reference data collected in the field (Congalton, 1991; Story and Congalton, 1986). Comparison of reference data to thematic data in ArcMap V.10 allowed the error matrix to be populated with information so that analysis could take place.

2.9 Spectral Characterization and Anatomical Study of Mangrove Leaf Samples

Leaf samples collected within the Solimon Bay study area were acquired to characterize the anatomical and spectral reflectance properties of the dominant four

species of mangrove characterizing the area. The resulting data were used to assist in selection and justification of Landsat TM band selection for the supervised classification.

2.9.1 Study Area for Foliar Collection

In March 2010 an area was identified for mangrove leaf sample collection at Solimon Bay, Mexico, a secluded bay with an associated mangrove habitat located along the coast and within the Municipality of Tulum (Figure 10).

**Municipality of Tulum, Quintana Roo Mexico
and Solimon Bay Study Site**

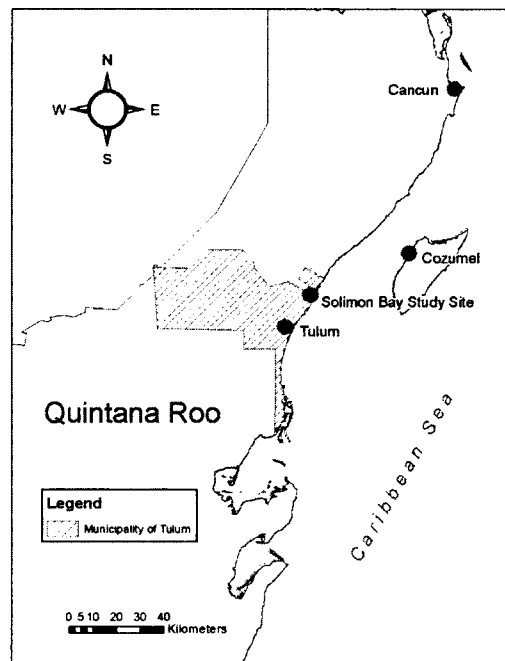


Figure 10 Municipality of Tulum including the Town of Tulum and the Solimon Bay Study Site

Solimon Bay was chosen as a study site because it was known to contain the four mangrove species (see below) and associated habitat types (defined below) that were of interest to this project, and it occurs within the lands made accessible to us through project partners Centro Ecologico Akumal (CEA).

Solimón Bay measures 1,360 meters along its mouth and is protected by a fringing barrier reef. The coastline within the study area is oriented along a northeast/southeast axis, including barrier beach, dune, mixed littoral forest and several mangrove habitats. The mangrove is dominated by *R. mangle*, and includes patches of *L. racemosa*, *A. germinans*, and *C. erectus*. These species assemblages represent two major habitat classification; Fringe and Dwarf mangrove (Lugo and Snedaker, 1974). While a few stands of ‘fringing’ mangrove (5-8 meters height) are present along the coastline, the majority of the Solimón Bay area is filled with densely packed ‘dwarf’ mangrove (1-2 meters height). Both ‘fringing’ and ‘dwarf’ habitats are dominated by *R. mangle*. On the western limit of Solimón Bay, patches of sawgrass (*Cladium jamaicense*) mix with mangrove. Beyond the mangrove area to the northwest begins low scrub forest that transitions into the semi deciduous tropical forest dominated by such species as Gum Tree (*Manilkara zapota*), Gumbo Limbo (*Bursura simaruba*), Poisonwood (*Metopium brownei*) and Fig (*Ficus maxima*) that typify the Yucatan Peninsula (Lee, 1996; Mazzotti et al., 2005) and are classified as ‘Not Mangrove’ in this study. Solimón Bay has been developed along the coastal strip with vacation homes built on the coastal dune between the beach and mangrove area.

Due to the difficulty of moving through the dense rhizophores (i.e. prop roots) of *R. mangle*, deep marles and knee-deep standing water, existing property lines (*mensuras*) that had been cut through the mangrove were used for access to the interior of the mangrove stand and served as transects along which samples were collected. *Mensuras* run parallel and perpendicular to the coastline, providing a relatively predictable pathway

through the site and are visible in imagery provided by Google Earth. The Solimon Bay area also serves as a reference site for classification, discussed in greater detail below.

2.9.2 Collection Methods for Leaf Samples

Leaf samples were collected every 50-100m along a *mensura* transect. At each sampling point, foliar samples (Figure 11) of each mangrove species present were collected with pruning shears, placed into a Ziploc bag with a wet paper towel to maintain high leaf moisture, then placed in a cooler with frozen blue ice for return to the base facilities (small microscopy lab and dorm room) for later analysis.

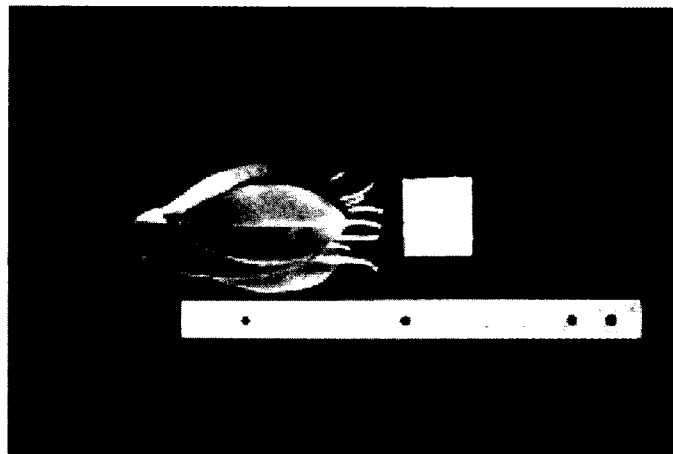


Figure 11 Foliar Sample Ready for Scan

Each sample bag was marked with a unique site number. Once returned to the base facility, each numbered bag was stored in a refrigerator until ready for analysis. Additionally, surface and porewater salinity samples were collected at each leaf collection site using a stainless steel ‘sipper’ and plastic syringe (Portnoy and Valiela, 1997). Porewater samples were obtained from an approximate depth of 30cm, corresponding with the average rooting depth of the species encountered (Moore, 2011). Salinity values were recorded in the field using a temperature corrected handheld

refractometer (VWR Scientific SW series [VWR item no. 12777-992])* . Foliar samples collected in this manner were used for both anatomical and spectral analysis.

In most cases, mangrove height and canopy closure were estimated and observations of soil type were noted (Table 5). Photographs and videos were taken for each site in order to supplement any observations recorded by our team. All of this information was recorded into a handheld Tripod Data Systems, Inc. RECON GPS unit* using SoloField® Software (TDSWay, 2007)* . SoloField® permits the creation of attribute menus that greatly speed up the process of data collection and later data organization. Moreover, each record is geo-referenced and can be exported from SoloField® as a shapefile so that it may be easily incorporated into a geographic information system (GIS) database.

Species:	Soil type (marle, bedrock, organic etc.)
Sample #:	Percent Canopy Closure
Type [dwarf, fringing etc. based on (Lugo and Snedaker, 1974)]	Salinity at Surface (ppt)
Mangrove Height (m)	Salinity Subsurface (ppt)
Flowering? (Y/N)	Sub surface Salinity Depth (cm)
Fruiting (Y/N)	Comments
Surface Water Depth (cm)	Camera Reference

Table 5 Data field form for Solimon Bay Study Site

A total of 30 foliar samples for both medial and distal leaves of *R. mangle* were processed. 11 samples of *L. racemosa* and five samples of *A. germinans* were also processed. There were no samples of *C. erectus* collected.

* Specific brand name is cited for clarity and does not imply endorsement.

2.9.3 Measuring Spectral Reflectance Properties of Leaf Samples

Foliar samples were processed at the field lab at the Centro Ecologico Akumal by separating the distal and medial leaves of the dominant *R. mangle*. Once prepared, samples, in optically-dense stacks of seven leaves, were then scanned in a standardized laboratory setting (Vogelmann et al., 1993) using the GER 2600 Field Spectrometer (VIRIS) (Figure 12) so that spectral reflectance properties could be recorded.



Figure 12 The VIRIS in use with leaf samples in the foreground

Each stack of seven leaves was scanned three times, rotating the stack 90 degrees between scans. Following scanning, a total of 81 spectral index values were then calculated using UNH software (Vogelmann et al., 1993). Only one of these indices was of interest to this project (the 5/4 ratio). The TM 5/4 ratio is an indicator of foliar moisture content. Other indices such as the Red Edge Inflection Point (REIP) were only used as an indicator of foliar chlorophyll concentration, a measure of plant health. It is important to note that Landsat TM bands are too broad to discriminate REIP values, thus REIP is not helpful for determining which band

combinations to use. Spectral reflectance curves were generated using UNH software (Vogelmann et al., 1993).

2.9.4 Mangrove Leaf Anatomy Analysis

This analysis was conducted to detect differences in the cellular structures and cellular arrangements of the three dominant mangrove species, *R. mangle*, *L. racemosa*, *A. germinans* found at the Solimon Bay Study site. The external morphology of the leaf samples was studied with a dissecting scope and the internal anatomy was studied with using a compound microscope. Hand cross-sections were taken from the mid-regions of the distal and medial leaves of samples from each mangrove species using a slicing motion with a razor blade and studied with a compound microscope. Multiple cross-sections were placed in a petri dish containing a small amount of water to prevent them from drying out. A 1:1 glycerin/water solution was then placed with a pipette on a clean slide and the best cross-sections were then transferred onto the slide and a covered with a coverslip. All of the samples were closely examined and the best cross-sections were further examined under higher magnification. These sections were photographed directly through the eyepiece of the compound microscope since no camera adapter was available at the time. In addition, small pieces of intact leaves were transferred to fixative FAA (formalin acetic acid and 70% EtOH), left for 24 hours and then transferred to 70% EtOH for storage and transport to UNH. Each of these pieces of leaves were then embedded in paraffin and thin sectioned using standard microtechnical procedures (Johansen, 1940). This procedure was repeated for all of the samples of each mangrove type. This part of the study was conducted by a UNH undergraduate, Ms. Natallia Leuchanka, as part of her IROP research program in Mexico (2010) and Belize (2011).

3.0 Results

3.1 Mangrove Leaf Anatomical Analysis

As noted above, the leaves of each of the three dominant mangrove species collected in Solimon Bay were analyzed for detailed cellular structure in order to develop insight into the spectral differences, if any, characterizing these species. Below is given a description of the cellular features of each species.

3.1.1 *Avicennia germinans* (Black mangrove)

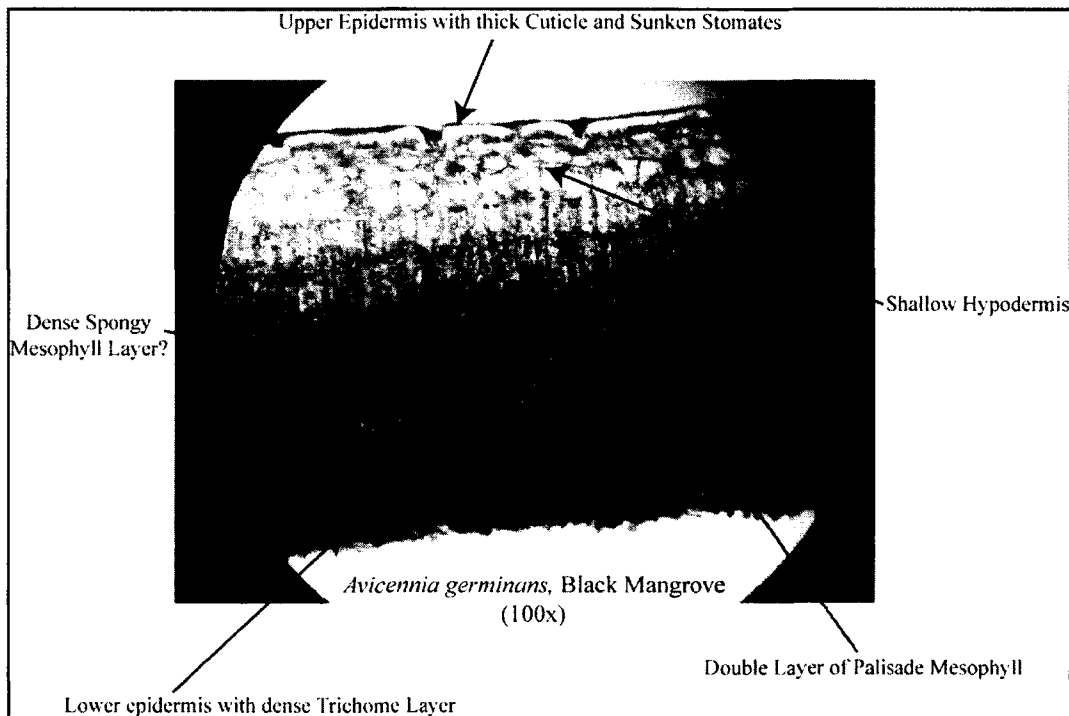


Figure 13 Thin Section of *A. germinans* Leaf (100x)

Figure 13 clearly illustrates the anatomy of a healthy leaf of *A. germinans*, the black mangrove. The leaf of *A. germinans* is dorsiventral. The thick cuticle and sunken stomates on the leaf's upper epidermis help restrict nonstomatal water loss (Tomlinson, 1986). Beneath the upper epidermis is a well-defined shallow hypodermis, these are the

'colorless', water storage cells that are common to many mangrove species (Tomlinson, 1986) and accounts for their thick, succulent leaves, as do the dense palisade and spongy mesophyll layers beneath the hypodermis. The mesophyll cells for this sample appear turgid and the outline of the individual cells is well defined and smooth. The color of the palisade mesophyll is much darker green than those of the other two species analyzed. The lower epidermis has a dense capitate trichome layer that is consistent with Tomlinson's (1986) description of *A. germinans*. This trichome layer covering the lower leaf surface is what gives it its characteristic gray/brown color.

3.1.2 *Rhizophora mangle* (Red mangrove)

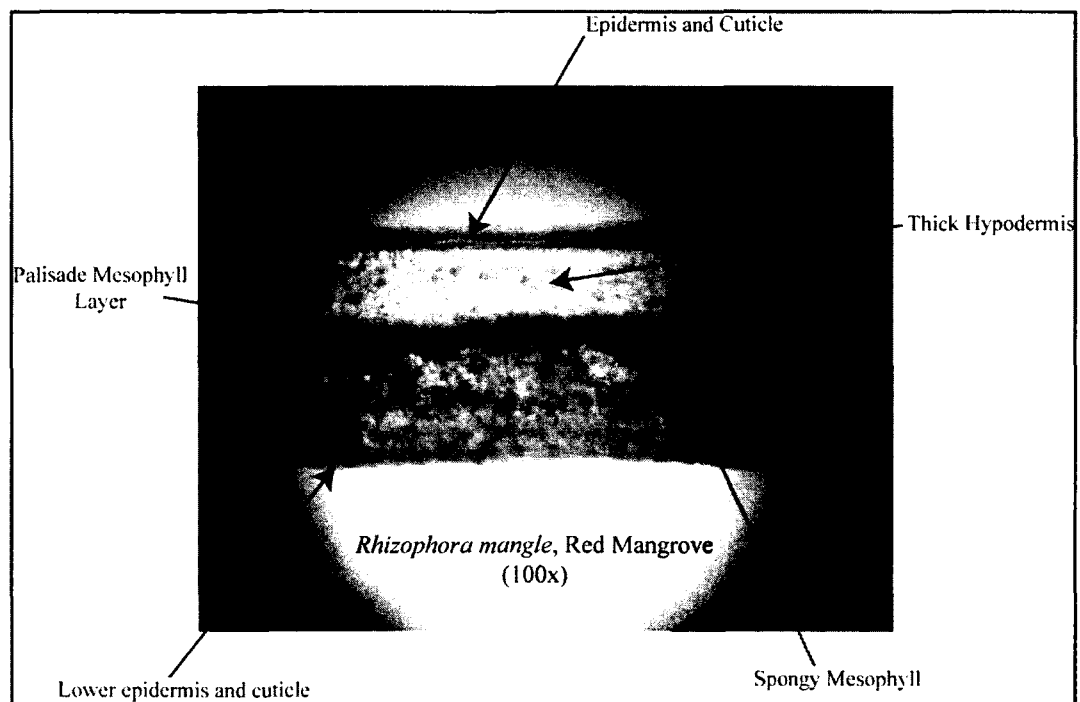


Figure 14 Thin Section of *R. mangle* leaf (100x)

Figure 14 shows a very well defined cross section of a *R. mangle* leaf. The leaf of *R. mangle* is dorsiventral and has five very well defined layers; the epidermis

and cuticle; the hypodermis; the palisade mesophyll; the spongy mesophyll; and the lower epidermis. The hypodermis and mesophyll cells for this sample appear turgid and the outline of the individual cells is well defined and smooth. The upper epidermis of the leaf has a thick cuticle with a very thick and well-defined hypodermis of 'colorless' water storage cells beneath it. The palisade mesophyll and spongy mesophyll layers are also thick and well defined. The dark green color of the palisade mesophyll layer is an indication of healthy quantities of leaves and a reflection of the leaf color. The thickness of these cell layers demonstrates why the leaf of *R. mangle* is so succulent. A closer examination of the hypodermis (Figure 15) of *R. mangle* shows cellular inclusions that could be salt or calcium oxalate. Present on the lower epidermis are trichomes and also sunken stomates.

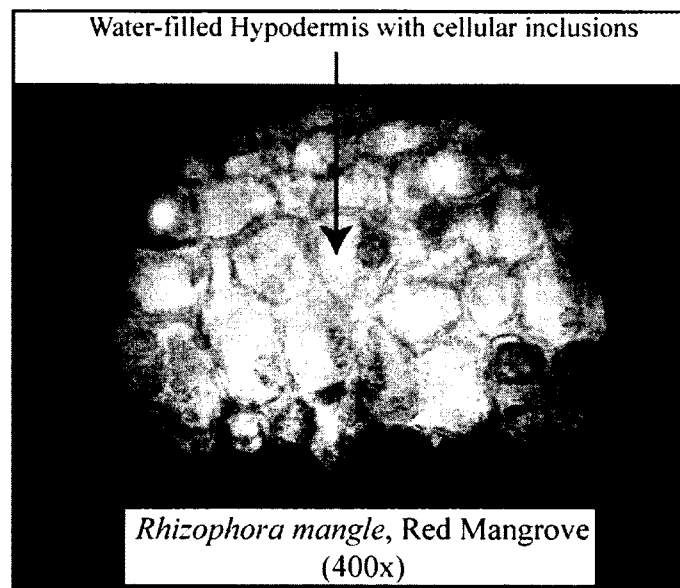


Figure 15 *R.mangle* water storage cells (400x)

3.1.3 Laguncularia racemosa (White mangrove)

The leaf of *L. racemosa* is isolateral with the 'colorless' water storage tissue occupying the center of the leaf (Figure 16). While there is good separation between each of the layers, the individual cell structure observed in Figure 16 is not as well defined as in the other two species. The top and the bottom of the leaf have thick, well-defined mesophyll layers. The fact that the green upper palisade mesophyll layer is unobstructed by the presence of water storage cells should influence the reflectance in TM Band 3. The water storage cells are loosely packed and not well organized. Non-sunken stomates are found on both the upper and lower surfaces of the leaf. Of the three cross sections examined, the sample of the *L. racemosa* is distinctly different from those of *A. germinans* and *R. mangle*, due to the isolateral structure of the leaf and ill defined cell shapes. Because of this difference, it would be logical to hypothesize that the reflectance characteristics of *L. racemosa* will be more different from than similar to the other two mangrove species.

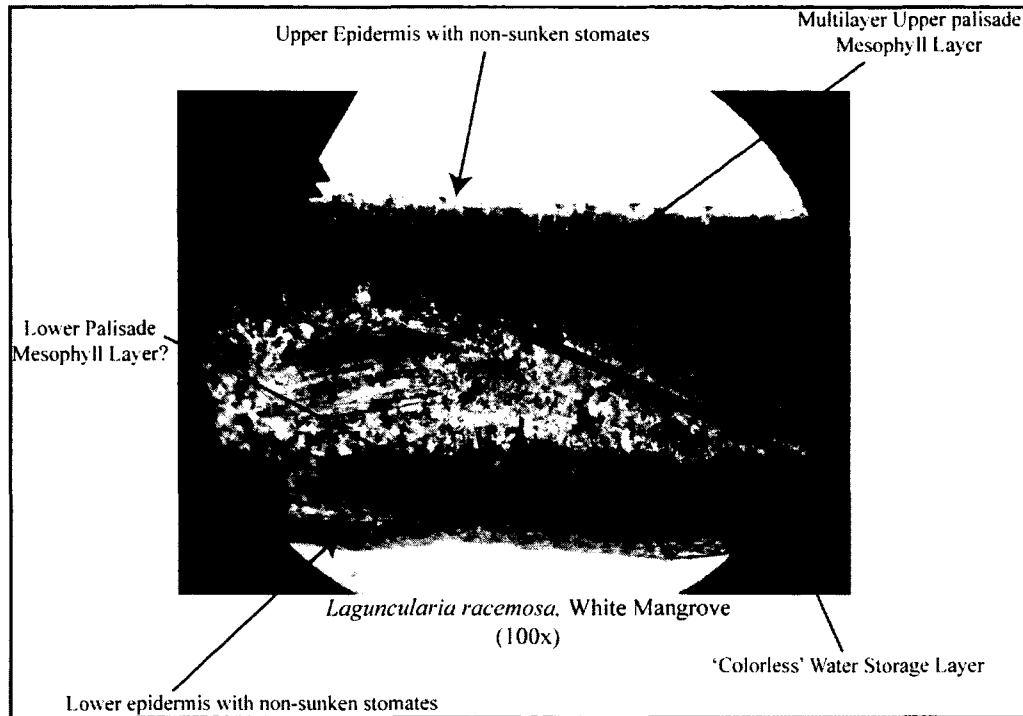


Figure 16 Thin section of *L. racemosa* leaf (100x)

3.2 Spectral Characterization of Mangrove

The three mangrove species are observed to have distinct spectral characterizations that likely relate to the cellular structure of ‘colorless’ water storage cells, palisade mesophyll cells and spongy mesophyll cells commonly found among all mangrove species occurring at Solimon Bay (Figure 19). This relates well to the statement by Jensen (2007) that the ‘dominant factors controlling leaf reflectance are (found in) the *leaf pigments in the palisade mesophyll* (in the visible), the *scattering of near-infrared energy in the spongy mesophyll* and the *amount of water in the plant*’, likely in the short-wave infrared. Given this statement, and the anatomical structure of the three species of mangrove examined, particular attention should be given to the visible portion of the spectrum (400 nm - 700 nm; TM Bands 2 and 3) which relates to leaf pigment, the near infra-red (700 nm - 1400 nm; TM Band 4/NIR Plateau) portion

which relates to spongy mesophyll and the short-wave infrared range from 1400 nm – 2600 nm (TM Bands 5 and 7) where leaf moisture content can have a significant impact.

The strongest separation of all three species is along the NIR plateau suggesting that there are major differences in the spongy mesophyll layers. The reflectance feature of the NIR plateau is a characterization of healthy leaf tissue (Rock et al., 1986). While not as distinct as the NIR plateau, the reflectance values seen in Band 3 confirm that the leaf pigment contained in the three species is the influence of leaf chlorophyll content. *A. germinans* has the lowest reflectance in band 3 while *L. racemosa* has the highest. This is supported by the darker green color due perhaps to greater density of chloroplasts observed in *A. germinans*. Subtle but distinct differences are seen across in band 5 and band 7. This confirms that water storage cells play a role in the spectral characterization of mangrove species. There is an interesting reversal of reflectance values on either side of band 5. This is very likely due to cellular/foiar water content. The 1400 nm and 1900 nm water absorption features are overtones of the primary water absorption in the TIR, with the 1900 nm absorption stronger than the one at 1400 nm. Therefore, the leaves with the greatest amount of water will reflect the least in band 7. Based on analysis of the reflectance curves for each species, there is enough separation and differences, that each of the three species can be spectrally characterized. These characterizations are based on anatomical differences seen in all three species.

In order to further understand the reflective properties of mangrove and how they relate to surrounding forest vegetation, the average reflectance curves of the three main species were compared with two non-mangrove species, *Ficus cotinifolia* and *Ficus maxima* (Figure 20). Both species are commonly found in the surrounding forest

environment and have succulent leaves similar to mangrove. Ryan Huntley as part of his Masters thesis at UNH collected the two samples provided to this study on April 1st, 2005 in the forest environment of Quintana Roo (Huntley, 2005). They were sampled using the same methods outlined above. As predicted, the reflectance of mangrove in the 1400nm to 2400nm range is much lower than the non-mangrove species. This is accentuated in both TM bands 5 and 7 with very prominent separation of mangrove and non-mangrove species. A comparison of the TM 5/4 means (Table 6, Figure 17) for all species demonstrates that the mangrove species have values for water content below those of the *Ficus* species. Interestingly, the REIP values (Table 6, Figure 18) for both the *Ficus* species are much higher than the mangrove species. In addition, the *Ficus maxima* sample has high reflectance along the NIR plateau. This suggests that even though the *Ficus* has lower water content, it has adapted to be able to tolerate these lower water levels associated with the regions dry season and still remain healthy. The strong separation seen in the middle infrared corroborates the visual interpretation of the Landsat imagery and the ability of bands 5 and 7 to highlight areas of mangrove. The drier forest vegetation also validates the use of imagery from the dry season in order to accentuate these differences.

Species	REIP		TM 5/4		N
	Avg.	Std. Dev.	Avg.	Std. Dev.	
Avicennia germanins	708.14	9.11	0.489	0.027	5
Rhizophora mangle (Distal)	710.76	8.58	0.410	0.026	30
Rhizophora mangle (Medial)	718.11	5.63	0.411	0.038	30
Laguncularia racemosa	712.69	9.23	0.437	0.042	11
Ficus maxima	723.80	1.35	0.515	0.020	4
Ficus cotinifolia	723.47	2.33	0.512	0.011	7

Table 6 Average Spectral Indices (REIP, 5/4) for Solimon Bay Mangrove Samples and Two Non-Mangrove Samples

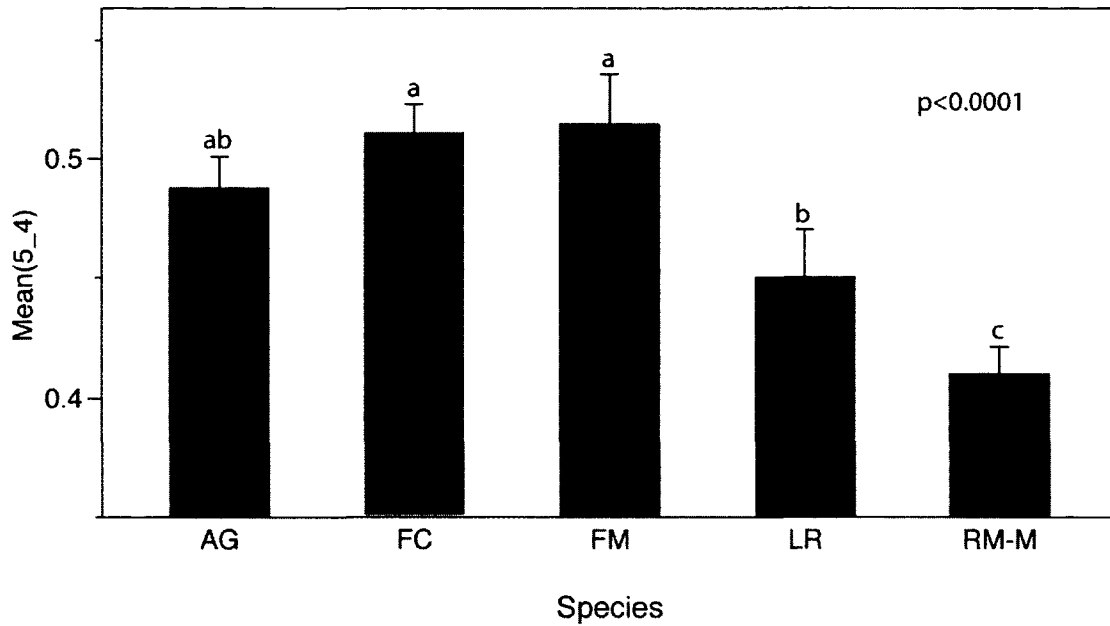


Figure 17 Plot of the mean 5/4 ratio for Black Mangrove (AG), *Ficus cotinifolia* (FC), *Ficus maxima* (FM), Red Mangrove Medial (RM-M), and White Mangrove (LC). Overall analysis by ANOVA followed by multiple comparisons using Student's *t* (<0.05). Error bars constructed using 1 standard error from the mean.

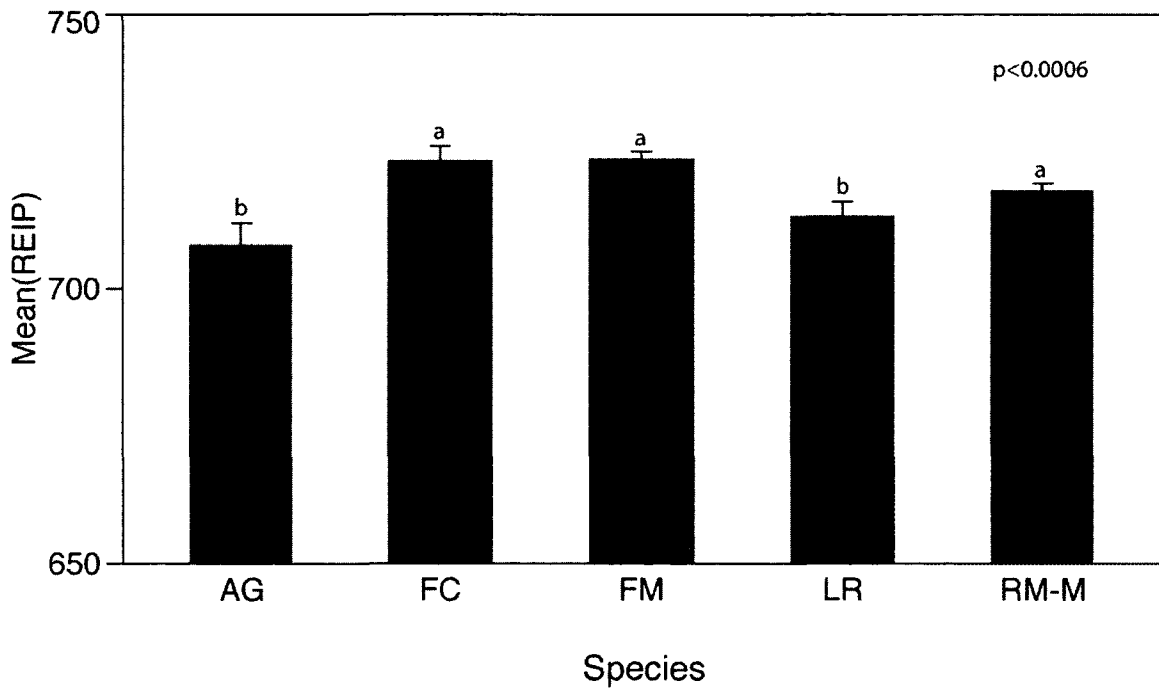


Figure 18 Plot of the mean REIP value for Black Mangrove (AG), *Ficus cotinifolia* (FC), *Ficus maxima* (FM), Red Mangrove Medial (RM-M), and White Mangrove (LR). Overall analysis by ANOVA followed by multiple comparisons using Student's *t* (<0.05). Error bars constructed using 1 standard error from the mean.

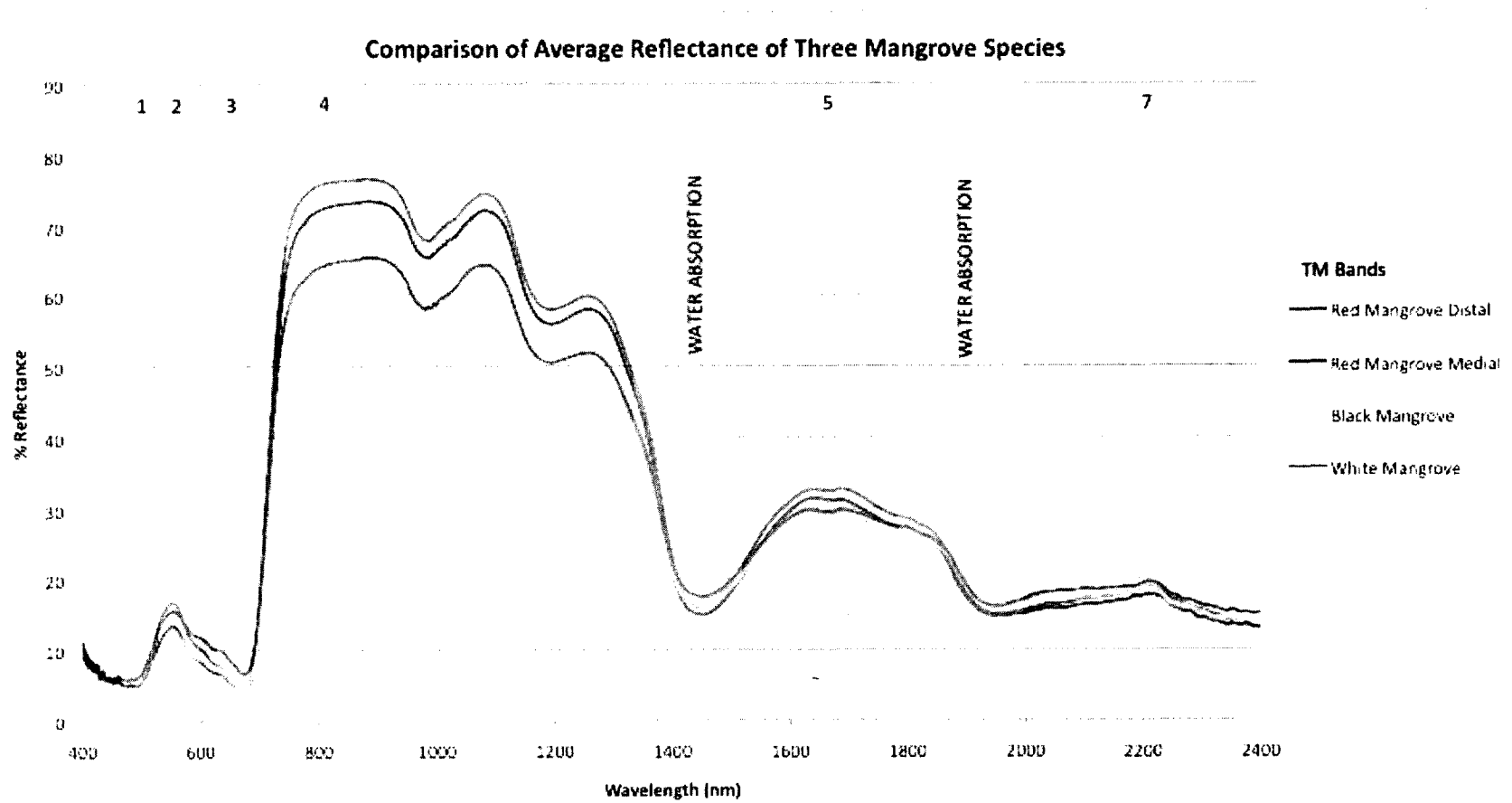


Figure 19 Reflectance Curves for 3 Mangrove Species, Solimon Bay, Mexico

Comparison of Average Reflectance of Three Mangrove Species with Ficus Maxima and Ficus Cotinifolia

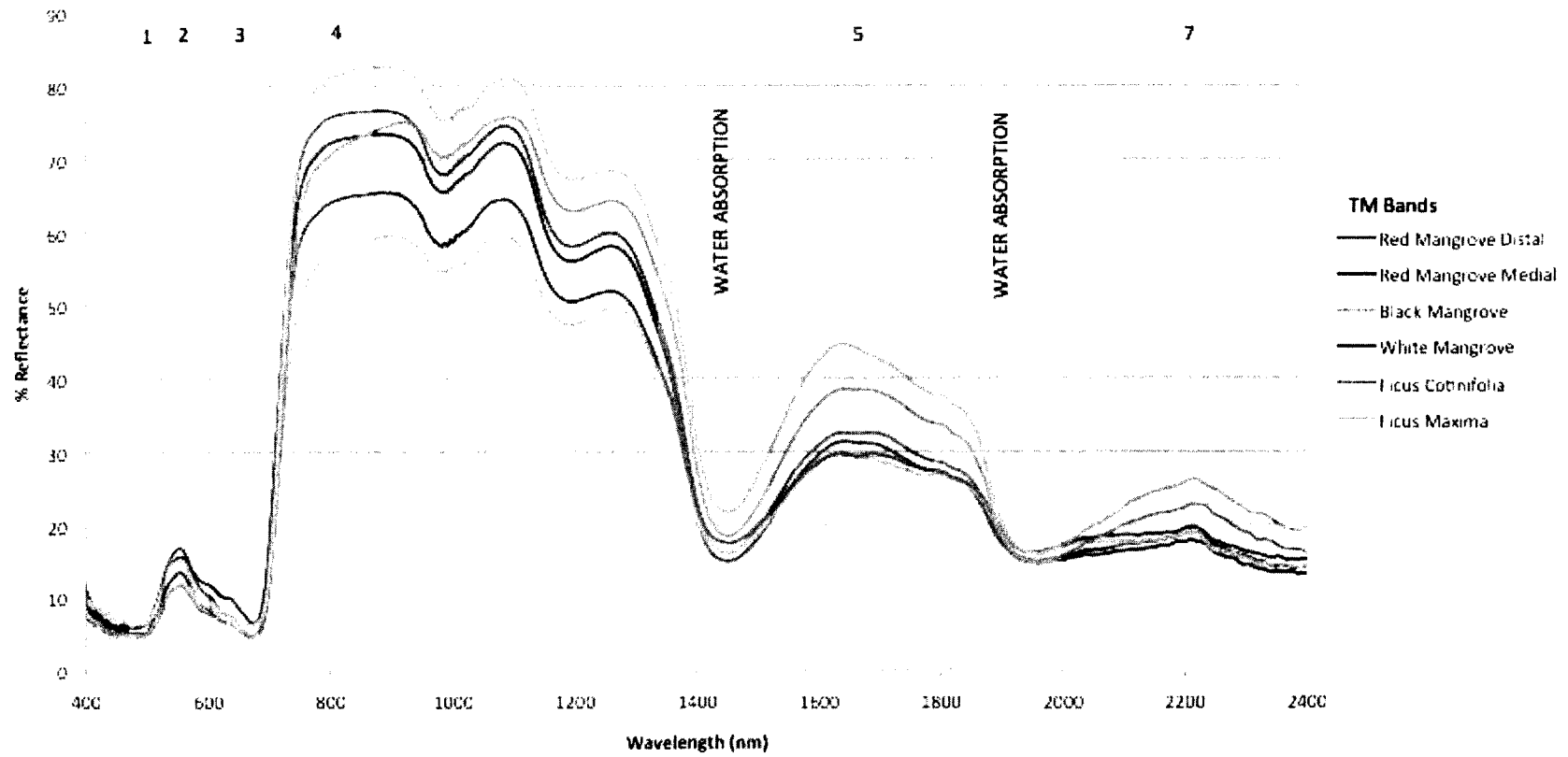


Figure 20 Comparison of Average Reflectance of Three Mangrove Species with Two Non-Mangrove Species

3.2 Thematic Map Results

3.2.1 Thematic Map Accuracy Assessment

The June 5th-13th, 2011 sites were spread throughout the study area and were visited and ground reference sample points were collected. A total of 35 ‘mangrove’ and 46 ‘not mangrove’ points were collected. Of these points, 5 ‘mangrove’ points and 8 ‘not mangrove’ points were discarded due to issues with minimum distances from other points or spatial autocorrelation as outlined in the methods. Reference data were crosschecked with the thematic map in GIS and an error matrix was populated (Table 7). An overall accuracy of 88% was returned. Both producers and users accuracy produced acceptable results.

		Reference Data		Row total
		M	NM	
Classified Data	M	29	6	35
	NM	2	29	31
Column Total		31	35	58
Overall Accuracy	88%			
Producers Accuracy		Users Accuracy		
Mangrove (M)	94%	Mangrove (M)		83%
Not Mangrove (NM)	83%	Not Mangrove (NM)		94%

Table 7 Mangrove Accuracy Assessment Error Matrix

3.2.2 Thematic Map Classifications

The final thematic map was created from the supervised classifications of the 13 band-stacked image (Figure 21). A total of 18,268 polygons that met the minimum mapping unit of 3x3 pixels (8,100m²) and that covered an area of 95,808 hectares were classified for areas of mangrove and not mangrove (forest and sawgrass) (Table 8).

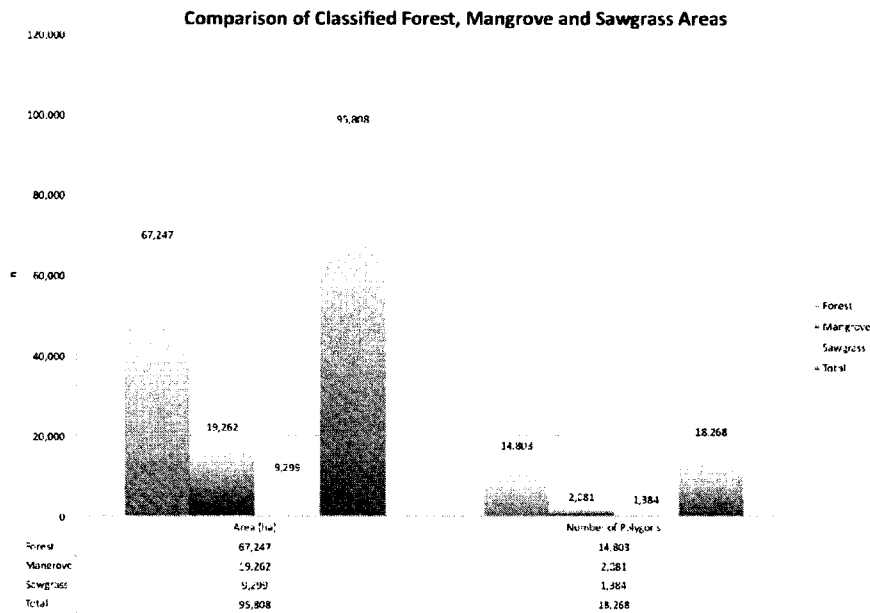


Table 8 Comparison of Classified Mangrove and Not-Mangrove Areas

The non-mangrove class of forest was the dominant vegetation class to be classified with 67,247 ha, while mangrove had 19,262 ha and sawgrass had 9,299 ha.

Final Supervised Classification Showing Polygons Meeting the Minimum Mapping Unit

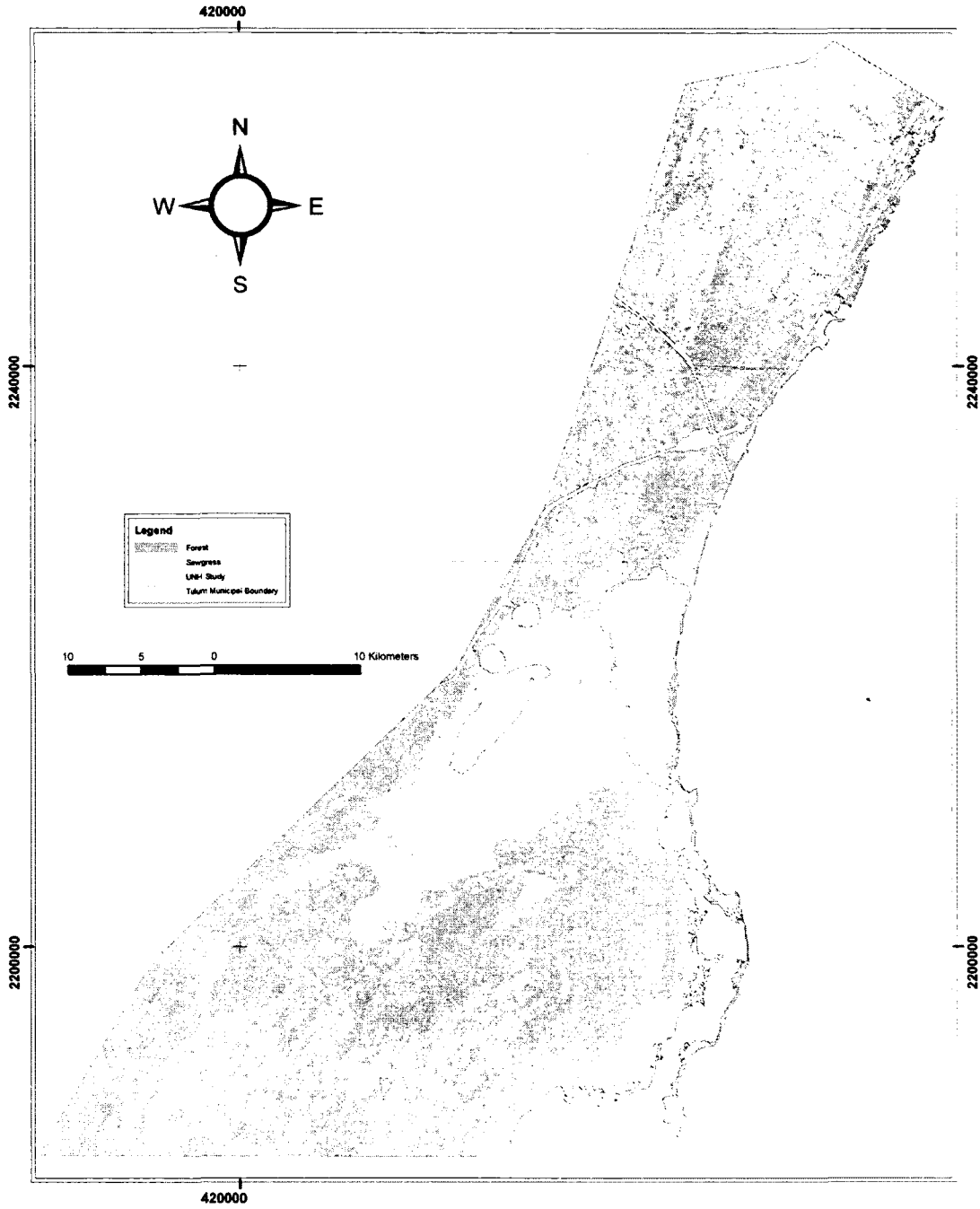


Figure 21 Final Supervised Classification Showing Polygons Meeting the MMU

Adding to the significance of these findings are large inland depressions a distance of 15 kilometers from the coast that were identified by the classification to contain mangroves. The existence of mangrove habitat in these areas was confirmed by field visits during the accuracy assessment component of this study. Inland areas of mangrove are uncommon and the large areas discovered by this study could not only play a role in expanding conservation areas for the region, but also by advancing the body of knowledge about these rare habitats. In addition, cenotes large enough to meet the minimum mapping unit and known to contain mangrove were accurately classified within the thematic map. The ability to identify 'cenote' mangrove habitats could also play a role in the expansion of conservation areas to include the region's aquifer system. It also highlights the need to further explore the relationship between the regions aquifer system and mangrove.

Furthermore, the thematic map was able to accurately distinguish between two classes of mangrove (fringe and dwarf) (Figure 22). While the possibility of separating individual species of mangroves using Landsat TM data was not demonstrated in this study, the ability to differentiate fringe and dwarf mangrove is a positive step towards the potential for species differentiation.

These results are still encouraging as they indicate an area of mangrove much larger and more extensive than published in the previous study done by CONABIO in 2009.

Areas of Mangrove Identified by this Study by Class (Fringe and Dwarf)

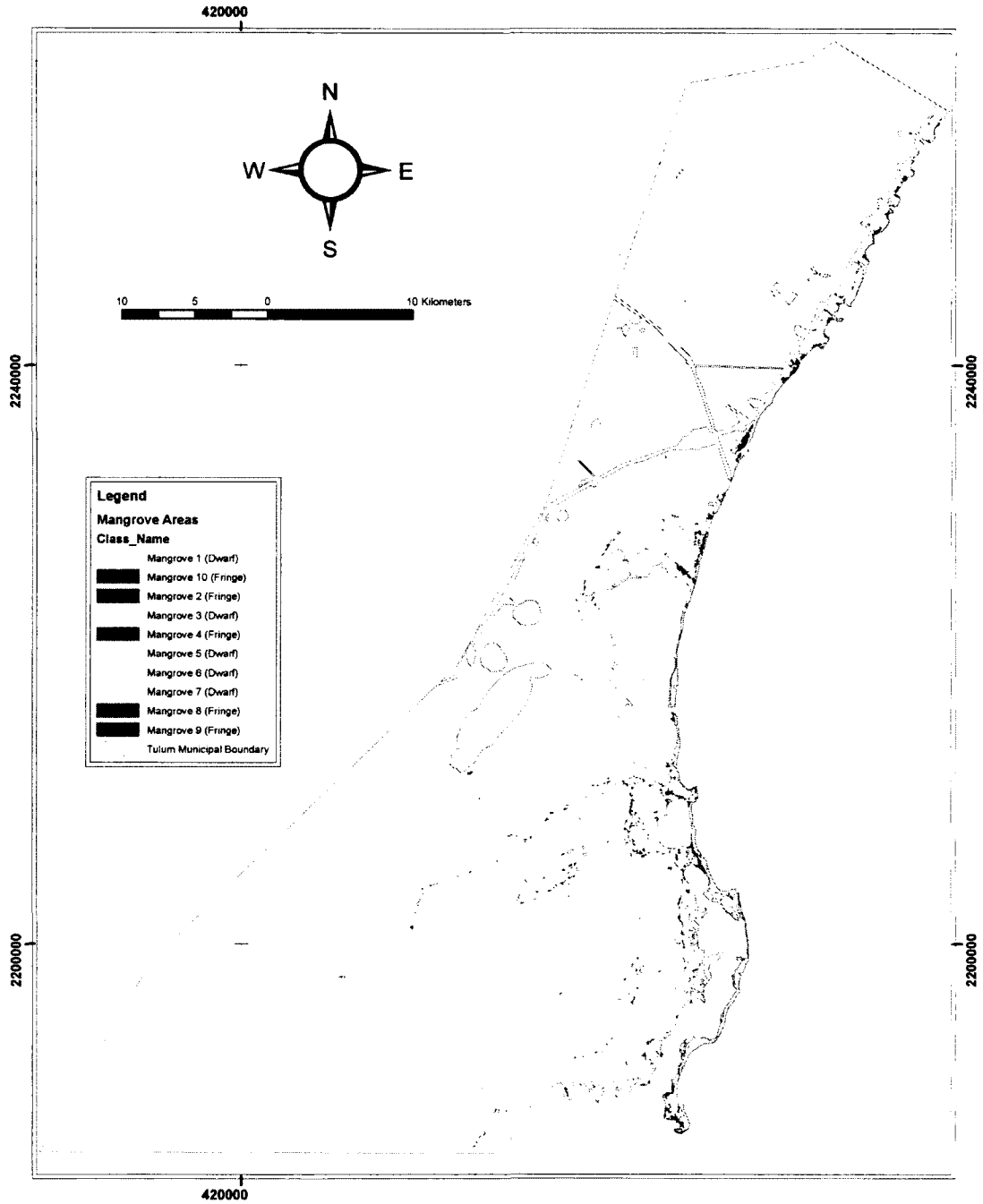


Figure 22 Areas of Mangrove Identified by this Study by Class

4.0 Discussion

4.1 Leaf Anatomy and Reflectance Properties of Mangrove

Through an analysis of leaf cross sections of the three major species of mangrove found in the region (*Rhizophora mangle*, *Avicennia germinans*, *Laguncularia racemosa*), this study sought to better understand the influence that anatomical differences among the mangrove species have on their reflectance properties since such anatomical differences may result in potentially diagnostic reflectance properties of the species (Tucker and Sellers, 1986).

Based on analysis of VIRIS data for the three main species of mangrove it has been determined that all three species have differences significant enough in TM bands 2, 4, 5 and 7 to allow them to be individually characterized. These differences can be attributed to differences in the leaf pigment, spongy mesophyll and 'colorless' water storage cells. Whether these differences would apply to the whole spectrum of mangrove species would only be answered by further analysis of the anatomical and spectral properties of each species.

Since water storage cells are an anatomical feature common to all mangrove species, and these water storage cells showed subtle but good separation in TM bands 5 and 7 for all three species, the same could apply for all mangrove species. Thus, the ability to individually characterize the reflectance properties of *R. mangle*, *A. germinans*, *L. racemosa* is a significant step towards the creation of a worldwide database of mangrove reflectance properties. Future studies should center around a coordinated effort to collect, scan and analyze the spectral reflectance properties of mangrove species

from around the world. A library of reflectance properties of mangroves would greatly benefit the effort to map mangrove communities worldwide.

Furthermore, the decision to use Landsat TM data acquired from the dry season was validated by comparing the reflectance properties of forest vegetation of similar succulence to mangrove to see if the reflectance of mangrove species varied from surrounding non-mangrove forest vegetation. Comparison of these reflectance values showed strong separation in TM bands 5 and 7. Such strong separation demonstrates how well the much drier forest vegetation stands from the mangrove vegetation due to a lack of leaf moisture content. This was further confirmed by visual analysis and of the Landsat TM imagery using the FCC band combination of 7,5,3. Interestingly, band 7 had a double effect of not only being able to help in the discrimination between leaf moisture in mangrove and non-mangrove classes, but also in the differences in soil moisture. Figure 23 illustrates the difference in soil moisture very nicely between the drier 1984 image and the more moist conditions present in the 2000 image (Case and Gerrish, 1984; Lawrence et al., 2001). The fact that mangrove is able to exist in these moist soil conditions that band 7 accentuates so nicely, and that differences in leaf moisture content between mangrove and non-mangrove species are picked up by band 7, played a significant role in the ability of the supervised classification to perform so well.

**Comparison of drier conditions present in 1984 vs. 2000
Rancho San Eric, Tulum**

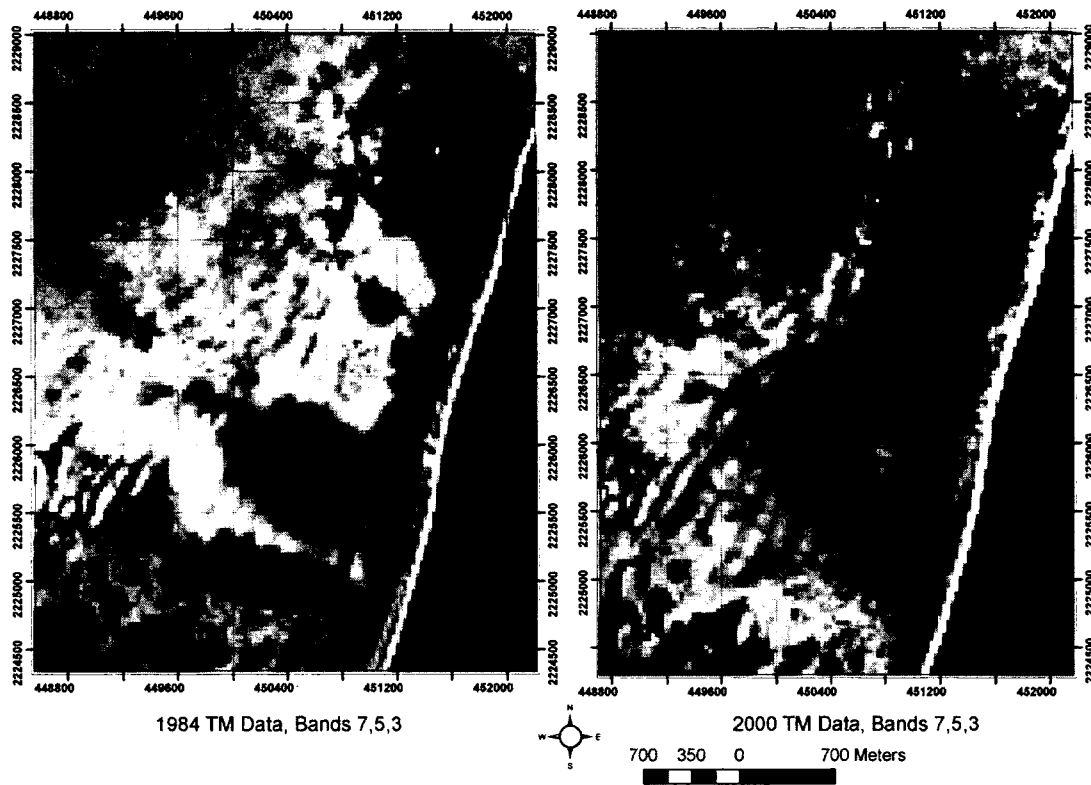


**Figure 23 Comparison of potential moisture conditions in the
1984 and 2000 Thematic Mapper data sets**

4.2 Map Accuracy

The 88% overall accuracy achieved for this project was an acceptable result. However, there are several potential sources of error that could have played a factor in the final accuracy assessment. The most obvious is the fact that the image used for the classification was acquired 11 years prior to field studies being conducted. Changes in landcover from 2000 to 2011 could be factors for errors present in the final accuracy assessment. It would be interesting to redo the classification once an image closer in date to the field study becomes available. Another source of error, is potentially areas where mixed vegetation of *C. jamaicense* and mangrove were confused. The subtle boundaries

between these vegetation changes could be difficult for the 30m resolution of the Landsat TM 5 to pick up. As a result, errors in classification in either direction could have occurred. Finally, the areas of grassland along the Vigia Chico road in Sian Ka'an were a cause of error and confusion for the model. Identified as mangrove, these areas were in fact, inundated low areas with grasses. Since they had not been factored into the original classification system they were deemed 'non-mangrove' for the accuracy assessment. There appear to be more of these areas in close proximity to the Vigia Chico road. In future studies, these areas should be classified separately as they are distinct from all other habitats classified in this study.

4.3 The Thematic Map

4.3.1 Forest Classification

The final supervised classification was able to adequately discriminate areas of mangrove and non-mangrove. The non-mangrove class of forest was the dominant vegetation class (Table 8) to be classified. It is interesting to observe that in the final supervised classification that shows all of the polygons (Figure 24), that there are subtle variations in the forest vegetation throughout the study area.

Final Supervised Classification Showing All Polygons

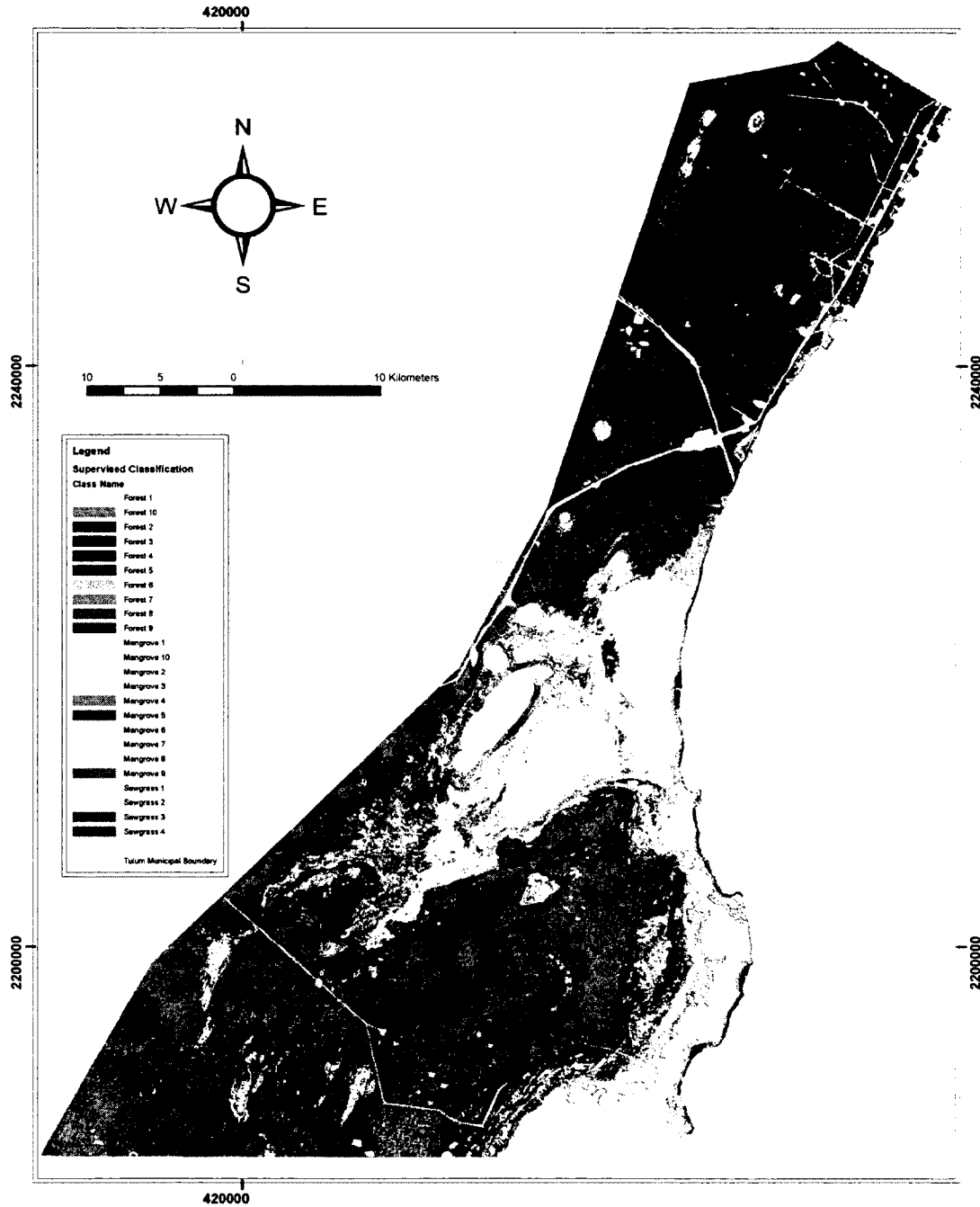


Figure 24 Final Supervised Classification of the Study Area (Showing all polygons)

It should be noted that for the supervised classification there were no differentiations made for the forest class when assigning training areas to it. In other words, forest was considered to be one homogeneous vegetation type. The variations in forest vegetation seen in Figure 24 could be attributed to a number of factors from differences in specific forest vegetation types (palm forest vs. deciduous forest), human disturbance, elevation, hurricane storm damage, wildfires and surface geology. In addition, Figure 21 shows that while there are large areas of contiguous forest, there are also large fragmented areas of forest that do not meet the minimum mapping unit. This is particularly evident in the northern limits of the study area and again suggests that there may be underlying reasons for these areas as explained above. Hurricane storm damage, forest fires and human disturbance could all be contributors to forest fragmentation.

Figure 21 also shows that large forested areas surround two of the areas of inland mangrove identified by this study (Laguna Madera and Laguna Selva Maya). These areas of forest are similar in appearance to the 'halos' of vegetation that appear around cenotes (Huntley, 2005). The vegetation 'halos' around cenotes have been attributed to the readily available source of water that the cenotes provide and that forest vegetation benefits from. This suggests that there is a relationship between the seasonally inundated inland mangrove areas, the possible microclimate that they create and the surrounding forest vegetation. The increased moisture in these areas could also act as protection for the forest from the forest fires that frequent the region. While the classification of forest type was not the focus of this particular study, these results indicate that a more detailed classification of forest types would warrant a follow-up study. Such a study would be of additional benefit to regional conservation efforts.

4.3.2 Sawgrass Classification

Areas of sawgrass (*Cladium jamaicense*) were discriminated well by this study (Figure 21). The ability to differentiate sawgrass from other vegetation types is important, as it will give natural resource managers, particularly in the Sian Ka'an Biosphere Reserve a better understanding of the distributions of habitats. Since a minimum of ten training classes were required for the study and only four sawgrass areas were used for training, this evidence can only be presented anecdotally. However, the evidence does suggest that sawgrass possesses characteristics that set it apart from the two other main classes in this study (mangrove and forest). The fact that sawgrass is a sedge and grows in large homogeneous areas would be factors allowing it to stand out from the leafy vegetation of the mangrove and forest. Furthermore, although there is no literature to support this, it is possible that sawgrass is a C4 plant. Plants that are classified as C4 have anatomical differences that allow them to fixate carbon in a manner that is distinct from that of C3 plants (Raven Peter H., 1976). Comparisons of fluorescence signals taken from hyperspectral data have shown that C4 plants can be distinguished from C3 plants (Liangyun, 2010). Thus, if future studies can confirm that sawgrass is indeed a C4 plant, then the methods outlined by Liangyun could aid in furthering the ability to differentiate sawgrass from surrounding mangrove and forest habitats. The study by Liangyun reinforces the value of, and need for hyperspectral data to be acquired for this region thus broadening and enriching the characterization of vegetation for the area.

4.3.3 Mangrove Classification

A total area of 19,262 ha was classified as mangrove (Figure 22) by this study.

The results are encouraging as they indicate an area of mangrove much larger and more extensive than published in the previous study done by CONABIO in 2009. Perhaps the most interesting discovery made by this study is the existence of mangrove habitat in isolated areas up to 15 kilometers from the coast, and in cenotes. These findings are discussed in further detail below.

It is important to state that, and as noted in the methods, the class of ‘overwash’ mangrove was masked out of the Landsat image due to confusion with other areas. As result, areas of ‘overwash’ mangrove are missing from the final tally for total classified mangrove areas. The majority of the ‘overwash’ areas that were masked out are located in Laguna Caapechen in the Sian Ka’an Biosphere Reserve. It is also important to state that there were discrepancies between mangrove classes and non-mangrove classes along the Vigia Chico road within the Sian Ka’an Biosphere Reserve. Areas identified as ‘mangrove’ in the classification, were, in fact, a non-mangrove habitat that was neither forest nor sawgrass. The inability of the supervised classification to make a distinction would need to be addressed in further studies. Therefore, there are also areas non-mangrove habitat that *are* included in the final tally.

A comparison of the classified mangrove polygons by size (Table 9) reveals that the majority of them are small ($1 > 5$ ha). This is a positive finding in that it shows that the classification was able to map well within the parameters of the MMU. However, such a large number of small polygons suggest that there are many, small, potentially

fragmented areas of mangrove throughout the study area. From the standpoint of conservation, these areas pose a challenge, as smaller more fragmented areas are more difficult to consolidate and conserve.

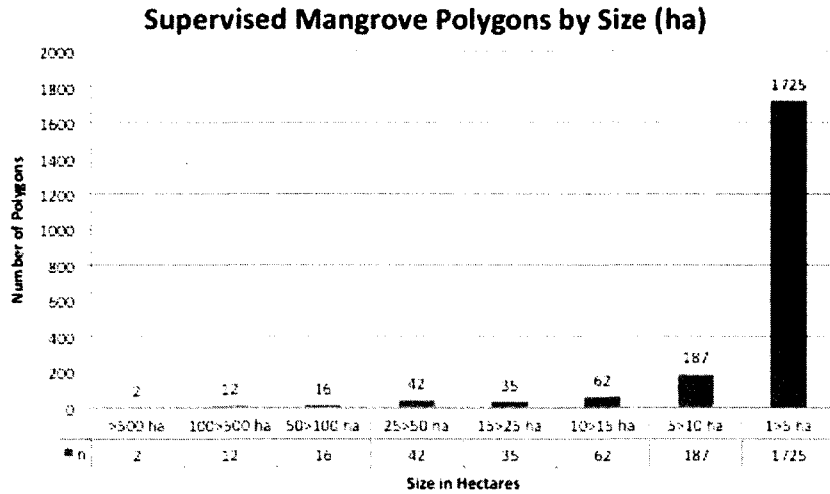


Table 9 Supervised Mangrove Polygons by Size (ha)

Furthermore, the thematic map was able to accurately distinguish between two classes of mangrove (fringe and dwarf) (Figure 22, Table 10). The areas of fringe that were identified fit with the areas they would normally be associated (e.g. protected lakeshores of the Sian Ka'an Biosphere Reserve). The comparison of mangrove areas by type seen in Table 10 also helps illustrate the dominance of the dwarf mangrove type over fringe. The success of the classifications ability to discriminate fringe and dwarf mangrove types can be attributed to the training areas that were used.

Mangrove Areas (ha) and Number of Polygons by Type

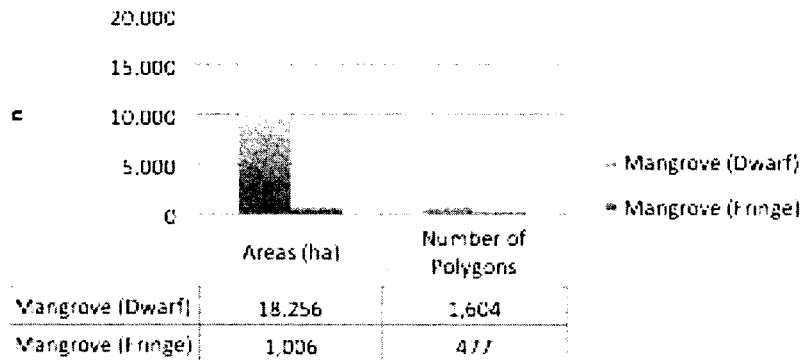


Table 10 Mangrove Areas (ha) and Number of Polygons by Type

The spectral differences between fringe and dwarf mangrove could be related to proximity as evidenced by the presence of fringe mangrove around and within cenotes and by lakeshores. Future work in the area should include further study of leaf anatomy between the fringe and dwarf classes and also the generation of spectral reflectance curves of fringe. Studies of this nature will only help better understand the differences between them and allow for more accurate classification.

The possibility of separating individual species of mangroves using Landsat TM data was not demonstrated in this study. However, the ability to be able to discriminate at by type (fringe and dwarf) and to characterize the spectral reflectance properties of individual mangrove species is potentially a positive first step towards the use of hyperspectral data to further explore mangrove zonation, and species differentiation both locally and internationally.

While some may look at the thematic map as the end result of this project, it is only one small part that opens up new avenues for investigation with many questions to be answered. While an 88% overall accuracy is encouraging, there is always room for

refinement of the model. Further refinement should include more training classes for *C. jamaicense* so that it may stand alone as its own class. The variations in forest cover seen in the final supervised classification suggest that the forest vegetation for the area is not homogeneous and could be classified in more detail. A better understanding of the distribution of *C. jamaicense* and characterization of forest habitats and types will only benefit the managers of the regions natural resources. Mangrove habitats were adequately identified and mapped by the model. Refinement could be applied in order to lessen the confusion between mangrove, *C. jamaicense*, and the grass habitats encountered in the Sian Ka'an Biosphere Reserve. Additional time could be spent to allow the model to include areas of overwash mangrove that were not represented in the thematic map. The ability for the model to correctly discriminate between mangrove types (dwarf and fringe) was a welcome outcome. This clearly shows that there is a difference spectrally between these two mangrove types. Further investigation using high-resolution hyperspectral instruments like the VIRIS combined with anatomical analysis of the two types would help to understand the differences and improve the model. The Landsat 5 TM data has done an admirable job of classification with the one shortcoming of the ability to distinguish at the species level. While the Landsat 5 TM data is an excellent first pass, airborne hyperspectral data would allow for much more detailed inventory of habitats, potentially to a species level. The groundwork laid out in this study will only serve to further improve how the model works.

4.4 Inland Mangrove Habitats

Inland mangrove habitats have been described from around the world, yet they are a rarity (Ellison and Simmonds, 2003; Lugo, 1981). One of the common factors that allows these habitats to exist is that they are found in areas of karst geology (Lugo, 1981). Inland mangrove areas are thought to be influenced by groundwater flows associated with the porous nature of karst geology even though they can be kilometers from the coast (Ellison and Simmonds, 2003). Given that the karst geology of the region around Tulum has well-developed solution cave systems that act as conduits for both fresh and saltwater (Beddows, 2004) it is not surprising that inland mangrove habitats are found in this area. The large depressions associated with the Holbox Fracture (Laguna Madera, Laguna Selva Maya, Laguna Union, Laguna Chumkopo) and the cenotes (karst windows to the aquifer) that were identified by this study to have mangrove (Figure 25), represent two different types of inland mangrove habitat with connections to the regions aquifer system.

Despite being isolated from the sea these communities are described as healthy habitats. Ellison and Simmonds (2003) reported from Lake MacLeod in Western Australia, rates of primary production, and mangrove biomass per unit area that were equivalent to mangroves found in normal coastal situations. Lugo (1981) identified a large intact inland mangrove habitat in the Bahamas 50 km from the sea that is similar in species composition to the Tulum. The Lake Windsor site he describes had all four of the species that are found in Mexico present.

Unprotected Inland Areas of Mangrove

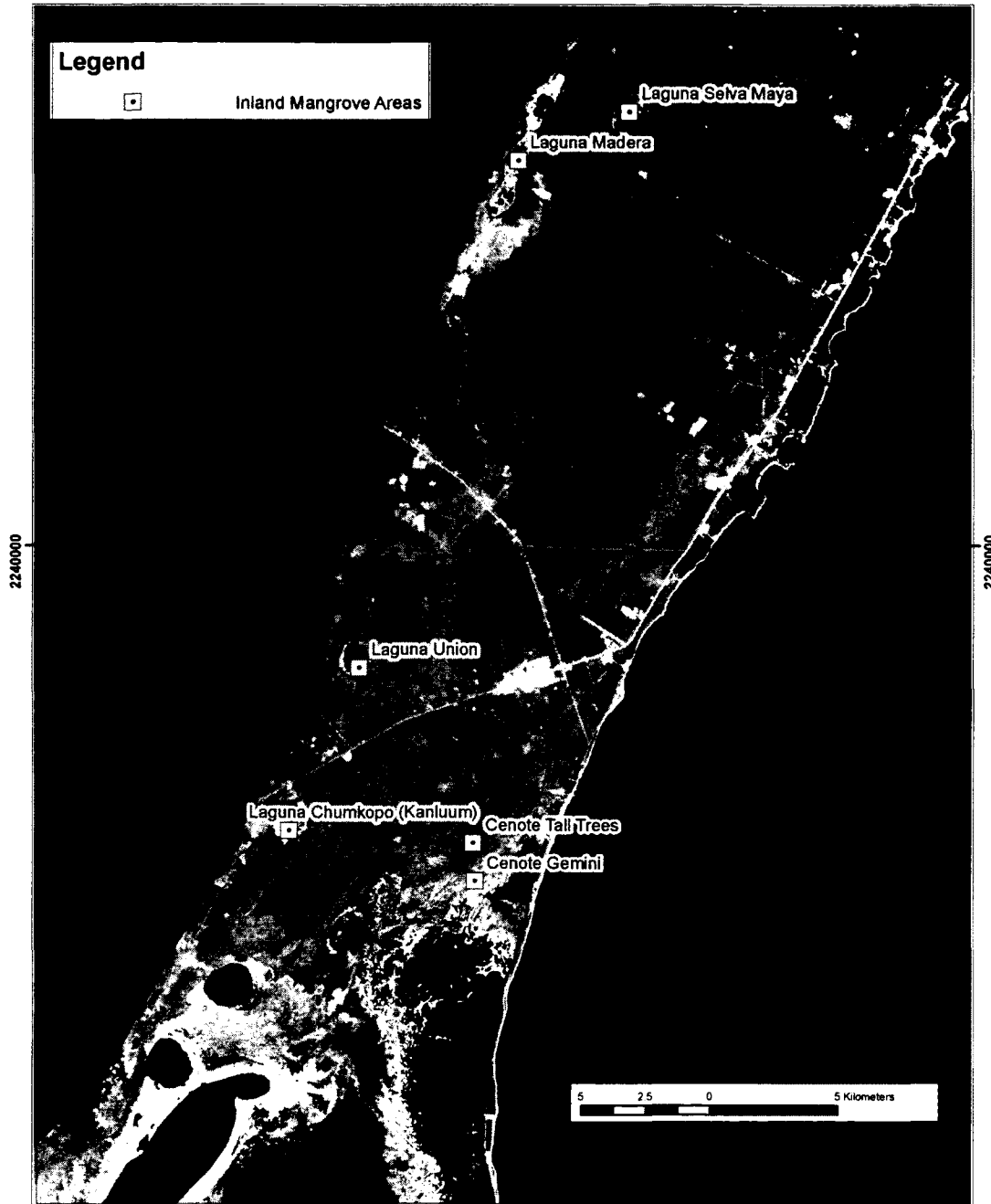


Figure 25 Unprotected Inland Areas of Mangrove

Measurements of soil and surface water yielded high values (surface salinity range: 25.0 ppt-72.8 ppt; soil salinity range: 25ppt-119ppt) that are typical of the arid climate in

which they were found. *A. germinans* and *L. racemosa* grew in areas of higher salinity while *R. mangle* and *C. erectus* occupied areas of lower salinity. Of the sites found in the literature, the one described by Lugo is the closest geographically and in the species found. However, there are more differences than similarities to the sites found in and around Tulum. Foremost among these differences is that salinities of pore water samples taken in two of the inland mangrove areas were much lower and bordered on freshwater bodies. The average salinity of Laguna Madera measurements was 0.95 ppt while the measurement made at Laguna Selva Maya was 2.0 ppt. These both represent very low salinity measurements and also suggest that there is a salinity gradient heading towards the coast from these two inland areas.

The second major difference is that the species diversity is lower than in the study by Lugo, perhaps due in large part to the lower salinity levels. Only *R. mangle* and *C. erectus* were found consistently in the areas around Tulum (Table 11).

R. mangle was observed to have very brittle branches that would snap off. This is contrary to *R. mangle* observed by the beach that had much more typically supple branches. One can only speculate about these differences, but they may have something to do with the lower salinity levels.

Name	Distance from Coast (km)	Substrate	Mangrove Species Present	Salinity Subsurface (ppt)
Laguna Selva Maya	11.1	Marle, organic	Red Mangrove, Buttonwood	2.0
Laguna Madera	15	Marle, organic, bedrock	Red Mangrove, Buttonwood	0.95
Laguna Union	9.5	Marle	Red Mangrove, Buttonwood	n/a
Laguna Chumkopo (Kanluum)	10	Marle	Red Mangrove, Buttonwood, White Mangrove	n/a
Cenote Gemini	2.6	Open Water, Organic	Red Mangrove	n/a
Cenote Tall Trees	2.8	Open Water, organic, Bedrock	Black Mangrove?	n/a

Table 11 Characteristics of Inland Mangrove Areas

One intriguing question that has not yet been answered relates to the origins of inland mangrove habitats. A number of theories exist to explain these origins. Lugo (1981) postulates that mangrove propagules are distributed by hurricanes, while others claim that they are remnants of past communities cut off by sea level change and geological enclosure (Ellison and Simmonds, 2003). The cenotes of the Yucatan Peninsula provide evidence that these mangrove areas are indeed remnants from mangrove communities cut off by sea level rise during the Holocene. Gabriel et al. (2009) examined core samples from Cenote Aktun Ha, located 8.5 km from the coast, and found a pollen record that indicates that the cenote evolved from a marsh once

dominated by *R. mangle*. Using ^{14}C -dating, wood fragments from the bottom of the core where *R. mangle* pollen was located were dated to $6,840 \pm 100$ cal year BP. Further analysis of the core towards the surface indicates that over time, and as sea levels rose, there was a decrease in *R. mangle* pollen. What is striking, is that Cenote Aktun Ha is located directly between the two large present day inland mangrove areas of Laguna Madera and Laguna Union. The presence of the *R. mangle* pollen in Cenote Aktun Ha that dates back to the Holocene would support the theory that the present day inland mangrove areas are remnants of Holocene period mangrove communities. It would also suggest that the cenotes are able to provide ideal conditions that allow mangrove habitats to grow out of, or recede into during episodes of sea level and climate change.

The discovery of inland cenote habitats is one of the more exciting outcomes of this study, and is the one that will have the greatest impact for conservation efforts. That mangrove habitats are found inland is not only interesting, but also is very relevant for conservation. The fact that these mangrove communities exist in such low levels of salinity, so close to freshwater conditions, suggests that suitable habitat for protecting mangrove extends all the way inland whether mangrove is there or not. The implications for extending the search for mangrove and mangrove habitat further inland by using hyperspectral data could expand conservation areas beyond their current limits.

This study also suggests that cenotes and the aquifer system for this region are vectors for inland mangrove. Cenotes possibly provide habitat connectivity, suitable hydrology or other requirements that promote 'mangrove oasis' from which mangrove habitats can grow out of or recede into with changes in sea level as evidenced by the study of Gabriel et al. (2009). Cenotes and the aquifer system have very little if any

environmental protection under Mexican law. By identifying ‘mangrove oasis’, potentially, the laws protecting mangroves in Mexico can serve blanket protection to the regions aquifer. While the results of this project show that the large majority of mangrove habitats within the study area fall under protected areas, the inland mangrove habitats of cenotes and lagunas fall outside of them. An effort needs to be undertaken to ensure their conservation.

4.5 Comparison of CONABIO and UNH studies

A previous study by CONABIO conducted in 2008 that used remote sensing techniques, was able to identify and map a total 317 polygons representing 8,040 ha within the study area (CONABIO, 2009). By contrast, the UNH study has expanded the total number of mapped areas of mangrove to 2,081 polygons covering 19,262 ha. This represents a 140% increase on the previously mapped area (Figure 26, Table 12).

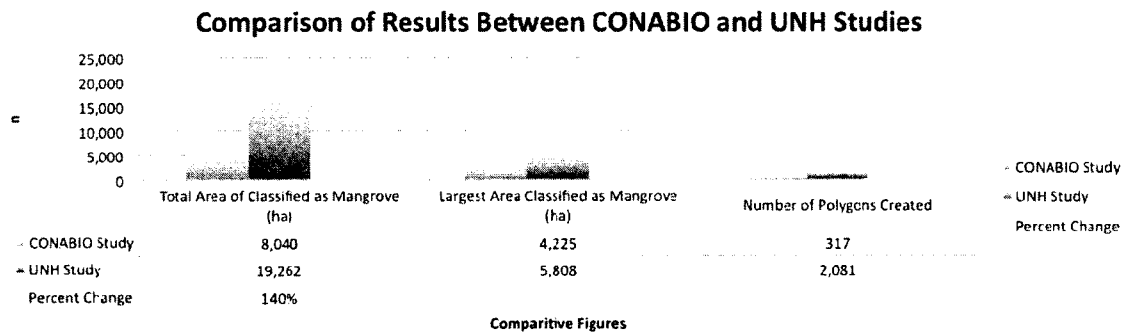


Table 12 Comparisons of Results Between CONABIO and UNH Studies

Differences in these two studies can be attributed to one factor; the scope of the study area. The scope of the CONABIO study was nationwide and was focused only on coastal areas. The UNH study was more focused geographically and took advantage of

my knowledge of the area to expand further inland to areas known to have mangrove habitat (cenotes) and areas suspected of having mangrove habitat (the depressions and lakes associated with the Holbox fracture). Thus the UNH study extended the boundaries of its study area beyond those of which the CONABIO study had used. Another potential issue might have been that for the CONABIO study, SPOT 5 10-meter data were used. While SPOT 5 has a higher spatial resolution than Landsat TM data, it has reduced spectral resolution, with only 3 bands covering portions of the visible and near infrared spectrum. One would infer then that the capability of the SPOT 5 sensor to identify areas of mangrove would be less than that of the Landsat 5 TM sensor. However, when comparing the two studies, there is a good deal of intersection in the common areas studied. This suggests that the SPOT and Landsat TM data were able to resolve mangrove at an equal rate. Thus, the difference in the amount of mangrove that was identified is most attributable to the fact that the UNH study extended into areas not covered by the CONABIO study.

Areas of Mangrove Identified by CONABIO and UNH Studies

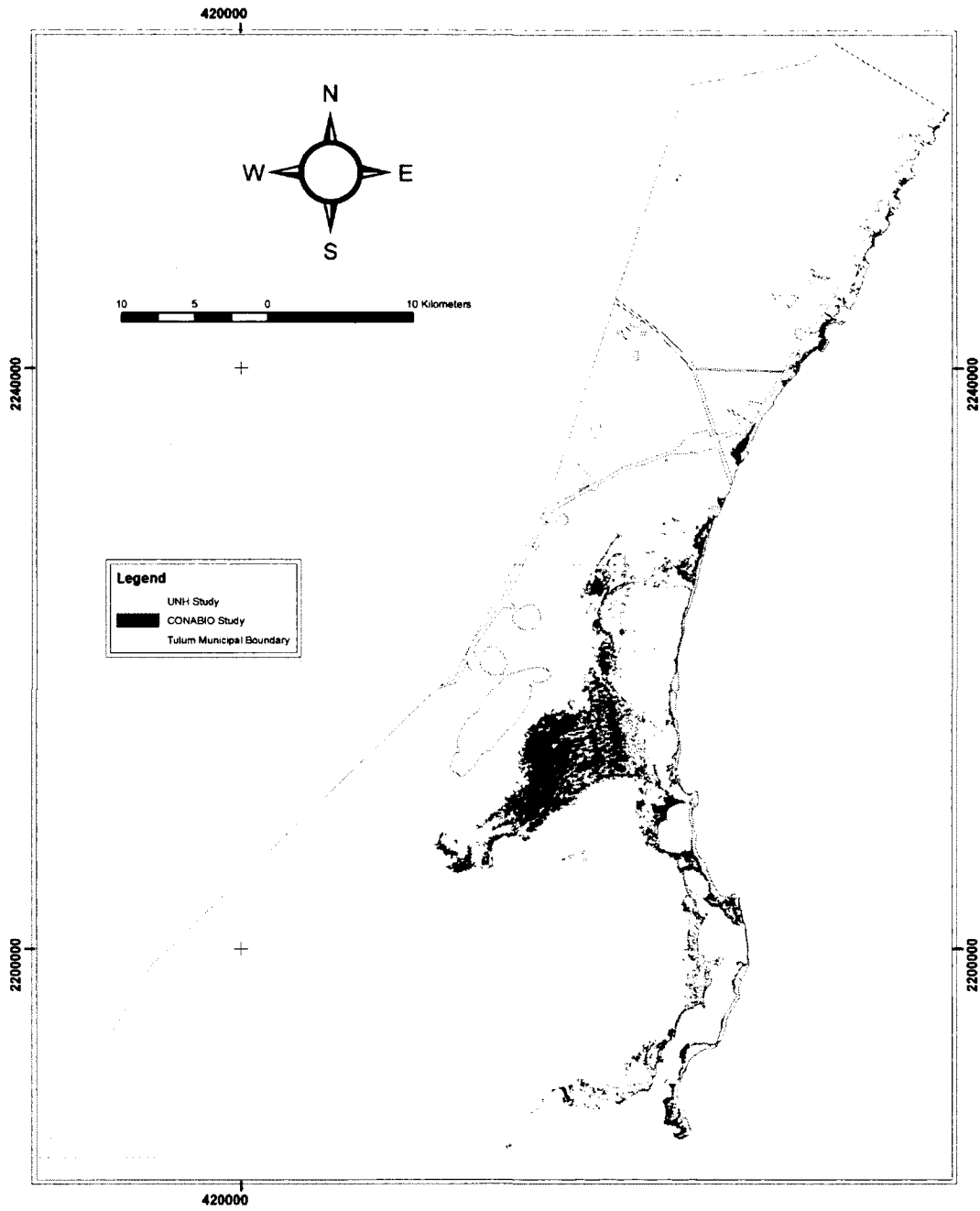


Figure 26 Overlays of CONABIO and UNH Studies

4.6 Implications for Mangrove Conservation

Figure 27 shows that the majority of the mangrove identified within the study area fall within protected areas. This accounts for 89% (17,061 ha) of the mangrove that was classified. The remaining 2,196 ha of unprotected mangrove are in privately owned property or ejido (communally owned) lands. Unprotected areas are distributed both in close proximity to the coast and inland areas already described (Figure 28). The largest contiguous area (658 ha) of unprotected mangrove is located in the southern boundary of the Ejido Jose Maria Pino Suarez that borders the northern limit of the Sian Ka'an Biosphere Reserve. This sharp border that divides the protected from unprotected areas is clearly visible and should be a priority area for conservation due to its close proximity to Sian Ka'an. These mangrove serve as an ecological buffer that protects and nourishes the reserve.

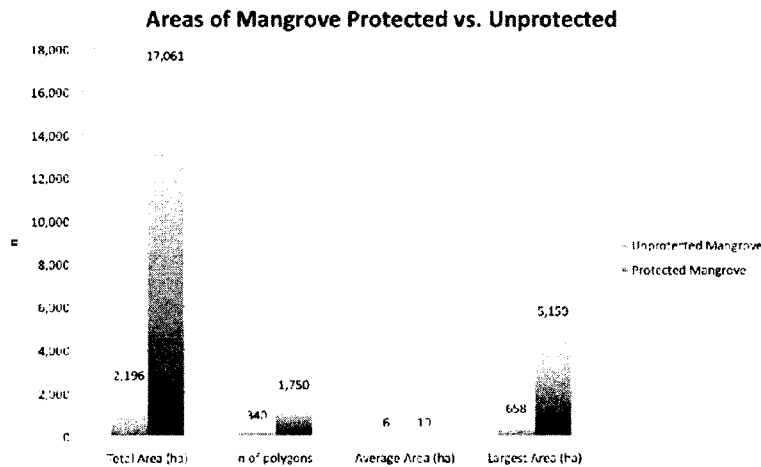


Figure 27 Areas of Mangrove, Protected vs. Unprotected

Despite the fact that the large majority of mangrove is found within protected areas, the remaining unprotected areas should not be discounted. Due to the high rate of development occurring on along the coastline, priority should be given to these areas for

active conservation. Conservation of coastal mangrove is a key element to maintaining the health of the Mesoamerican Barrier Reef, which draws tourists to the area and helps to sustain the regions economy. And due to their rarity and potential for scientific discovery, the inland mangrove habitats (e.g. lagunas, cenotes) identified by this study should also be considered of extremely high value and worthy of conservation.

Unprotected Areas of Mangrove Identified by the UNH Study

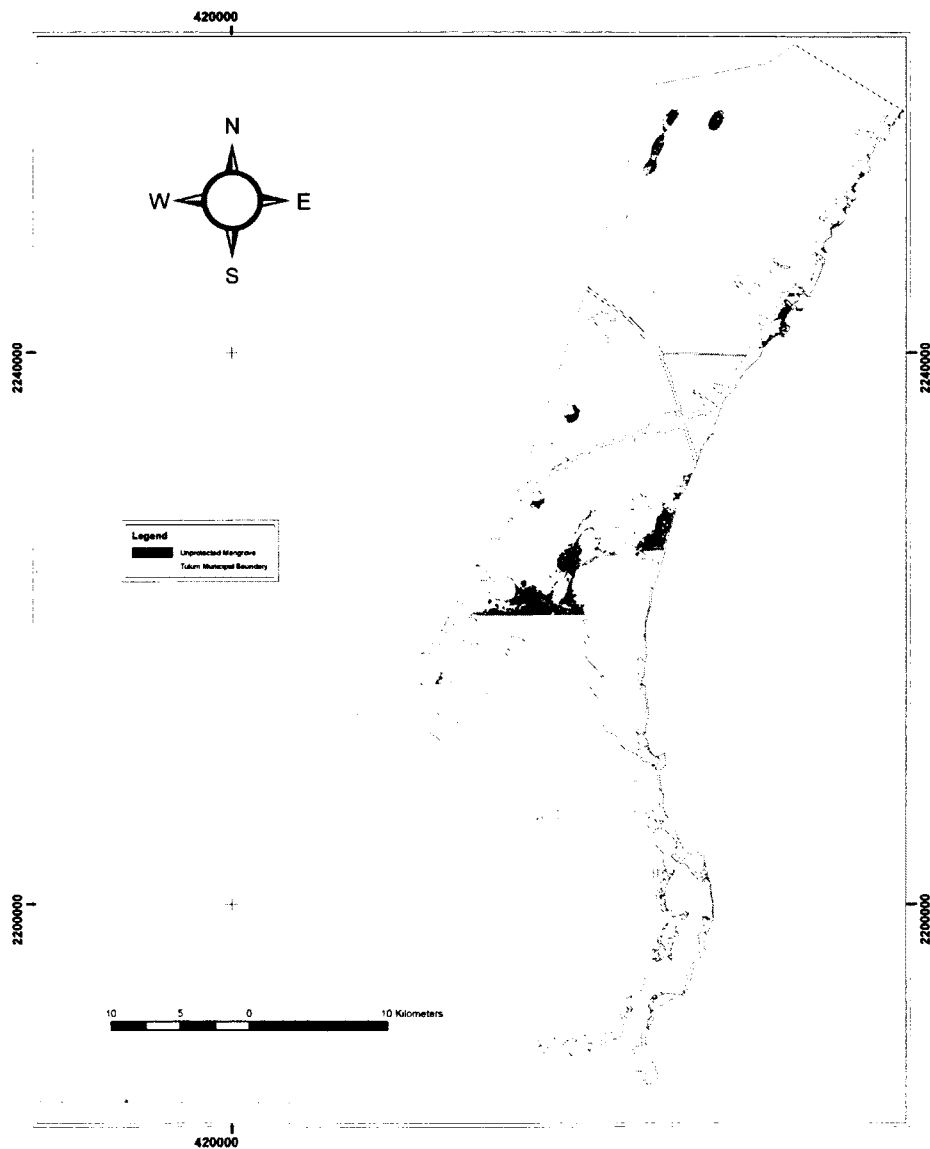


Figure 28 Unprotected Areas of Mangrove Identified by the UNH Study

5.0 Conclusions

This study was able to successfully identify and map areas of mangrove within and around the municipality of Tulum Quintana Roo Mexico using remote sensing techniques. Anatomical differences between the three main species of mangrove found in the area were examined and compared to high-resolution spectral reflectance data so that each species could then be spectrally characterized. The spectral reference data for mangrove was also compared to two common types of forest vegetation revealing significant differences in reflectance values between them associated with TM bands 5 and 7. These differences were also noted during visual analysis of the TM data. A vector-based map with an overall accuracy of 88% was created that identified 140% more mangrove areas than in a previous study. The supervised classification was able to discriminate mangrove and non-mangrove (forest, sawgrass) habitats. Although sawgrass (*Cladium jamaicense*) was grouped with forest habitats for classification, anecdotal evidence suggests that it can be classified on its own in future studies.

As a result of the classification, which expanded its scope further inland than previous studies, large inland mangrove habitats (lakes, cenotes, depressions) were identified and confirmed by field visits. The furthest distance inland for one of these sites is 15 kilometers from the coast. These inland habitats of mangrove are of high ecological value due to their scarcity worldwide. Unlike other similar habitats where hypersaline conditions have been documented, the habitats found in the course of this study had very low salinity levels. The implications that mangrove can exist in such low salinity conditions suggests that mangrove that suitable habitat for protecting mangrove extends all the way inland whether mangrove is there or not. The presence of mangrove in cenote

environments also suggests that cenotes and the aquifer system they connect are vectors for inland cenotes. Due to the high rate of development in this region, both along the coast and inland, the mangroves of this area need to be the focus of conservation efforts. The ability to link mangrove, which is protected under Mexican law, to the cenotes, lakes and depressions of the area would serve a double purpose to protect and conserve these valuable natural resources. It is my great hope that this study will act as a springboard to action.

Hypothesis 1

H1: Detailed hyperspectral analysis (i.e. VIRIS data) of foliage of mangrove leaves will allow species of mangroves to be spectrally characterized, based on diagnostic reflectance properties.

Hypothesis 1 is supported by the findings of this project.

Hypothesis 2

H2: The diagnostic reflectance properties will be related to differences in leaf anatomical properties.

Hypothesis 2 is supported by the findings of this project.

Hypothesis 3

H3: Analysis of Landsat Thematic Mapper multispectral imagery, combined with the VIRIS data, will allow dominant mangrove types to be detected and mapped.

Hypothesis 3 is supported by the findings of this project.

Hypothesis 4

H4: Use of this model will allow the detection of mangrove in areas where it was previously not known to exist.

Hypothesis 4 is supported by the findings of this project.

References

- AllBusiness.com. (2007) President Felipe Calderon Signs Legislation to Protect Coastal Wetlands; Governors Threaten to Defy New Law, Source: <http://www.allbusiness.com/north-america/mexico/4049966-1.html>.
- Alongi D.M. (2008) Mangrove forests: Resilience, protection from tsunamis, and responses to global climate change. *Estuarine Coastal and Shelf Science* 76:1-13.
- Beddows P.A. (2004) Groundwater Hydrology of a Coastal Conduit Carbonate Aquifer: Caribbean Coast of the Yucatan Peninsula, Mexico. , School of Geographical Sciences, University of Bristol, Bristol.
- Blasco F., Gauquelin T., Rasolofoharinoro M., Denis J., Aizpuru M., Caldairou V. (1998) Recent advances in mangrove studies using remote sensing data. *Marine and Freshwater Research* 49:287-296.
- Camilleri J.C., Ribí G. (1983) Leaf Thickness of Mangroves (*Rhizophora-Mangle*) Growing in Different Salinities. *Biotropica* 15:139-141.
- Case R.A., Gerrish H.P. (1984) Atlantic Hurricane Season of 1983. *Monthly Weather Review* 112:1083-1092.
- CONABIO. (2009) Manglares de México: Extensión y distribución. 2a ed., Comisión Nacional para el Conocimiento y Uso de la Biodiversidad, México. pp. 99.
- Congalton R.G. (1988) Using Spatial Auto-Correlation Analysis to Explore the Errors in Maps Generated from Remotely Sensed Data. *Photogrammetric Engineering and Remote Sensing* 54:587-592.
- Congalton R.G. (1991) A Review of Assessing the Accuracy of Classifications of Remotely Sensed Data. *Remote Sensing of Environment* 37:35-46.
- Congalton R.G. (2011) Personal Communication, Durham, NH.
- Congalton R.G., Balogh M., Bell C., Green K., Milliken J.A., Ottman R. (1998) Mapping and monitoring agricultural crops and other land cover in the Lower Colorado River Basin. *Photogrammetric Engineering and Remote Sensing* 64:1107-1113.
- Congreso del Estado de Quintana Roo. (2008) Decreto de Creación del Municipio de Tulum, in: Periódico Oficial de Quintana Roo (Ed.).
- Cornejo R.H., Koedam N., Luna A.R., Troell M., Dahdouh-Guebas F. (2005) Remote sensing and ethnobotanical assessment of the Mangrove forest changes in the Navachiste-San Ignacio-Macapule lagoon complex, Sinaloa, Mexico. *Ecology and Society* 10.
- Crist E.P., Cicone R.C. (1984) Application of the Tasseled Cap Concept to Simulated Thematic Mapper Data. *Photogrammetric Engineering and Remote Sensing* 50:343-352.
- Ellison A.M., Farnsworth E.J. (1996) Anthropogenic disturbance of Caribbean mangrove ecosystems: Past impacts, present trends, and future predictions. *Biotropica* 28:549-565.

- Ellison J., Simmonds S. (2003) Structure and Productivity of inland mangrove stands at Lake MacLeod, Western Australia. *Journal of the Royal Society of Western Australia* 86:pp. 21-26.
- ERDAS. (2010) *Imagine V. 10.0 Systems Guides*, ERDAS, Inc., Atlanta, GA.
- ESRI. (2010) *ArcMap V. 10.0*, Environmental Systems Research Institute, Inc. , Redlands, CA.
- Ewel K.C., Twilley R.R., Ong J.E. (1998) Different kinds of mangrove forests provide different goods and services. *Global Ecology and Biogeography* 7:83-94.
- FAO. (2007) *The world's mangroves, 1980-2005 : A thematic study in the framework of the Global Forest Resources Assessment 2005 Food and Agriculture Organization of the United Nations*, Rome.
- Forestwatch. (2011) *Using Imagery in Forest Watch*, Source: <http://www.forestwatch.sr.unh.edu/imagery/spectral.shtml>.
- Gabriel J.J., Reinhardt E.G., Peros M.C., Davidson D.E., van Hengstum P.J., Beddows P.A. (2009) Palaeoenvironmental evolution of Cenote Aktun Ha (Carwash) on the Yucatan Peninsula, Mexico and its response to Holocene sea-level rise. *Journal of Paleolimnology* 42:199-213. DOI: Doi 10.1007/S10933-008-9271-X.
- Gates D.M., Keegan H.J., Schleter J.C., Weidner V.R. (1965) Spectral Properties of Plants. *Applied Optics* 4:11-&.
- GloVis. (2011) *Landsat Product Type Descriptions*, United States Geological Survey.
- Gopal S., Woodcock C. (1994) Theory and Methods for Accuracy Assessment of Thematic Maps Using Fuzzy-Sets. *Photogrammetric Engineering and Remote Sensing* 60:181-188.
- Green E.P., Clark C.D., Mumby P.J., Edwards A.J., Ellis A.C. (1998) Remote sensing techniques for mangrove mapping. *International Journal of Remote Sensing* 19:935-956.
- Held A., Ticehurst C., Lymburner L., Williams N. (2003) High resolution mapping of tropical mangrove ecosystems using hyperspectral and radar remote sensing. *International Journal of Remote Sensing* 24:2739-2759.
- Heumann B.W. (2011) Satellite remote sensing of mangrove forests: Recent advances and future opportunities. *Progress in Physical Geography* 35:87-108.
- Hogarth P.J. (1999) *The Biology of Mangroves* Oxford university Press, Oxford, UK.
- Hunt E.R., Rock B.N., Nobel P.S. (1987) Measurement of Leaf Relative Water-Content by Infrared Reflectance. *Remote Sensing of Environment* 22:429-435.
- Huntley R. (2005) *Characterizing Vegetation Associated with Cenotes in Quintana Roo, Mexico Using Remote Sensing and Field Methods*, Department of Natural Resources, University of New Hampshire, Durham, New Hampshire. pp. 208.
- Instituto Nacional de Estadística y Geografía. (2010) *Censo de Población y Vivienda*.
- Jensen J.R. (2007) *Remote sensing of the environment : An earth resource perspective*. 2nd ed. Pearson Prentice Hall, Upper Saddle River, NJ.
- Johansen D.A. (1940) *Plant Microtechnique* McGraw-Hill, New York.

- Kaplowitz M.D. (2000) Identifying Ecosystem Services Using Multiple Methods: Lessons from the Mangrove Wetlands of Yucatan, Mexico. *Agriculture and Human Values* 17:169-179.
- Kaplowitz M.D. (2001) Assessing mangrove products and services at the local level: The use of focus groups and individual interviews. *Landscape and Urban Planning* 56:53-60.
- Kathiresan K., Bingham B.L. (2001) Biology of mangroves and mangrove ecosystems. *Advances in Marine Biology*, Vol 40 40:81-251.
- Lawrence M.B., Avila L.A., Beven J.L., Franklin J.L., Guiney J.L., Pasch R.J. (2001) Atlantic Hurricane Season of 1999. *Monthly Weather Review* 129:3057-3084.
- Lee J.C. (1996) *Amphibians and Reptiles of the Yucatan Peninsula* Cornell University Press, Ithaca and London.
- Liangyun L. (2010) Discriminating C3 and C4 Plants from Hyperspectral Data, *Geoscience and Remote Sensing Symposium (IGARSS), 2010 IEEE International*. pp. 4252-4255.
- Lugo A.E. (1981) The Inland Mangroves of Inagua. *Journal of Natural History* 15:845-852.
- Lugo A.E., Snedaker S.C. (1974) The Ecology of Mangroves. *Annual Review of Ecology and Systematics* 5:39-64.
- Mazzotti F.J., Fling H.E., Merediz G., Lazcano M., Lasch C., Barnes T. (2005) Conceptual ecological model of the Sian Ka'an Biosphere Reserve, Quintana Roo, Mexico. *Wetlands* 25:980-997.
- Meacham S.S. (2007) Freshwater Resources in the Yucatan Peninsula in: L. Holliday, et al. (Eds.), *Sustainable Management of Groundwater in Mexico: Proceedings of a Workshop (Series: Strengthening Science-Based Decision Making in Developing Countries)*, National Academies Press, Merida, Yucatan, Mexico. pp. 6-12.
- Moore G. (2011) Personal Communication, Durham, New Hampshire.
- Murray M.R., Zisman S.A., Furley P.A., Munro D.M., Gibson J., Ratter J., Bridgewater S., Minty C.D., Place C.J. (2003) The mangroves of Belize Part 1. distribution, composition and classification. *Forest Ecology and Management* 174:265-279.
- Pasqualini V., Iltis J., Dessay N., Lointier M., Guelorget O., Polidori L. (1999) Mangrove mapping in North-Western Madagascar using SPOT-XS and SIR-C radar data. *Hydrobiologia* 413:127-133.
- Poder Ejecutivo Federal. (2011) *Ley General de Vida Silvestre*, in: *Diario Oficial de la Federación* (Ed.), Mexico.
- Polidoro B.A., Carpenter K.E., Collins L., Duke N.C., Ellison A.M., Ellison J.C., Farnsworth E.J., Fernando E.S., Kathiresan K., Koedam N.E., Livingstone S.R., Miyagi T., Moore G.E., Vien N.N., Ong J.E., Primavera J.H., Salmo S.G., Sanciangco J.C., Sukardjo S., Wang Y.M., Yong J.W.H. (2010) The Loss of Species: Mangrove Extinction Risk and Geographic Areas of Global Concern. *Plos One* 5.
- Portnoy J.W., Valiela I. (1997) Short-term effects of salinity reduction and drainage on salt-marsh biogeochemical cycling and *Spartina* (cordgrass) production. *Estuaries* 20:569-578.

- Rasolofoharinoro M., Blasco F., Bellan M.F., Aizpuru M., Gauquelin T., Denis J. (1998) A remote sensing based methodology for mangrove studies in Madagascar. *International Journal of Remote Sensing* 19:1873-1886.
- Raven Peter H. E., R.F., Curtis, H. (1976) *The Biology of Plants* Worth Publishers, Inc., New York City.
- Rock B.N., Hoshizaki T., Miller J.R. (1988) Comparison of Insitu and Airborne Spectral Measurements of the Blue Shift Associated with Forest Decline. *Remote Sensing of Environment* 24:109-127.
- Rock B.N., Vogelmann J.E., Williams D.L., Vogelmann A.F., Hoshizaki T. (1986) Remote Detection of Forest Damage. *Bioscience* 36:439-445.
- Rock B.N., Williams D.L., Moss D.M., Lauten G.N., Kim M. (1994) High-Spectral-Resolution Field and Laboratory Optical Reflectance Measurements of Red Spruce and Eastern Hemlock Needles and Branches. *Remote Sensing of Environment* 47:176-189.
- Salvador R., San-Miguel-Ayanz J. (2003) The effect of histogram discontinuities on spectral information and non-supervised classifiers. *International Journal of Remote Sensing* 24:115-131. DOI: Doi 10.1080/01431160110070654.
- Story M., Congalton R.G. (1986) Accuracy Assessment - a Users Perspective. *Photogrammetric Engineering and Remote Sensing* 52:397-399.
- TDSWay. (2007) SoloField for Windows CE, Tripod Data Systems Inc, Corvallis, OR.
- Terchunian A., Klemas V., Segovia A., Alvarez A., Vasconez B., Guerrero L. (1986) Mangrove Mapping in Ecuador - The Impact of Shrimp Pond Construction. *Environmental Management* 10:345-350.
- Tomlinson P.B. (1986) *The Botany of Mangroves* Cambridge University Press, Cambridge Cambridgeshire ; New York.
- Trimble. (2011) Trimble NOMAD Rugged Handheld Computer, Trimble Navigation Limited.
- Tucker C.J., Sellers P.J. (1986) Satellite Remote-Sensing of Primary Production. *International Journal of Remote Sensing* 7:1395-1416.
- Valiela I., Bowen J.L., York J.K. (2001) Mangrove forests: One of the world's threatened major tropical environments. *Bioscience* 51:807-815.
- Vogelmann J.E., Rock B.N., Moss D.M. (1993) Red Edge Spectral Measurements from Sugar Maple Leaves. *International Journal of Remote Sensing* 14:1563-1575.

Appendices

Appendix A:

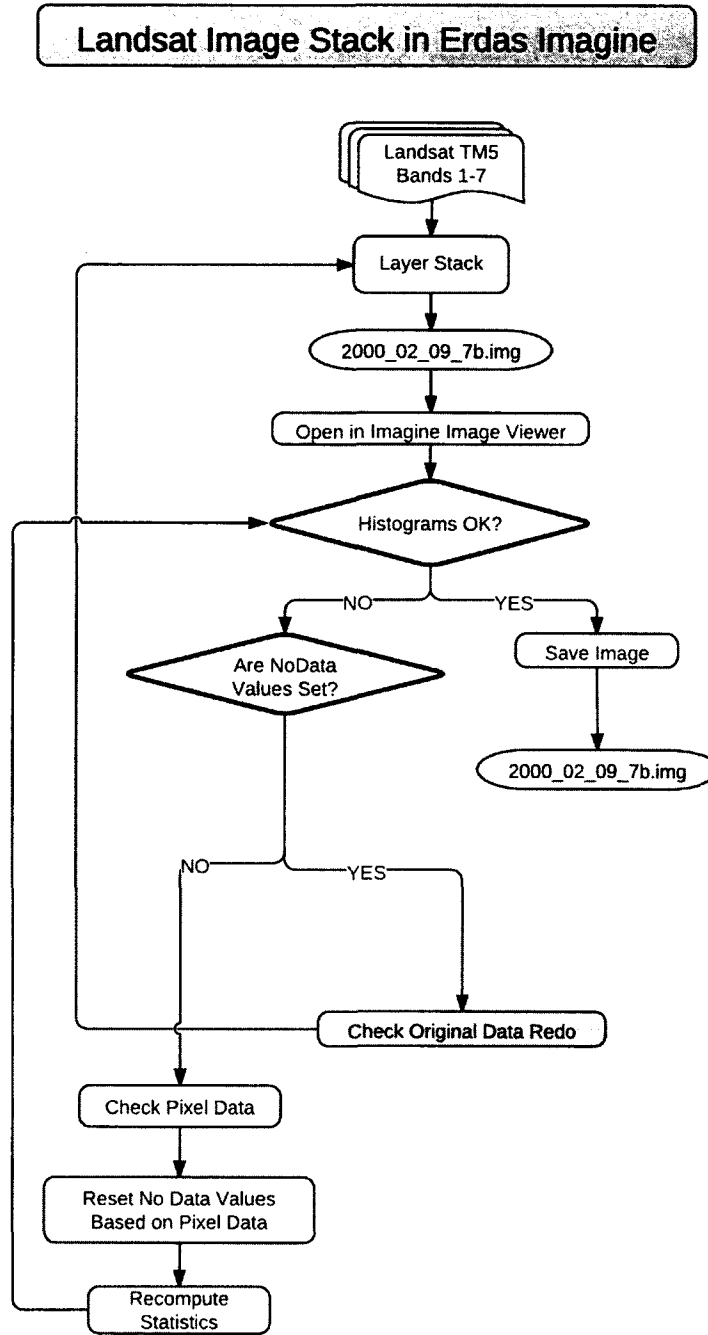


Figure A 1 Flowchart for Image Stacking in ERDAS Imagine V.10

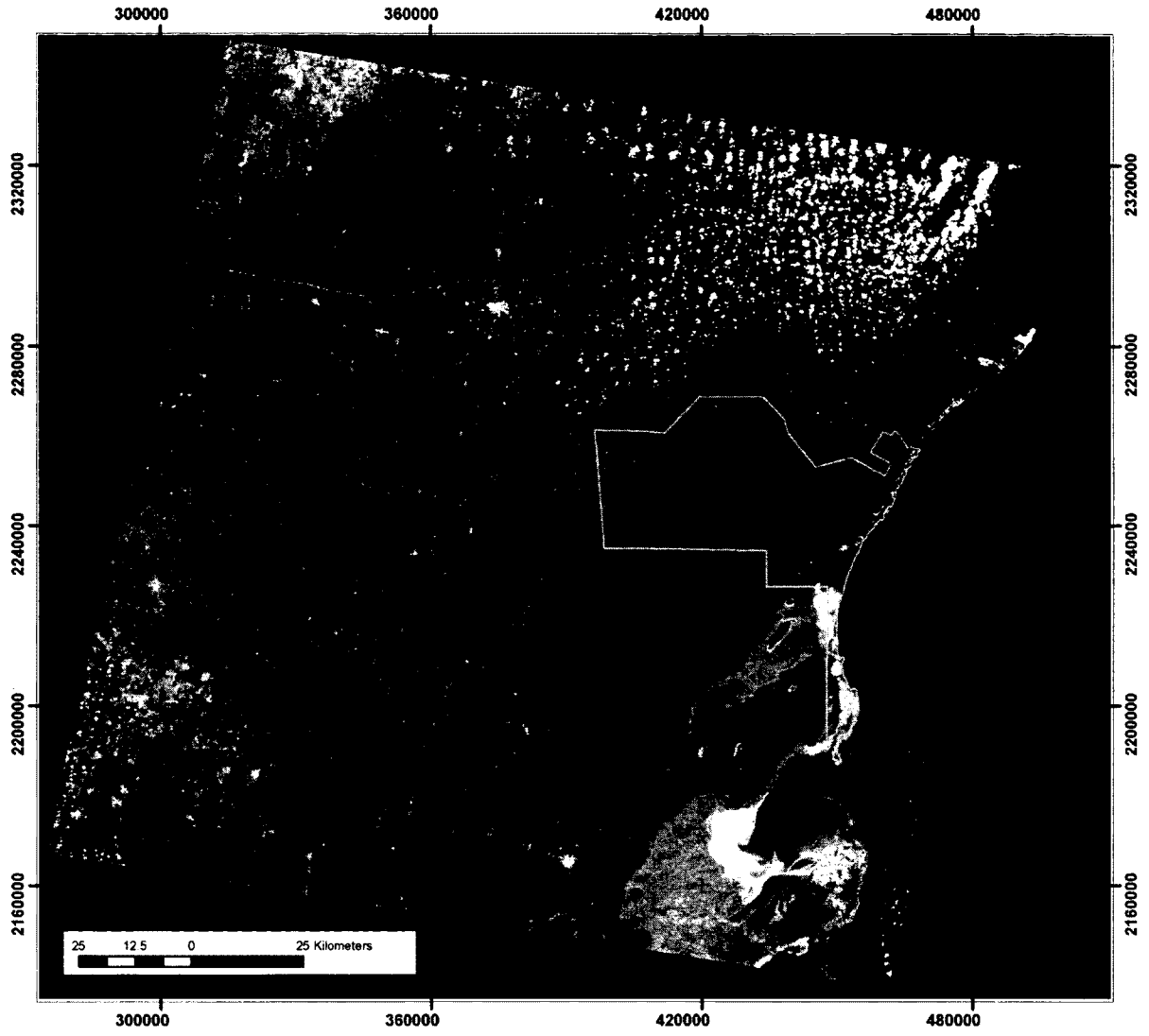


Figure A 2 Full Extent of Landsat 5 TM Image (FCC bands 4,3,2) Path 19 Row 46, Acquired February 9th, 2000 with Tulum Municipal Boundary

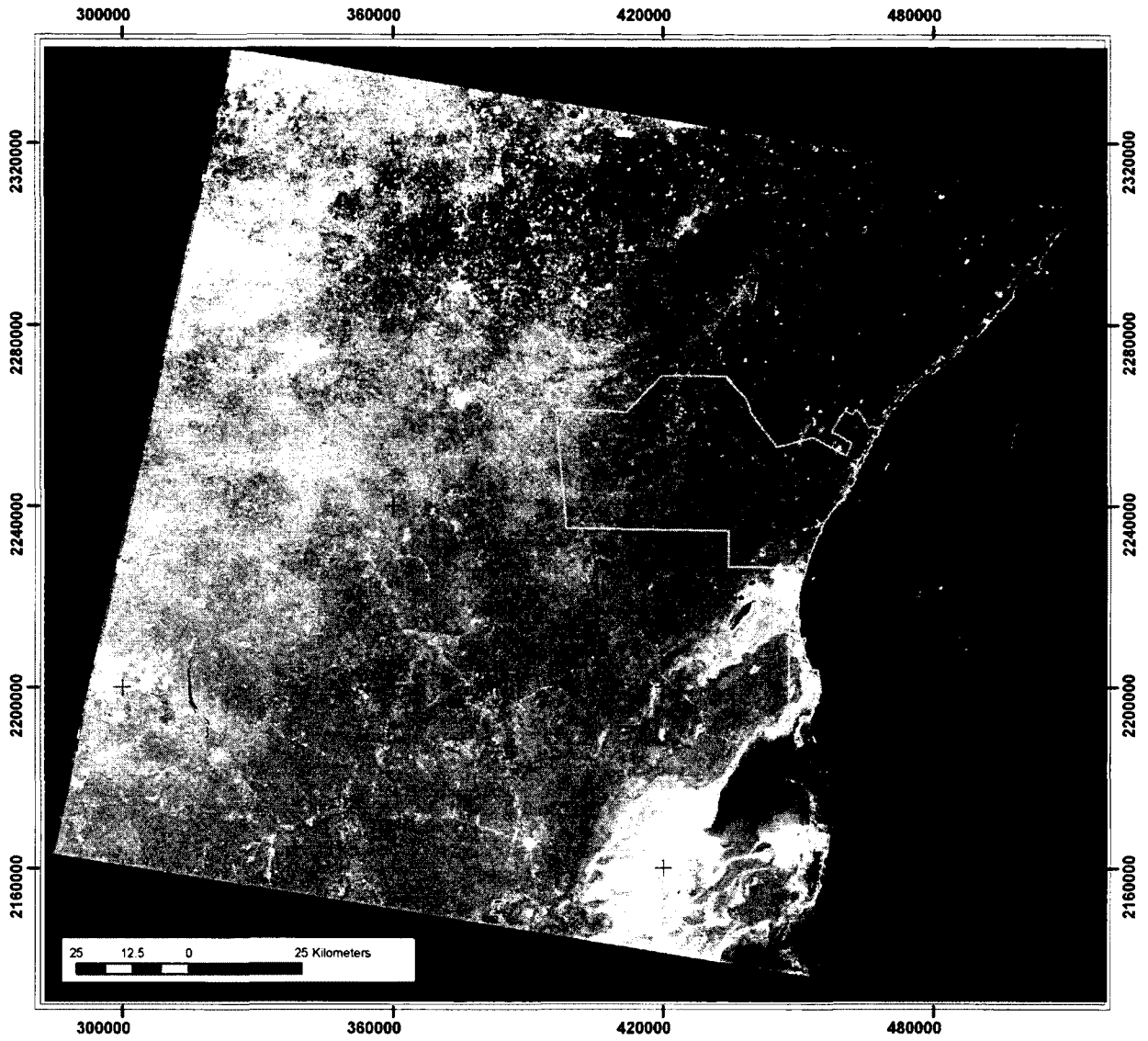


Figure A 3 Full Extent of Landsat 5 Image (FCC Bands 4,3,2) Path 19 Row 46, Acquired April 17th, 1984 with Tulum Municipal Boundary

10 Class Unsupervised Classification

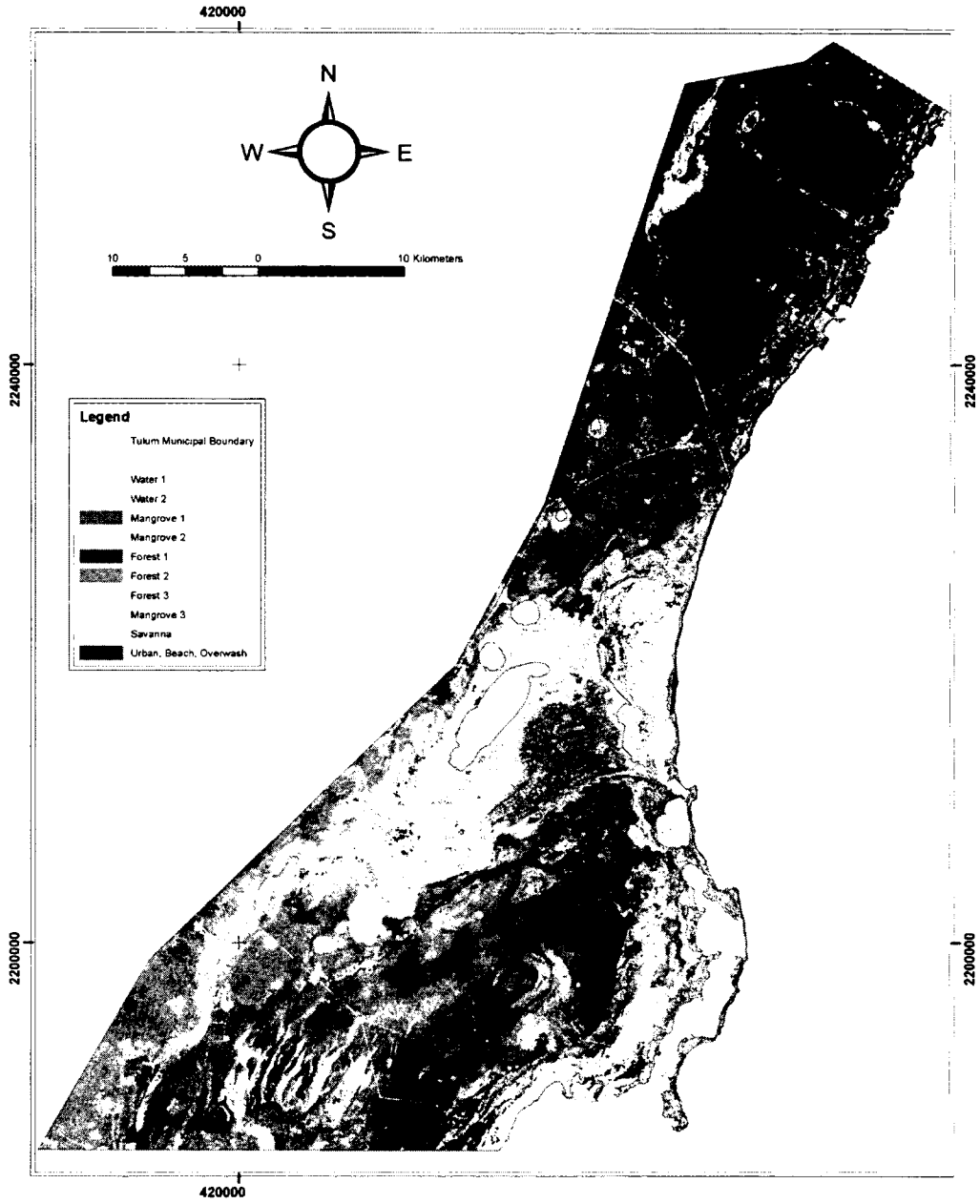


Figure A 4 10 Class Unsupervised Classification of the Study Area

Derivative Band Creation and Stacking in Erdas Imagine (5/4 Ratio, Principal Components Analysis)

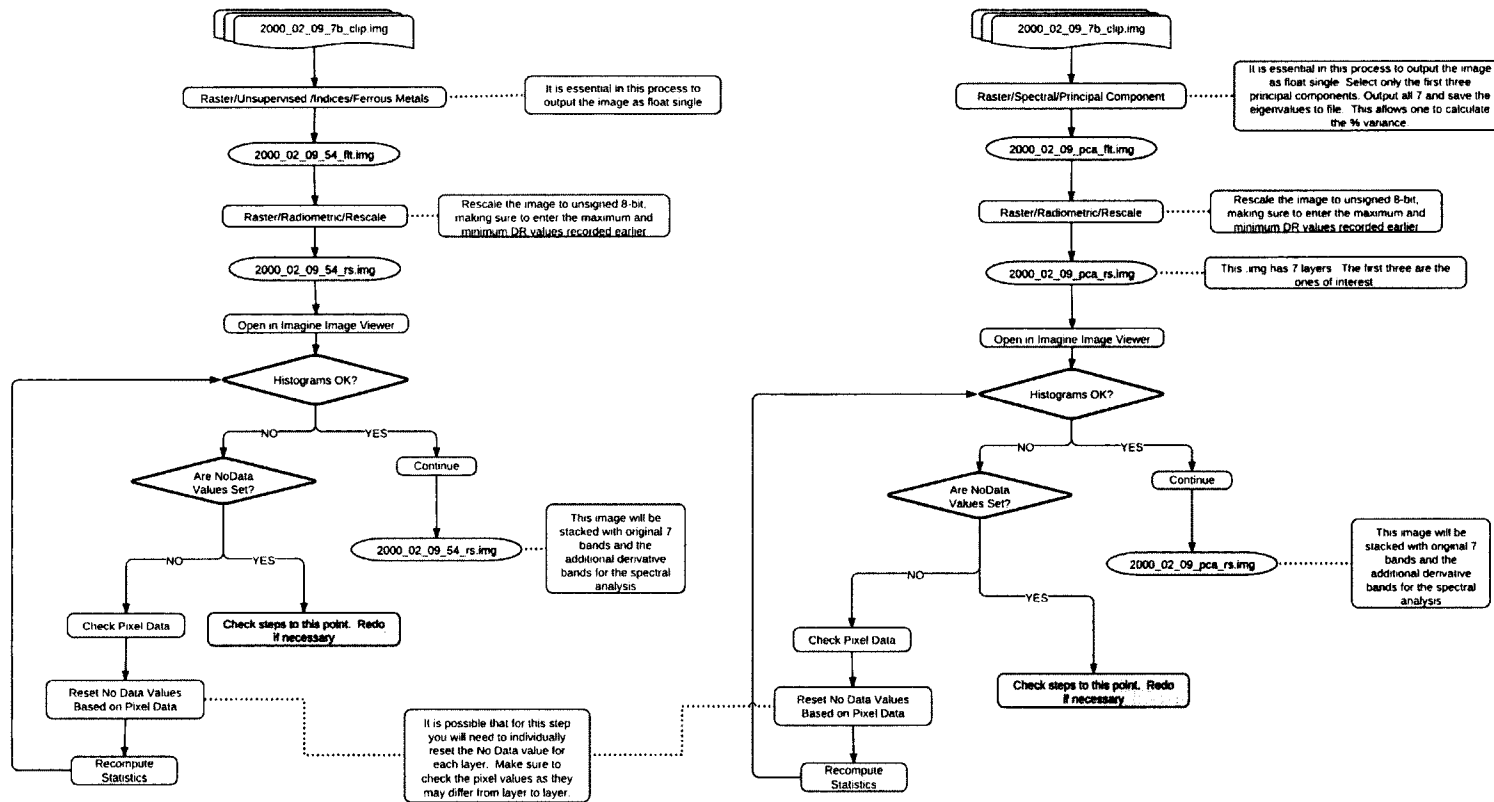


Figure A 5 Derivative Band Creation (5/4 ratio, Principal Components Analysis) in ERDAS imagine V.10

Derivative Band Creation and Stacking in Erdas Imagine (NDVI, Tasseled-Cap)

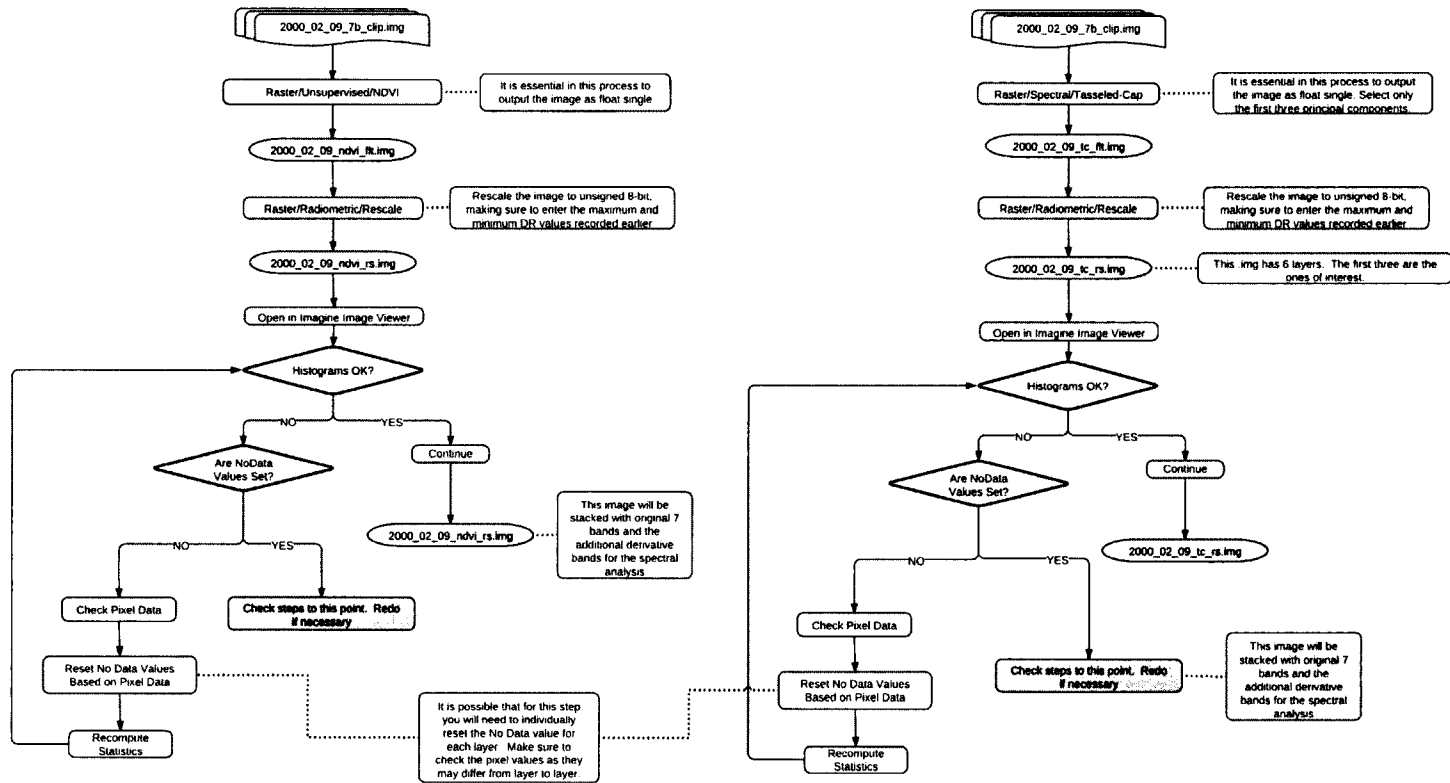


Figure A 6 Derivative Band Creation (NDVI, Tasseled-Cap) in ERDAS Imagine

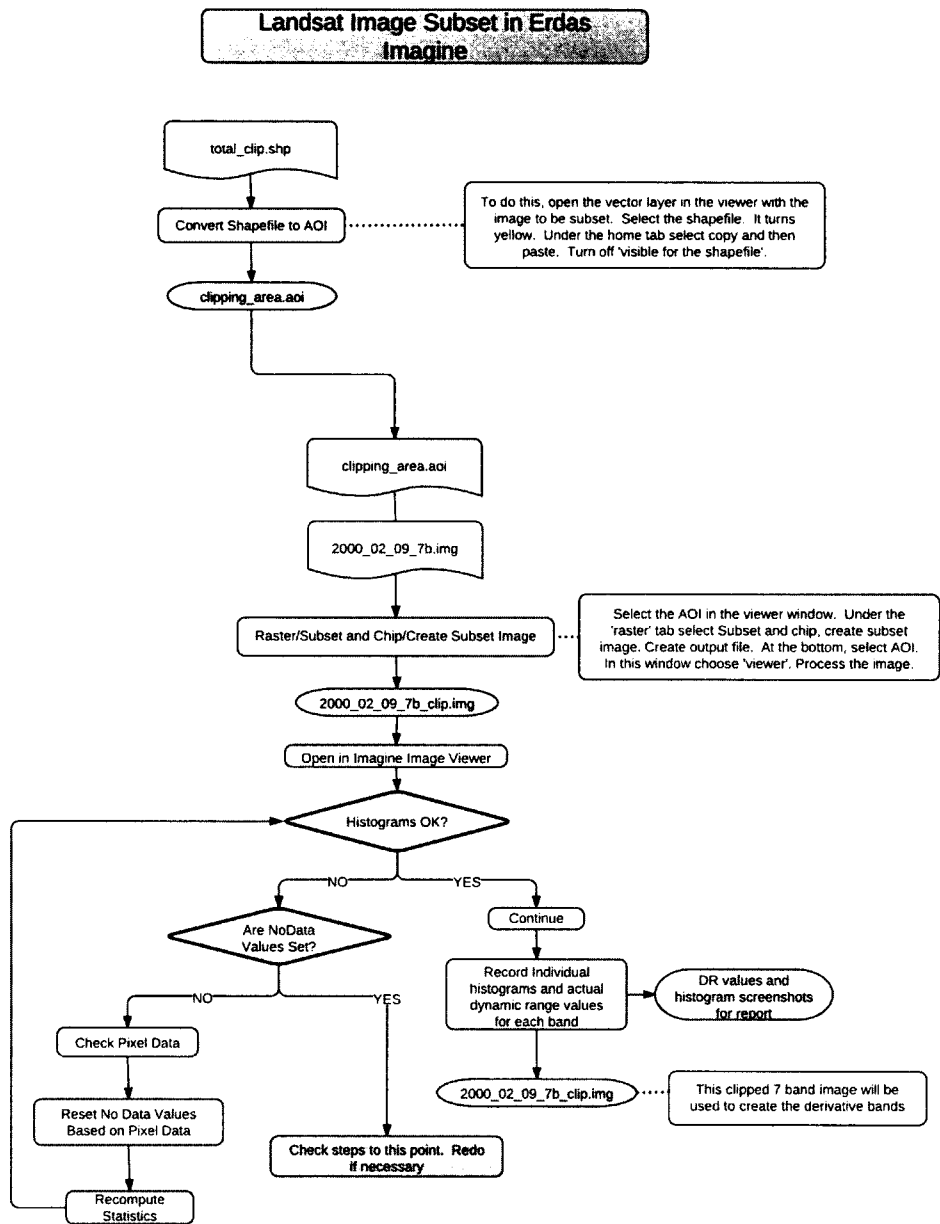


Figure A 7 Flowchart for Landsat Image Subset and Masking in ERDAS Imagine

Accuracy Assessment Reference Points

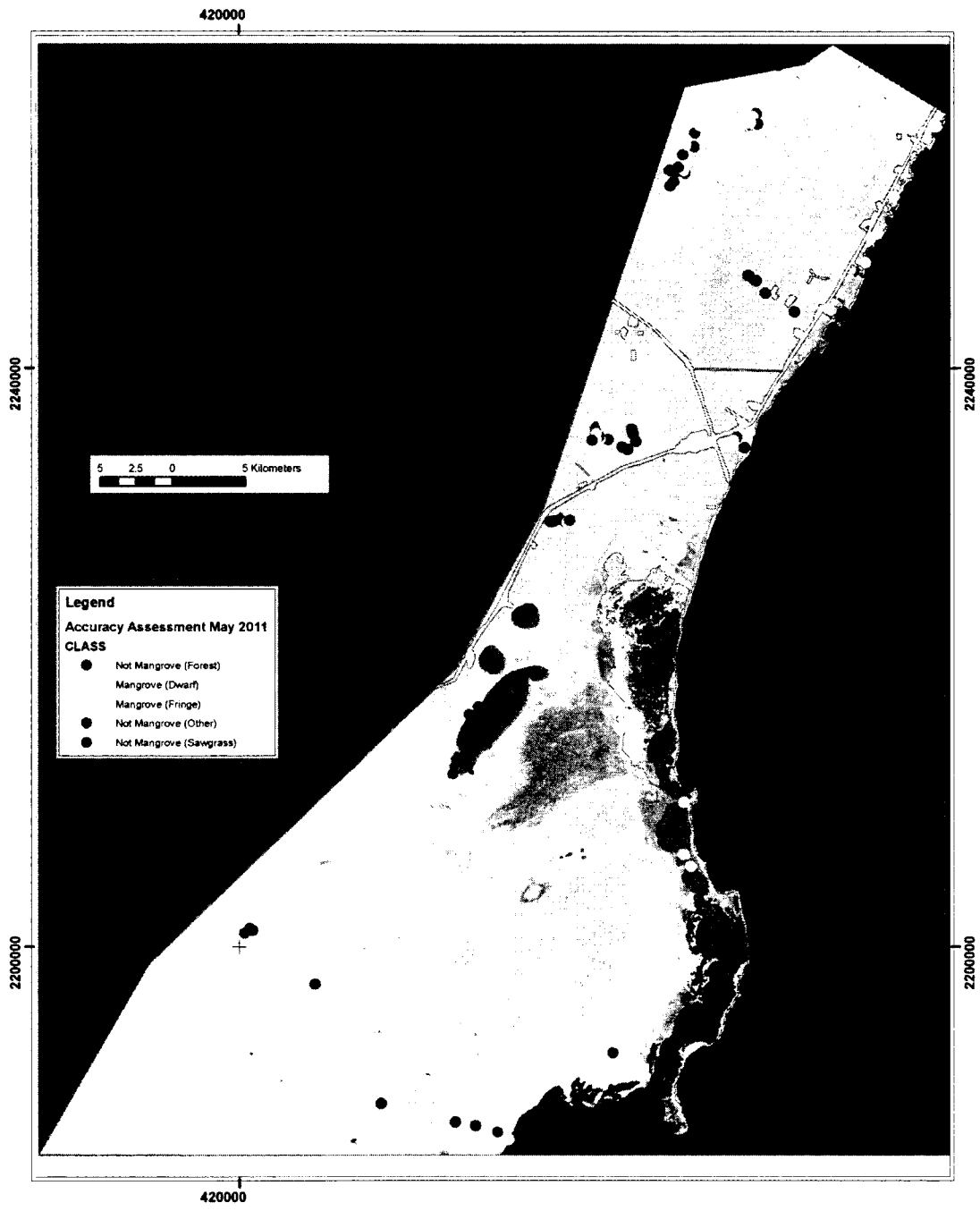


Figure A 8 Accuracy Assessment Reference Points